



Analysis of soluble high-affinity PD1 variants

Natalia Krajewska

Master of Science (by Dissertation) in Cell and Molecular Biology

Department of Biological Science

University of Essex

Date of submission: May 2020

CONTENTS

Title Page	Page 1
Contents	Page 2
Abstract	Page 4
1.1. Pancreatic Cancer Progression	Page 6
1.2. Pancreatic cancer microenvironment	Page 7
1.3. Immunological responses to tumours	Page 10
1.4. Immune evasion in pancreatic cancer	Page 12
1.5. The PD-1/PD-L1 signalling pathway	Page 13
1.6. PD1/PD-L1 signalling in cancer	Page 17
1.7. Targeting the PD1/PD-L1 signalling pathway in cancer	Page 19
1.8. Increasing binding affinity of proteins	Page 20
1.9. Mesenchymal stem cells as drug delivery vector	Page 21
1.10. Aims and hypotheses	Page 22
2.1. Generation of the pcDNA.sPD1 ^{WT}	Page 24
2.2. Generation of variants with higher binding affinities	Page 24
2.3. Generation of the sPD1.pFUSE constructs	Page 24
2.4. Agarose Gel Electrophoresis parameters	Page 25
2.5. DNA gel extraction	Page 25
2.6. Plasmid Miniprep	Page 25
2.7. DNA Plasmid Midiprep	Page 25
2.8. <i>E. Coli</i> culture conditions	Page 26

<u>2.9. CHO cell Culture</u>	<u>Page 26</u>
<u>2.10. CHO cell transfection</u>	<u>Page 26</u>
<u>2.11. ELISA</u>	<u>Page 27</u>
<u>2.12. Solid-phase protein competition assay</u>	<u>Page 27</u>
<u>2.13. Unspecific Binding Testing</u>	<u>Page 27</u>
<u>2.14. Surface staining and FACS analysis</u>	<u>Page 28</u>
<u>2.15. Adenoviral vector generation for sPD1 expression</u>	<u>Page 29</u>
<u>2.16. Mesenchymal stem cell transduction</u>	<u>Page 29</u>
<u>3.1. Designing a soluble PD1 DNA construct</u>	<u>Page 31</u>
<u>3.2. sPD1^{WT} protein production</u>	<u>Page 35</u>
<u>3.3. Testing sPD1^{WT} binding to PD-L1 in a cellular competition assay</u>	<u>Page 36</u>
<u>3.4. Establishing parameters of the microplate-based sPD1 Competition Assay</u>	<u>Page 38</u>
<u>3.5 Generation of sPD1 variants with mutations to increase binding affinity to PD-L1</u>	<u>Page 41</u>
<u>3.6 Generation of a soluble High Affinity Consensus (HAC) sequence PD1 variant</u>	<u>Page 45</u>
<u>3.7. Protein affinity testing to PD-L1 of the sPD1^{HAC} protein</u>	<u>Page 50</u>
<u>3.8. Analysis of sPD1^{HAC}.IgG binding to PD-L1 in a cellular competition assay</u>	<u>Page 54</u>
<u>3.9. sPD1^{HAC}.IgG adenoviral vector generation</u>	<u>Page 55</u>
<u>4.1 Discussion</u>	<u>Page 58</u>
<u>4.8 Conclusions</u>	<u>Page 63</u>
<u>Bibliography</u>	<u>Page 64</u>

ABSTRACT

Despite achieving significant clinical impact in several major cancer types such as melanoma or Hodgkin's lymphoma, immunotherapies have not had much success in the treatment of pancreatic cancer. This cancer is characterised by a pro-inflammatory and immunosuppressive stroma which causes aggressive cancer growth and results in drug resistance. In this study we seek to overcome some of the challenges associated with drug delivery into the pancreatic cancer microenvironment and design a checkpoint inhibitor therapeutic to inhibit PD1/PD-L1 signalling. Mesenchymal stem cells (MSCs) offer an alternative drug delivery method for delivering this treatment to the pancreas due to their ability to infiltrate tumours and deliver a therapeutic payload. In this study soluble PD1 (sPD1) variants were generated with increased binding properties to PD-L1. The sPD1 variants were analysed using solid-phase protein competition studies as well as live pancreatic cell assays to assess their immune checkpoint inhibitory functions. These studies revealed that one variant - expressed as an IgG fusion protein, that can completely outcompete wild-type PD1, even at very low concentrations. MSCs were then successfully engineered to produce and secrete this variant. These cells were termed MSC.sPD1. This way of delivering therapeutics into the tumour microenvironment holds great promise, however it should be noted that MSCs have been associated with several undesirable effects, and further research needs to be conducted on MSC.sPD1 to confirm their safety and efficacy.

INTRODUCTION

Within the last decade, cancer immunotherapies have truly revolutionized cancer treatment. Unlike other mainstream anti-cancer therapies which typically directly target cancer cells, immunotherapies target the immune system and the tumour microenvironment (TME) instead (Yu and Cui, 2018). By aiding the activation of immune system cells these therapies can promote powerful anti-tumour effects. Among these therapies, checkpoint inhibitors -a type of targeted treatment that blocks checkpoint proteins on immune cells, have achieved remarkable progress in recent years. Checkpoint proteins are receptors which normally regulate the duration of immune responses and maintain self-tolerance. Blocking inhibitory checkpoint proteins has greatly improved significant outcomes in certain cancers such as melanoma (Topalian et al., 2012), Hodgkin's lymphoma (Ansell et al., 2015) and non-small cell lung cancer (Borghaei et al., 2015), however immunotherapies have had little success in the treatment of pancreatic cancer. This cancer is characterised as very aggressive and with a particularly poor prognosis. Survival rates for pancreatic cancer are less than 5% - one of the lowest among other cancers (Pancreatic Cancer UK, 2019). It is the 7th leading cause of cancer death in both males and females (Bray et al., 2018). The age-standardised incidence rate of pancreatic cancer in the western world has been observed to increase by 1.03% per year between 1973 and 2014 (Saad et al., 2018). Epidemiological projections predict that by 2030 it will be the 2nd leading cause of cancer-related deaths in USA and Europe after lung cancer, surpassing colorectal, breast and prostate cancer (Rahib et al, 2014). Taking these worrying statistics into consideration, it is clear that new treatments for pancreatic cancer are greatly needed.

There are several factors which will be reviewed in this paper, that contribute to the poor prognosis and treatment outcomes of pancreatic cancer: I) A lack of symptoms and biomarkers in the early stages of tumorigenesis, II) A high metastatic tendency during early stages of cancer, III) Drug resistance as a result of a dense, fibrous stroma which surrounds the tumour, IV) A highly immunosuppressive TME resulting in cancer immune evasion. The aforementioned factors make pancreatic cancer a complex and unique disease, making it hard to treat. In our study we seek to overcome some of the current challenges associated with drug delivery into the pancreatic cancer microenvironment.

1.1. Pancreatic Cancer Progression

Pancreatic cancer can arise from either endocrine or exocrine cells, however exocrine tumours are much more common and make up 95% of cancer cases. Of the exocrine sub-type, it is the pancreatic ductal adenocarcinoma (PDAC) that accounts for the majority of the tumours; 90% of all pancreatic cancer malignancies are of this type. Pancreatic cancers are tumours derived from epithelial cells in the lining of the pancreatic duct. Progression of the disease occurs in a stepwise manner characterised by the transition of a normal pancreatic duct to non-invasive precursor lesions which eventually develop into an invasive neoplasia (Koorstra et al., 2009). This progression is accompanied by an accumulation of genetic mutations which lead to various molecular and morphological changes in cells. Pancreatic intraepithelial neoplasia (PanIN) is the most common precursor of pancreatic cancer (Matthaei et al., 2011) – PanINs are microscopic lesions (<5 mm) which form in the small pancreatic ducts. They are flat or papillary and composed of columnar and cuboidal cells containing varying amounts of mucin (Guo et al. 2016).

The early genetic alterations present in PanINs include telomerase shortening, V-Ki-ras2 Kirsten rat sarcoma viral oncogene homolog (KRAS) activation and inactivation of tumour suppressor genes cyclin-dependent kinase inhibitor 2A/cyclin-dependent kinase inhibitor 16 (CDKN2A/16). KRAS mutation is present in 90% of pancreatic cancer cases and is one of the earliest genetic abnormalities in the tumour progression model for pancreatic cancer and is likely the driver of tumour formation (Löhr et al., 2005). The KRAS gene encodes membrane-anchored guanosine triphosphate hydrolase (GTP-ase) and if it gains oncogenic activity it causes a continuous induction of downstream signalling pathways (MAPK/Erk, PI3K/Akt) contributing to increased proliferative signals, invasiveness and inhibition of cell apoptosis. The CDKN2A gene encodes a cell-cycle checkpoint protein which inhibits the cell cycle at the G1/S checkpoint by binding to CDKs. Another early genetic abnormality is telomere shortening - detected in 90% of PanIN-1 cases compared to the normal ductal epithelium (van Heek NT et al., 2002). Telomere shortening results in chromosomal instability, abnormal fusion of chromosome ends and gene translocation due to inappropriate chromosome segregation during mitosis which all lead to further mutations. Epigenetic changes are also common in early pancreatic cancer and mostly include methylation of CpG islands which are present in the promoter regions of genes causing gene silencing. Microarray analyses have shown that hypermethylation begins in the early stages of PanINs and progressively increases during neoplastic progression (Sato et al., 2008).

The accumulation of mutational changes leads to progressive molecular remodelling in cancer cells causing increasing levels of nuclear and cytoskeletal abnormalities. These changes allow the cancer cells to gain the various hallmark properties associated with cancer: sustained cell division, evasion of growth

suppression, cell death evasion, replicative immortality, invasion and metastasis abilities, angiogenesis, altered cellular metabolism and suppression of immune responses (Hanahan and Weinberg, 2011). Ultimately PanINs can develop into an invasive pancreatic cancer, where they push out of the epithelium and infiltrate healthy tissue. The primary tumour affects the normal functioning of the pancreas by blocking ducts that deliver enzymes to the intestine and by disrupting endocrine gland functions thereby causing diabetes and other hormonal disorders. The tumour can also wrap around blood vessels and interfere with the function of other nearby organs. The most detrimental effect of this cancer however is its proneness to metastasis and the consequent formation of secondary tumours.

1.2. Pancreatic cancer microenvironment

The pancreatic cancer TME is fairly unique in its characteristics and is characterised by a dense fibrotic stroma that surrounds the tumour. At the core of the pancreatic cancer microenvironment lies the pancreatic stellate cell (PSC); the key player behind the fibrotic reaction and the remodelling of the TME. These normally quiescent cells are characterised by their ability to store retinoids within lipid droplets. Normally, they are involved in the regulation of the extracellular tissue matrix (ECM) turnover by regulating the synthesis and degradation of ECM proteins (Apte et al, 2012). In response to pancreatic injury or inflammation, PSCs activate and undergo morphological changes including the loss of retinoid droplets, acquisition of a spindle like shape and increased α -SMA (smooth muscle alpha-actin) expression (Bachem et al., 1998). Once active, PSCs begin to actively proliferate, migrate and take part in a fibrotic reaction where they increase their production ECM components such as collagen type I and type II laminin and fibronectin. They also contribute to matrix degradation via production of matrix metalloproteinases and their inhibitors (Apte et al., 2004). PSC activation is triggered by several interleukins, chemokines, growth factors (GFs) including platelet-derived GF (PDGF), vascular endothelial GF (VEGF), transforming GF- β (TGF- β) and tumour necrosis factor alpha (TNF- α) (Korc et al., 1991; Mews et al., 2002) These factors are present at sites of inflammation which includes tumour tissue.

During pancreatic cancer the pancreas is in a state of chronic pancreatitis which leads to a prolonged activation of PSCs and an excessive ECM protein production. The imbalance between ECM deposition and degradation causes the formation of a dense fibrotic stroma in a process known as desmoplasia. The stromal production is facilitated by an abundance of growth factors. This stroma accounts for a large portion of the pancreatic cancer tumour and can make up over 80% of the tumour mass (Erkan et al, 2012). A complex cross-talk exists between the stroma and cancer cells which has been shown to propagate tumour growth and progression (Figure 1.1.1). Concurrent subcutaneous co-injection of

PSCs and cancer cells into immunocompromised murine models resulted in significantly larger and more aggressive tumours with a stronger stromal reaction than those produced by an injection with cancer cells alone (Bachem et al., 2005). This network of interactions between PSC and cancer cells leads to a devastating, self-perpetuating cycle of continuous recruitment and activation of PSCs which propagates cancer growth. An increase in the cancer cell population in turn further promotes PSC activation. In addition to this, activated PSC cells also take part in autocrine signalling via the secretion of TGF, PDGF and connective tissue growth factor (CTGF). These factors cause further perpetuation of PSC activation resulting in even more ECM production (Masamune et al., 2009).

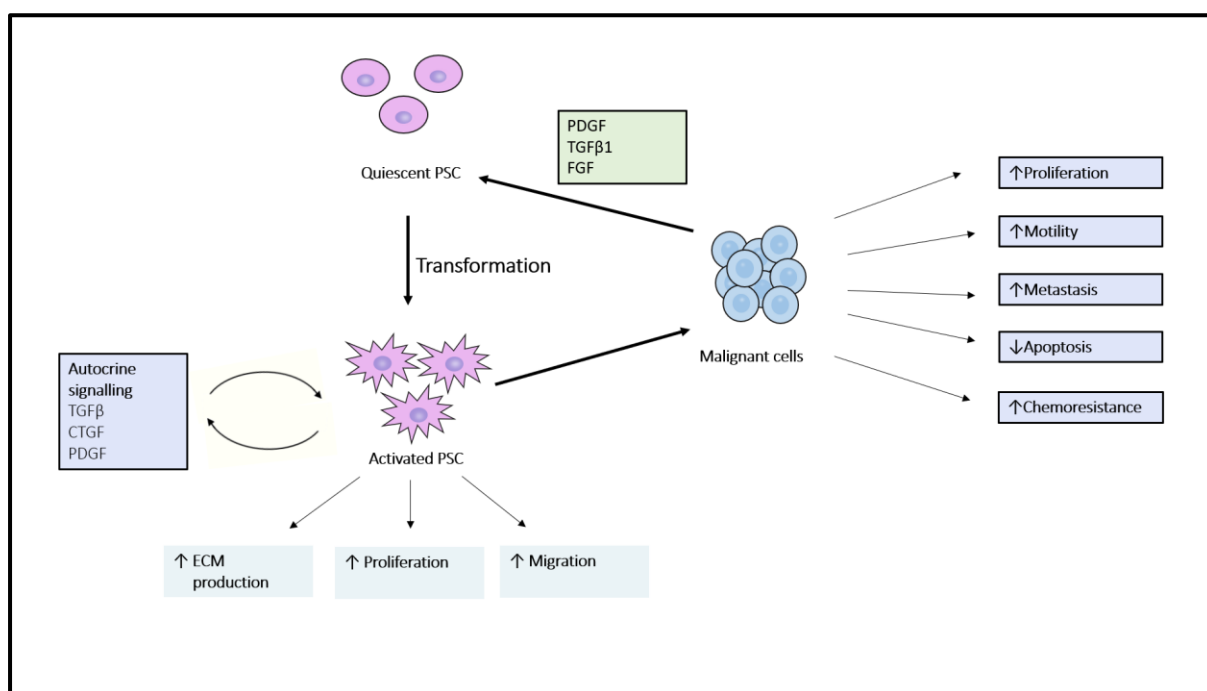


Figure 1.1.1 Bi-directional interaction between malignant cancer cells and pancreatic stellate cells (PSCs). Malignant cells stimulate PSC activation via secretion of platelet derived growth factor (PDGF), tissue growth factor- β 1(TGF β 1) and fibroblast growth factor (FGF). Activated PSCs increase their proliferation and migration rates and begin secreting extracellular matrix (ECM) components. PSCs take part in autocrine signalling and drive their own activation via the secretion of TGF β , platelet-derived growth factor (PDGF) and connective tissue growth factor (CTGF). Activated PSCs secrete a variety of agents which ultimately aid cancer growth by increasing proliferation, motility, metastasis, chemoresistance and decreasing apoptosis in cancer cells.

Activated PSCs can influence cancer progression via several mechanisms. Firstly, PSCs aid cancer metastasis and it has been reported that tumours with an increased number of PSCs have a significantly greater incidence of distant metastases (Hwang et al., 2008). This may be due to PSCs involvement in epithelial-mesenchymal transition (EMT) of cancer cells - one of the key events during cancer metastasis wherein epithelial cells gain mesenchymal-like migratory and invasive properties. When pancreatic cancer cells were co-cultured with PSCs, they exhibited loose cell contacts and a scattered

fibro-blast like appearance in comparison to mono-cultured cells (Kikuta et al., 2010). The study also reported a decreased expression of epithelial markers such as E-Cadherin and β -cadherin and an increased expression of mesenchymal markers such as Snail and vimentin. Research also shows that PSCs can co-migrate with pancreatic cancer cells to metastatic sites where they are likely to be involved in seeding and aiding cancer growth (Xu et al., 2010). Pancreatic cancer cells may also begin to secrete the ECM metalloproteinase inducer (EMMPRIN) which causes PSCs to increase secretion of the MMP2 protein. MMP2 is essential for the degradation of the basement membrane; a critical process during cancer invasion. Another important property of PSCs is their ability to prevent apoptosis in cells, further promoting the growth of the cancer cell population. Inhibition of apoptosis is thought to be related to the up-regulation of anti-apoptotic proteins including Bcl-2, Bcl-xL and survivin in PSCs (Ling et al. 2011).

As well as aiding cancer growth, the stroma also protects pancreatic cancer cells from therapeutic interventions. Despite pancreatic cancer having the same chemosensitivity *in vitro* as other cancers, pancreatic cancer patients have a higher resistance to chemotherapeutics than other cancers (McCarrol, 2014). Research points to the dense stroma as the main perpetrator of this resistance. Together, the prominent fibrosis and the increasing amount of proliferating cancer cells result in growth-induced stress which compresses lymph nodes and blood vessels which leads to an increased interstitial fluid pressure (IFP) and hypoxia. An increased IFP impairs drug perfusion and hypoxia further drives PSC activation to generate more fibrosis and creates a hypoxia-fibrosis cycle which indirectly contributes to chemoresistance by impairing drug delivery to cancer cells (McCarrol et al., 2014). On top of this, a state of hypoxia has been shown to induce a number of genes responsible for increased invasion, aggressiveness and metastasis of tumours (Chan and Giaccia, 2007). Hypoxia-inducible factor-1 α (HIF-1 α) has also been shown to upregulate the multidrug resistance gene which shows a distinct mechanism for stromal-induced chemotherapy resistance (Comerford et al., 2002). The secretions from PSCs have been also shown to confer a chemoresistant phenotype by suppressing H₂O₂ -induced apoptosis (Vonlaufen et al., 2008).

1.3. Immunological responses to tumours

The immune system also plays key roles in both the positive and negative regulation of pancreatic cancer development and progression and the cross-talk between immune and cancer cells is an important hallmark of cancer. The immune system employs several strategies to remove malignant cells from the body, utilising both the innate and adaptive systems. Several cell types of the immune system can recognise 'danger' such as pathogens, tumours and damaged tissues. This includes neutrophils, macrophages, dendritic cells (DCs), mast cells and natural killer (NK) cells. These cells can offer indirect

protection via the removal of viruses, reducing the risk of virally-induced tumours and pathogens, resolving inflammation and preventing the establishment of an inflammatory environment which may lead to tumorigenesis (Swann and Smyth, 2007). Activated innate system cells can release factors such as cytokines – interferons (IFNs), interleukins (ILs) and colony stimulating factors (CSF) – and chemokines which can cause local and systemic inflammation and alert the adaptive immune system to danger. The adaptive immune system employs more direct methods of tumour removal by attacking tumour cells and causing cell death. Mutations in cancer cell DNA lead to a production of abnormal proteins, termed neoantigens. These are processed and presented on the cell surface via the major histocompatibility complex (MHC) in a process known as antigen presentation and recognised by antigen presenting cells (APCs) such as DCs and macrophages. These cells internalize the neoantigen and deliver it to naïve T cells which reside within lymph nodes. The peptide-MHC complex (pMHC) on APCs is recognised by the naïve T cells which bind the pMHC via their T cell receptor (TCR) within an immunological synapse. When activated, the naïve T cells differentiate into CD8+ cytotoxic T cells which can destroy cancer cells directly and CD4+ Helper T cells which activate B cells and stimulate them to differentiate into memory cells and plasma cells and produce anti-tumour antibodies (Wachsmann et al., 2013). In addition to TCR stimulation, T cells require an additional signal known as the ‘co-stimulation’ signal to escape from anergy. Co-stimulatory signals are mostly delivered by the B7 family of molecules expressed on APCs (Greenwald et al., 2005). The most important co-stimulatory signal comes from CD80 on the APC which binds the CD28 receptor on the T cell and provides the required co-stimulation signal required for T cell activation. Together, these signals stimulate proliferation and rescue T cells from apoptosis (Chen and Flies, 2013).

Another member of the B7 family, B7 homolog 1 (B7-H1) (Ishida et al., 1992), was found to engage T cells during antigen presentation causing the secretion of IL-10 - an anti-inflammatory cytokine. It was therefore proposed that B7-H1 plays a role in the suppression of T cell effector functions. The corresponding receptor of B7-H1 on T cells was found to be PD1 and so B7-H1 is now also known as PD-L1. Other such negative regulatory signals exist including lymphocyte-activation gene 3 (LAG-3) and cytotoxic T-lymphocyte associated protein 4 (CTLA-4) and they have important roles in ensuring self-tolerance and providing protection against aggravated immune responses. The interplay between stimulatory and inhibitory signals determines the overall strength of the signal and thus the level of T-cell activation. A third signal is delivered by cytokines and regulates T cell differentiation and effector capacities. Activation of T cells leads to polarization of the Golgi and granule network and subsequent exocytosis of protease-filled granules. Pore-forming proteins assemble to form pore channels called perforins on the surface of the cancer cell. These channels allow entry of other proteases, most importantly granzymes which are serine proteases that trigger DNA fragmentation - an important

characteristic of apoptosis. T cells can also cause tumour death via the activation of the Fas surface receptor which leads to pro-apoptotic signalling (Ruddon, 2007).

At the molecular level, when the TCR recognises the pMHC a complex signalling pathway is initiated (Figure 1.3.1). It begins with the recruitment of Src-like tyrosine kinases such as LCK to the signalling complex which cause phosphorylation of intracellular chains of TCR and CD28 which recruits ZAP70 to CD3/TCR and PI3K to CD28. ZAP70 initiates multiple signalling events via phosphorylation of LAT - a membrane adaptor protein, which once phosphorylated binds multiple members of the GRB family of adaptor proteins such as GRB2 to facilitate the assembly of macromolecular signalling complexes which are necessary for efficient T cell activation. The recruited GRB2 together with SOS protein can now activate Ras (Okkenhaug and Vanhaesebroeck, 2003). This leads to the activation of the Raf and MEK kinases which ultimately activate the mitogen activated protein kinases (MAPKs) ERK1/2 (Huse, 2009) leading to activation of the Fos protein. The co-stimulatory interaction between CD80 and CD28 reinforces T cell activation signalling. The association of PI3K with the CD28 intracytoplasmic domain results in the production of PIP₃ (phosphatidylinositol [3,4,5]-triphosphate) which is required for AKT activation; this initiates the AKT-molecular target of rapamycin (mTOR) pathway and rescues T cells from anergy. It also stimulates the activation of rel/NF- κ B and Jun nuclear factors. Jun and Fos proteins form heterodimers, commonly referred to as AP-1 which is a transcription factor involved in the regulation of differentiation, proliferation and apoptosis. PLC γ 1 is also activated causing the release of Ca²⁺ ions from the endoplasmic reticulum and NFAT (Nuclear factor of activated T cells) which is required for the activation of the expression of PD-L1 (Oestreich et al.,2008). NFAT forms a protein complex with AP-1 during TCR activation and CD28 co-stimulation. The use of a NFAT-specific inhibitor significantly reduces PD1 expression, and the mutation of the NFATc1 consensus binding site causes complete loss of PD1 expression in T cells. Other transcription factors regulating PD1 include Foxo1, Notch and IRF9 (Bardhan, Anagnostou and Boussiotis, 2016). The outlined signalling events lead to reorganization of the cytoskeleton as well as transcriptional activation of multiple genes leading to T cell proliferation, differentiation and/or effector function.

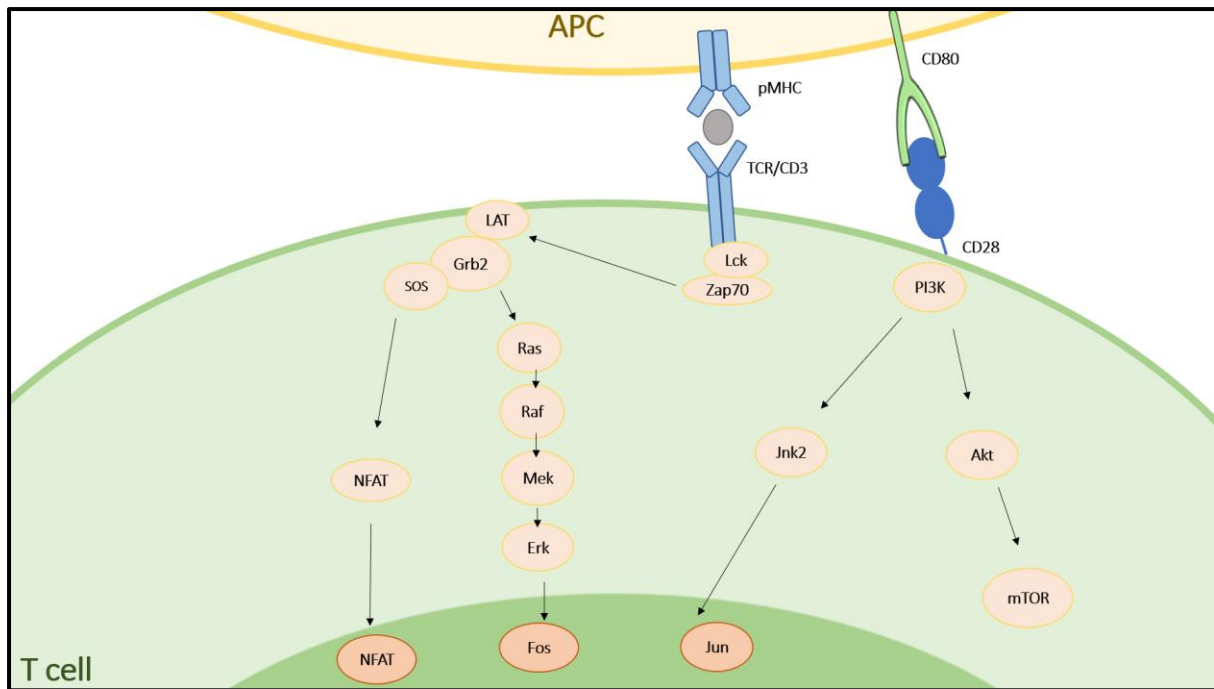


Figure 1.3.1. Signalling cascade in T cells resulting from T cell receptor (TCR) ligation with a peptide-bound major histocompatibility complex (pMHC), co-stimulated by the CD80 and CD28 interaction. TCR signalling recruits Lck which phosphorylates the TCR and recruits Zap70. Zap70 stimulates LAT which activates Grb2 and SOS leading to NFAT and Fos activation. PI3K is recruited to CD28 which initiates the Akt/mTOR signalling pathway and activates the Jun protein. Fos and Jun form a heterodimer in the nucleus called AP-1 which takes part in downstream signalling pathways to regulate proliferation, differentiation and T cell effector function. mTOR signalling also regulates growth and survival, motility and protein synthesis. NFAT activates PD1 expression on the surface of the T cell.

1.4. Immunosuppression in pancreatic cancer

The cancer immunoediting theory states that malignancies are either eliminated, reach equilibrium or achieve escape (Dunn et al, 2002). Eliminations occurs when effector immune system cells destroy early-stage genetically unstable cells. If the elimination event is unsuccessful the pancreatic cancer cells may enter a state of equilibrium where editing occurs. The immune system places a selective pressure on cancer cells and any cells with an acquired resistance to this elimination have an advantage. During this Darwinian selection, new pancreatic cancer variants emerge with novel mutations which can increase the overall resistance to immune attack. During the escape phase tumour cells continue proliferating excessively which may eventually lead to malignancies. Cancer cells reduce their immunogenicity through various different mechanisms. They may downregulate the expression of MHC class I molecules as well as the rate of neoantigen insertion into the MHC groove (Reeves and James, 2017). Both these actions decrease MHC presentation to T cells. A complete absence of MHC may result in full T cell evasion however it also leads to activation of NK cells which are normally inhibited by the

MHC (Kambayashi et al., 2001), therefore tumours must employ multiple mechanisms of tumour evasion. Tumours can start to secrete a variety of inhibitory cytokines and other small molecules to depress the immune system, such as TGF- β which suppresses NK and T-cell activation. Another method of immune evasion is the acquisition of mutations which switch on certain molecular pathways. Many tumours overexpress programmed death-ligand 1 (PD-L1) which, via binding to programmed death 1 (PD1) receptor on T cells contributes to strong inhibition in T cells. PD-L1 overexpression in tumours is often seen as an indicator of progression and poor prognosis in cancer (Escors et al., 2018).

Pancreatic cancer uses several tactics to effectively hide itself from the immune system, altering the immune microenvironment of the tumour in a unique way. Pancreatic cancer exist in an immune privileged environment and the proportion of inflammatory cells in murine pancreatic tumours was found to rise from 15.5% in normal pancreatic tissue to 50% in tumour tissue (Beatty et al., 2011). However, despite this influx of immune cells there is a drastic imbalance in the tumour infiltrate with a much higher population of pro-tumour cells than anti-tumour ones (Kunk et al., 2016). Populations such as regulatory T cells (Tregs), tumour-associated macrophages (TAMs), myeloid-derived suppressor cells (MDSCs), fibroblasts and mast cells are upregulated which ultimately protect tumour cells from being eliminated by the immune system and populations of anti-tumour immune cells such as NK cells, DCs and CD8+ T cells are downregulated (Kunk et al., 2016) Immune system defects such as this are present even in the early PanINs (Hiraoka et al., 2006) indicating that the immunosuppressive nature of TME could be a key driver of tumorigenesis. Tregs for example, induce tolerance against neoantigens and suppress tumour activity of T cells. Disruption of Tregs in murine models correlates with tumour growth inhibition (Tan et al., 2009). TAMs express a chemokine C-C motif receptor type 2 (CCR2) which mediates tumour proliferation, angiogenesis and chemotaxis of immune suppressive cells to the tumour stroma (Mitchem et al., 2013). MDSCs also exhibit specific pathways by which they inhibit the immune response and reducing these populations was found to cause tumour regression (Zhang et al., 2017). In order to develop an effective strategy against pancreatic cancer efforts should be focused on increasing the density of effector T-cells within the TME and inhibiting the immunosuppressive cells and receptors. Currently, much research is focused on the PD1 receptor due to the powerful inhibitory effects it has on immune responses.

1.5. The PD-1/PD-L1 signalling pathway

PD1 is the cognate receptor for PD-L1. It is a 288-amino acid type I transmembrane protein encoded by the PDCD1 gene in humans. It belongs to the B7 family of costimulatory molecules of antigen presentation. PD1 is absent on inactivated immune cells but becomes significantly upregulated after

activation of cells such as CD4⁺ and CD8⁺ T cells, B cells, monocytes, NK cells and DC cells (Agata et al., 1996). In naïve T cells PD1 expression is induced upon TCR activation and through cytokine receptors (Okazaki and Honjo, 2007). PD1 is composed of a single N-terminal immunoglobulin variable region (IgV)-like domain, a 20-amino acid stalk separating IgV from the plasma membrane, a transmembrane domain and a cytoplasmic tail which contains two tyrosine-based signalling motifs (Bardhan, Anagnostou and Boussiotis, 2016). Its expression is stimulated by the common γ chain cytokines interleukin-2 (IL-2), IL-7, IL-15 and IL-21 (Kinter et al., 2008). PD1 contains an immunoreceptor tyrosine-based inhibitory motif (ITIM) and an immunoreceptor tyrosine-based switch motif (ITSM) within its intracellular domain. ITIM is involved in the recruitment of SH2 domain -containing phosphatases and ITSM is necessary for the inhibitory function of PD1 (Neel et al., 2003).

The ligands of PD1 (PD-L1 and PD-L2) are type I transmembrane glycoproteins that adopt an immunoglobulin structure with an IgV distal region and an Ig constant (C) proximal region in its extracellular domain. They are anchored to the cell membrane via a hydrophobic transmembrane sequence followed by a short cytoplasmic region (Escors et al., 2018). PD-L2 expression is limited to professional APCs; it can be found on activated DCs, macrophages and bone marrow derived mast cells. PD-L1 is constitutively expressed on T and B cells, macrophages, DCs, mesenchymal stem cells (MSCs) and bone marrow-derived stem cells (Yamazaki et al., 2002) and widely expressed on non-hematopoietic cell lines such as lung cells, neurons, astrocytes, pancreatic islets or fibroblastic reticular cells. Additionally, PD-L1 is upregulated in many cell types, including cancer cells by several pro-inflammatory stimuli. In peripheral tissues, the immunosuppressive activity of PD1 is primarily mediated by PD-L1 interactions (Tsushima et al., 2007). Pro-inflammatory cytokines activate signalling cascades which cause transcription factor binding to the PD-L1 promoter. IFN- γ for example, activates the Janus kinase (JAK) and signal transducer and activator of transcription (STAT) pathway causing transcriptional activation of interferon regulatory factor 1 (IRF1) which binds to the PD-L1 promoter. TNF α and IFN- γ also activate the NF- κ B pathway which can transcriptionally activate PD-L1. Due to these pathways, high PD-L1 expression levels are associated with inflamed tissues. Up-regulation of PD-L1 can also be caused by epidermal growth factor receptor (EGFR) (Okita et al., 2017), hypoxia-inducible factor alpha (HIF-1 α) (Noman et al., 2014) and signalling pathways such as MAPK (Gong et al., 2011) and PI3K signalling pathway (Parsa et al., 2007).

Most crystallization studies of the PD1/PD-L1 complex report a 1:1 stoichiometry. Interestingly however, free PD-L1 was observed to form homodimers in several crystal structures, wherein the PD-L1 molecules form an asymmetrical unit (Lin et al., 2008; Chen et al., 2010). The dimeric binding of the PD-L1 molecules was found to create a rotating angle and occur via eight hydrogen bonds (Chen et al., 2010). Out of the known structures of B7 family, B7-1 forms a dimer in crystalline and solution state

(Ikemizu et al., 2000) and B7-2 exists as a dimer in CTLA-4/B7-2 complex but as a monomer in a free state (Zhang et al., 2003). It is therefore possible that the dimerization of PD-L1 is simply an evolutionary relic, however it may serve a functional purpose. The dimerization of the B7 members for example may be favoured on the T cell/APC interface as the two-dimensional arrangement of the molecules on the cell surface promotes oligomerization by decreasing the entropic penalty compared to when random distribution of individual B7 molecules (Zhang et al., 2003). These findings suggest that PD-L1 could be forming similar homodimers at the cell surface, however no experimental cell data exist to support the hypothesis as of yet. It is theorized that such a homodimer arrangement may not be possible due to the predicted glycosylation of the extracellular domains of PD-L1 which may create conformational clashes (Zak et al., 2015) however the dimerization theory cannot be ruled out and should be investigated further as it may provide a novel way of looking at binding of PD1 and PD-L1.

PD1 activation inhibits TCR-mediated signalling through dephosphorylation of proximal signalling molecules downstream of TCR (Figure 1.5.1). This impairs two important signalling cascades – the PI3K/Akt pathway and the Ras/Mek/Erk pathway, both of which are required to initiate T cell activation (Arasanz et al., 2017). Engagement of TCR causes the ITIM and ITSM motifs on the cytoplasmic tail of PD1 to become phosphorylated which leads to recruitment of SHP-1 and SHP-2 phosphatases to the intracellular domain (Chemnitz et al., 2004). TCR engagement with pMHC is sufficient for SHP recruitment, however PD1 must also be stimulated in order for T cell suppressive effects to occur. Upon PD1 stimulation, SHP begins to dephosphorylate the TCR signalling molecules – CD3, ZAP70 and PI3K kinases which results in downstream deactivation of their signalling targets. PD1 can also suppress T cell activation through indirect pathways by affecting T cell proliferation. The TCR signal causes an increase in CK2 kinase expression which phosphorylates the regulatory domain of PTEN which in turn decreases its phosphatase activity over PIP3 which is produced by PI3K. When PD1 is engaged, CK2 kinase expression is downregulated and PTEN can terminate the PI3K activities. This causes inhibition of the mTOR/Akt signalling pathway and results in T cells with lower proliferation and survival and higher proneness for apoptosis. SHP recruitment also causes activation of basic leucine transcription factor (BATF) which also impairs T cell proliferation and cytokine secretion (Quigley et al., 2010).

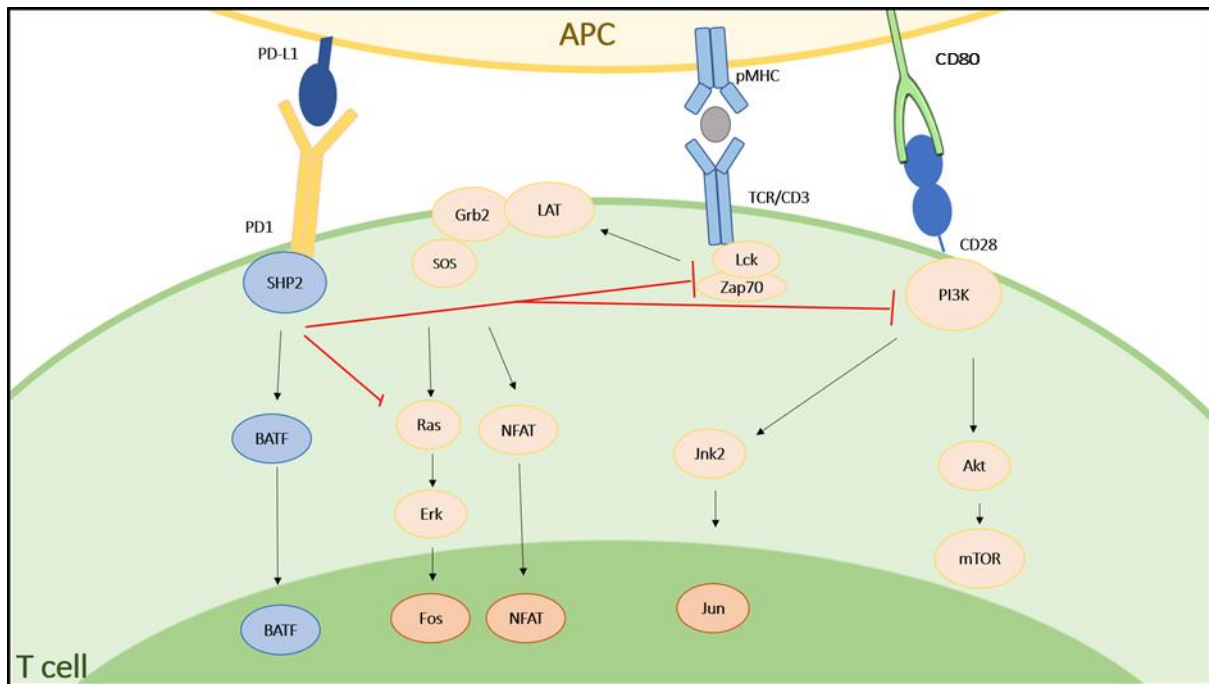


Figure 1.5.1. PD-L1/PD1 signalling causes dephosphorylation of downstream signalling molecules of T cell receptor (TCR) signalling thus inhibiting TCR signalling effects. PD1 activation recruits SHP2 which dephosphorylates Ras, Zap70 and PI3K, preventing their signalling pathways. This results in the inhibition of Akt/mTOR pathway and decreased production of Fos, NFAT and Jun transcription factors which activate genes involved in proliferation and cell survival. SHP2 also activates BATF which impairs T cell proliferation and cytokine secretion. Ultimately, PD1 signalling in T cells leads to an inhibition of their effector functions.

It has been observed that PD-L1 co-stimulation contributes to ligand-induced TCR down-modulation on CD8⁺ T cells (Karwacz et al., 2011). The details of this mechanism are not yet well-defined; however, most studies point to E3 ubiquitin ligases (especially CBL-B, c-CBL and ITCH) of the CBL family as the main mediators of this process. The CBL-B and ITCH E3 ubiquitin ligases have been shown to cause ubiquitination of CD3 and CD28 chains thus preventing their phosphorylation and association with the signalling kinases ZAP70 and PI3K (Fang and Liu, 2001). Interactions between PD1 and PD-L1 during dendritic cell presentation to T cells causes strong upregulation of CBL-b and c-CBL which contributes to antigen induced TCR down-modulation. It is very likely that this process also occurs in cancers. T cells that overexpress PD-L1 typically also have a low expression levels of surface TCR.

When T cells become activated, they undergo changes to their metabolism to cover the high energy requirements. Quiescent T cells generate energy by using glucose, fatty acids and amino acids to fuel oxidative phosphorylation. Once activated, they undergo metabolic reprogramming where oxidative phosphorylation still occurs, but aerobic glycolysis becomes the dominant form of metabolism. PD1 engagement causes a suppression of oxygen uptake and impairs the T cells ability to utilise glycolysis and instead promotes the use of fatty acids in beta-oxidation (Patsoukis et al., 2015). On top of this,

when T cells are stimulated during PD1 ligation, accumulation of polyunsaturated fatty acids occurs which are known to be suppressors of T-cell immunity. Therefore, another way PD1 may alter T-cell differentiation is by preventing T cells from appropriately remodelling their metabolism. As a result of these metabolic changes there is an increase in the T cell production of reactive oxygen species (ROS) derived from fatty acid oxidation (Tkachev et al., 2015). ROS is a harmful by-product of metabolism and is known to facilitate various harmful effects such as DNA damage. Therefore, the elevation of ROS and subsequent ROS-mediated DNA damage may be aiding cancer cells to acquire more mutations. Furthermore, ROS also have important roles in the regulation of the immune response during tumour development. More specifically, they greatly contribute to the inhibitory activities of tumour-induced immunosuppressive cells (Chen et al., 2016).

1.6. PD1/PD-L1 signalling in cancer

When T cells detect neoantigens presented by APCs, activation-induced regulatory receptors, including PD1 are expressed on their surface. TCR signalling on activated T cells leads to the production and secretion of inflammatory cytokines - the most potent of these being IFN- γ . Cytokines amplify the immune response attracting other immune system cells such as NKs and macrophages. They also lead to the expression of immunosuppressive factors including PD-L1 on stromal cells in the cancer microenvironment and immune system cells such as macrophages and myeloid suppressor cells (Spranger et al., 2013). This is an adaptive process which exists to limit immune and inflammatory responses. However, this process can cause PD-L1 upregulation in cancer cells too, in a process termed 'adaptive immune resistance' (Figure 1.6.1). In order for cancer cells to upregulate PD-L1 expression on their surface, a mutational event must first occur which changes cell-intrinsic mechanisms and results in altered activation of signalling pathways. The expression of PD-L1 on tumour cells can be facilitated via several mechanisms. Abnormalities in signalling pathways caused by oncogenic events such as activation of EGFR, MAPK or PI3K-Akt pathways and elevated STAT3 expression can upregulate PD-L1 expression in various cancers via transcriptional or post-translational mechanisms (Boussiotis, 2016). Amplifications of chromosome 9p24.1 cause increased gene dosage of PD-L1 and PD-L2 together with JAK2 in nodular sclerosing Hodgkin's lymphoma and primary mediastinal large B-cell lymphoma (Green et al., 2010). Recent studies also indicate that PD-L1 upregulation could be induced by radiotherapy; irradiation increased PD-L1 expression on tumour cells and myeloid-derived tumour suppressor cells (MDSC) and therefore suppressed radiation-induced immune responses (Deng et al., 2014). The occurrence of these mutations and expression of PD-L1 by cancer cells interferes with TCR signalling on T cells and effectively protects the cancer cell from detection by the host's immune system.

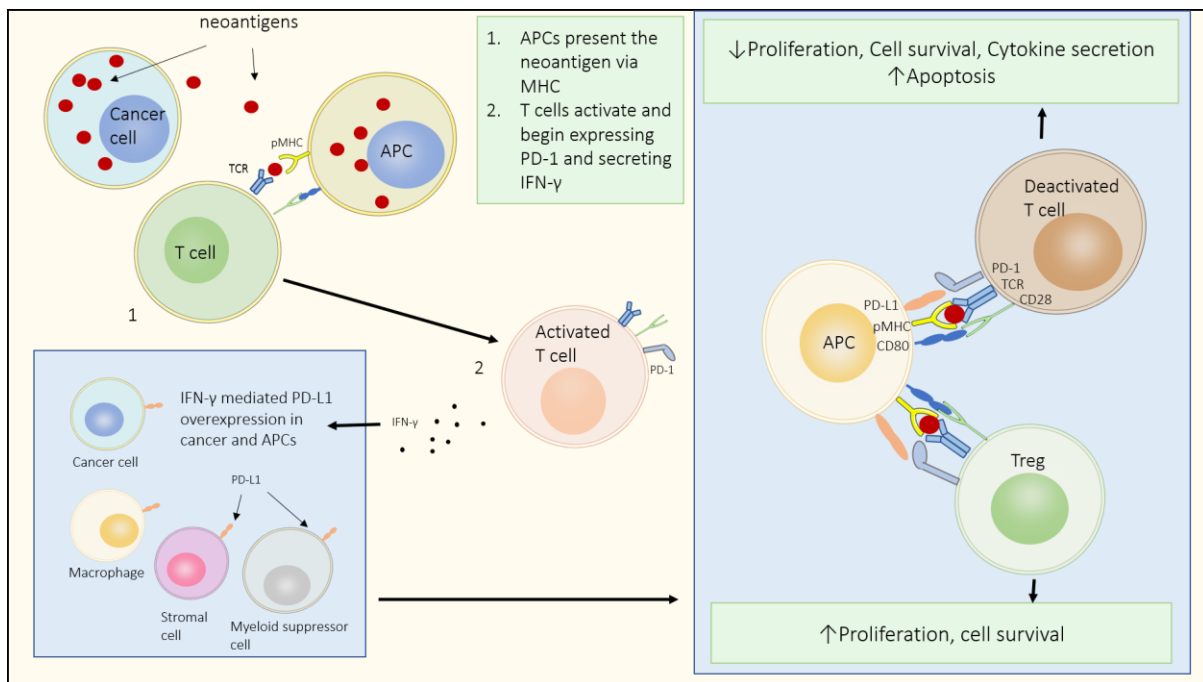


Figure 1.6.1. Adaptive immune resistance in cancer. Cancer cells produce neoantigens which are presented by antigen presenting cells (APC) via their major histocompatibility complex (MHC). T cells recognise the neoantigen with their T cell receptor (TCR) which leads to T cell activation. Activated T cells begin to express PD1 and secrete IFN- γ . IFN- γ induces PD1 ligand (PD-L1) expression in cancer cells, stromal cells and immune system cells such as macrophages and myeloid suppressor cells. Stimulation of PD1 on T cells causes inhibition of TCR signalling and leads to lower proliferation, cell survival and cytokine secretion and higher levels of apoptosis. On regulatory T cells (Tregs) which are immunosuppressive and inhibit T cell effector functions, PD1 signalling causes increased proliferation and cell survival. Both of these effects lead to increased immunosuppression in the tumour microenvironment and create a permissive environment for tumour immune evasion.

The expression of PD-L1 in the tumour and surrounding cell types causes inhibition of T cell functions which clearly aids cancer progression by allowing tumour immune escape. On top of this recent research implies that PD1/PD-L1 may also have regulatory functions in Tregs and since Tregs are immunosuppressive by nature, their aggregation in PD-L1 positive cancers exacerbates the already highly immunosuppressive cancer microenvironment. The involvement of the PD1/PD-1 pathway in Tregs has not been fully clarified yet, however it has been demonstrated that PD-L1 can induce Treg development *in vitro* and enhance their immunosuppressive functions. PD-L1 has been observed to convert naïve CD4⁺ T cells to Tregs via downregulation of Akt, mTOR and ERK2 and simultaneous upregulation of PTEN (Francisco et al., 2009). Another study evaluated Tregs in Melanoma patients receiving anti-PD1 therapy and reported that in responding patients Tregs exhibited decreased inhibitory activities (Woods et al., 2018). This suggests that PD1/PD-L1 inhibitors may exert their effects on Tregs as well as T cells and provide an alternative pathway of decreasing immunosuppression within

the TME. These findings indicate that anti-PD1/PDL1 therapy could be very beneficial in pancreatic cancer which has high population of Tregs.

1.7. Targeting the PD1/PD-L1 signalling pathway in cancer

Blocking PD1/PD-L1 interactions has been shown to be a very promising therapeutic strategy for PD-L1 positive cancers, and there are already several anti-PD1/PD-L1 therapies available for clinical use. Many studies have shown that systemic administration of PD-L1/PD1 blocking antibodies results in improved anti-tumour capacities of T cells (Hirano et al., 2005). Since 2012, PD-L1/PD1 blockade therapies have proven effective in the treatment of several human cancers. The first anti-PD-L1/PD1 agents to be approved by the FDA were Pembrolizumab and nivolumab - human monoclonal antibodies (mAbs) which target the PD1 receptor and prevent PD-L1/PD-L2 binding. Since then, other PD-L1/PD1 blocking mAbs have been approved for clinical use, including: atezolizumab, durvalumab and avelumab (Arasanz et al., 2017), which target PD-L1. PD1/PD-L1 checkpoint inhibitors have now been approved for the treatment of nine malignancies ranging from classical Hodgkin lymphoma to head and neck squamous cell carcinoma (HNSCC) (Balar and Weber, 2017) and significantly improved the survival of patients. Targeting PD1 has been especially effective in the treatment of advanced melanoma. With the use of checkpoint inhibitor therapies such as this one, the survival rates of melanoma patients have drastically improved over the past decade (Luke et al., 2017).

Despite the effectiveness in certain cancers, anti-PD1/PD-L1 therapy has not been successful in the context of pancreatic cancer. Until recently the poor effectiveness of anti-PD1/PD-L1 mAbs therapy in pancreatic cancer was accredited to a low expression of PD-L1 in this cancer. However, analysis of PD-L1 mRNA expression in 453 clinical pancreatic cancer samples revealed that PD-L1 expression was upregulated in 19% of the analysed pancreatic cancer cases. (Birnbaum et al., 2016). PD-L1 upregulated cancers displayed a profile of T cell exhaustion and were enriched in inhibitory molecules with pro-tumour populations present – Tregs and MDSCs. Anti-PD1/PD-L1 therapy therefore has the potential to be an effective way of treating PD-L1 positive pancreatic cancers. Anti-PD1/PD-L1 therapy would reactivate the exhausted T cells in the TME and may decrease the inhibitory activities of Tregs. As the frequency of CD8+ T cells in pancreatic cancer is fairly low, to optimize clinical outcomes this therapy should be combined with a treatment which increases T cell infiltration to tumours. For example, targeting tumours with tumour necrosis factor superfamily member 14 (TNFSF14) activates lymphotoxin β -receptor signalling causing a production of chemokines which recruit significant amounts of T cells, creating a T-cell-inflamed microenvironment in previously non-T cell-inflamed tumour tissues (Tang et al., 2017). This method of targeting tumours increases their responses to

checkpoint blockades and could significantly improve clinical outcomes of anti-PD1/PD-L1 therapy in pancreatic cancer.

However, the nature of pancreatic cancer makes drug delivery rather difficult. In contrast to many tumours that are dependent on neo-angiogenesis, pancreatic cancer is poorly vascularised in comparison to normal tissue (Olive et al, 2009). The lack of adequate vasculature causes poor perfusion and limits the delivery of therapeutic agents from the blood vessel into the TME. Since mAbs are administered intra-venously this poor vascularization in pancreatic cancer provides a major challenge for drug tumour entry. On top of this, mAbs have inherently poor tissue and tumour penetrance – in murine xenograft models, mAbs directed against tumour-specific antigens largely remained in the blood with only up to 20% of the administered dose reaching the tumour (Beckman et al., 2007). In pancreatic cancer the dense stromal barrier further restricts the ability of mAbs to enter the tumour site. Aside from these points, mAbs have other problems associated with their use. Due to their large size, antibodies diffuse poorly making them much less effective in the treatment of large tumours (Chen et al., 2019). The 'binding site barrier effect' is another limitation of mAbs, where high-affinity antibodies bind tightly to the first antigen they encounter - that is at the periphery of the tumour (Chames et al., 2009). They will not penetrate deeper within the tumour until the antigens on the periphery are saturated. Further limitation are the Fc effects of antibodies which lead to depletion of effector T cells.

Instead of a blocking antibody a soluble PD1 extracellular domain could be utilised as a competitive inhibitor, counteracting some of the limitation of mAbs. This molecule would be much smaller in size and would likely be much more effective in penetrating into the tumour site. The wild-type PD1 ectodomain does not have a strong binding affinity for PD-L1 and so may not be the best candidate for competitive inhibition in a therapeutic setting.

1.8. Increasing binding affinity of proteins

Protein binding affinity describes the strength of the binding interaction between a single biomolecule and its ligand. In a basic reversible bimolecular binding reaction, molecule A binds to molecule B - forming a complex. The strength of the interaction between two molecules is measured by the rate of the dissociation of the complex – the dissociation constant (K_D) (Pollard, 2010). The smaller the K_D value the greater the binding affinity between the ligand and its target. Binding affinity is influenced by non-covalent intermolecular forces such as hydrophobic and Van der Waals forces between the molecules, and the presence of other molecules. In this study we seek to enhance the affinity of the PD1 protein and generate mutants with increased binding characteristics to PD-L1 in order to antagonize the PD1/PD-L1.

Traditionally, design of high-affinity proteins was done experimentally, in a time-consuming and costly process. The newly developed computational methods have greatly reduced the time and cost of novel drug development. The most widely used computational method in drug design is docking and scoring which is an efficient method, however it is not the most accurate. It can predict binding modes of proteins and can discriminate between ones that will bind and ones that do not, however it cannot discriminate between drugs that differ by less than one order of magnitude in affinity (Genheden and Ryde, 2015). The alchemical perturbation method is another type of molecular modelling which is derived from statistical mechanics and is very accurate. However, it requires extensive sampling of the complex, the free ligand in solution as well as of the intermediate states. This makes the process quite computationally extensive (Genheden and Ryde, 2015). In between these modelling types lies a method of intermediate performance which samples just the complex and the free receptor and ligand molecules. The molecular modelling method to develop the high-affinity PD1 variants is of this intermediate sub-type, called Molecular Mechanics/Poisson Boltzmann Surface Area (MM/PBSA). In this method the free energy of the binding of ligand to receptor is estimated considering the bonded, electrostatic, van der Waals interactions and polar and non-polar contributions.

The MM/PBSA method was used to design PD1 variant proteins in an attempt to increase binding affinity. The variants were designed previously in collaboration with Professor Chris Reynolds and Dr Kevin Smith as part of a Pancreatic Cancer Research UK pilot project and analysed in the present study.

1.9. Mesenchymal stem cells as drug delivery vectors

The high-affinity sPD1 protein alone will not be able to penetrate the pancreatic stroma and reach the tumour site; it will require a delivery vector to do so. Mesenchymal stem cells (MSCs) have emerged as promising delivery vectors for the delivery of antitumor agents due to their incredible tendency to migrate towards sites of inflammation – such as tumours. These migratory properties have the potential to serve as drug-delivery vectors to deliver effective, targeted therapy to tumours (Gao et al., 2007). MSCs are heterogenous group of progenitor cells and play important roles in tissue regeneration. They are characterised by the expression (CD73, CD90, CD105) and lack of (CD34, CD45, CD19 CD11b, HLA-DR) haemopoietic cell markers on their surface. Additionally, they adhere to plastic in culture and have the ability to differentiate into osteoblasts, adipocytes and chondroblasts *in vitro* (Rojewski et al., 2008). It has been shown that MSCs are actively attracted to hepatic carcinoma, breast cancer and pre-metastatic niches (Xie et al., 2017; Ma et al., 2015; Arvelo et al., 2016). This tumour tropism is part of the normal tissue repair mechanism where MSCs are recruited to sites of tissue injury and inflammation. Tumour migration is thought to occur via a chemo-gradient where MSCs travel towards

inflammatory signals (Son et al, 2006) and the migration is regulated by various cytokines (such as VEGF, PDGF, HGF, HMGB1) (Eliopoulos et al., 2008).

Due to these features, MSCs have been genetically modified in many studies to express peptides and protein with anti-tumour properties. The first such application of MSCs in targeted cancer therapy was a delivery of IFN- β which successfully inhibited the growth of malignant cells (Studený et al., 2002). The study found that the tumour microenvironment preferentially promotes engraftment of MSCs compared to other tissues and the MSCs successfully produced biological agents in mouse tumour models. Significant anti-cancer effects against tumours of brain, ovary, liver kidney and pancreas were observed with MSCs genetically engineered to express suicidal genes (thymidine kinase, cytosine deaminase, carboxylesterase) (Song et al., 2011; Yin et al., 2011). Several anticancer therapies using MSCs are in various stages of clinical development such as MSCs modified to express TNF-related apoptosis -inducing ligand (TRAIL) and induce cell death of tumours (Cheng et al., 2019). These studies show supporting evidence that the use of MSCs to deliver therapeutics to pancreatic cancer will be effective.

1.10. Aims and hypotheses

The computationally-designed PD1 variants will be designed as soluble proteins (sPD1) and their binding properties to PD-L1 analysed. The variant with the strongest binding affinity will be selected and engineered into mesenchymal stem cells (MSCs) for expression. The hypothesis is that the MSCs containing the sPD1 – termed MSC.sPD1 – will travel to the inflamed pancreas via a chemokine gradient. The MSC.sPD1 will then secrete sPD1 into the TME. sPD1 will strongly bind to PD-L1 on cancer cells, T cells as well as the surrounding cells in the TME and will outcompete the binding of PD1 on T cells. This will block the PD1/PD-L1 -mediated inhibition of TCR signalling and will allow cytotoxic T cells to respond to neoantigens once more (Figure 1.10.1). Additionally, it may disrupt PD1 signalling on Tregs and inhibit their immunosuppressive functions. Altogether these effects will allow the immune system cells to begin destroying the tumour again.

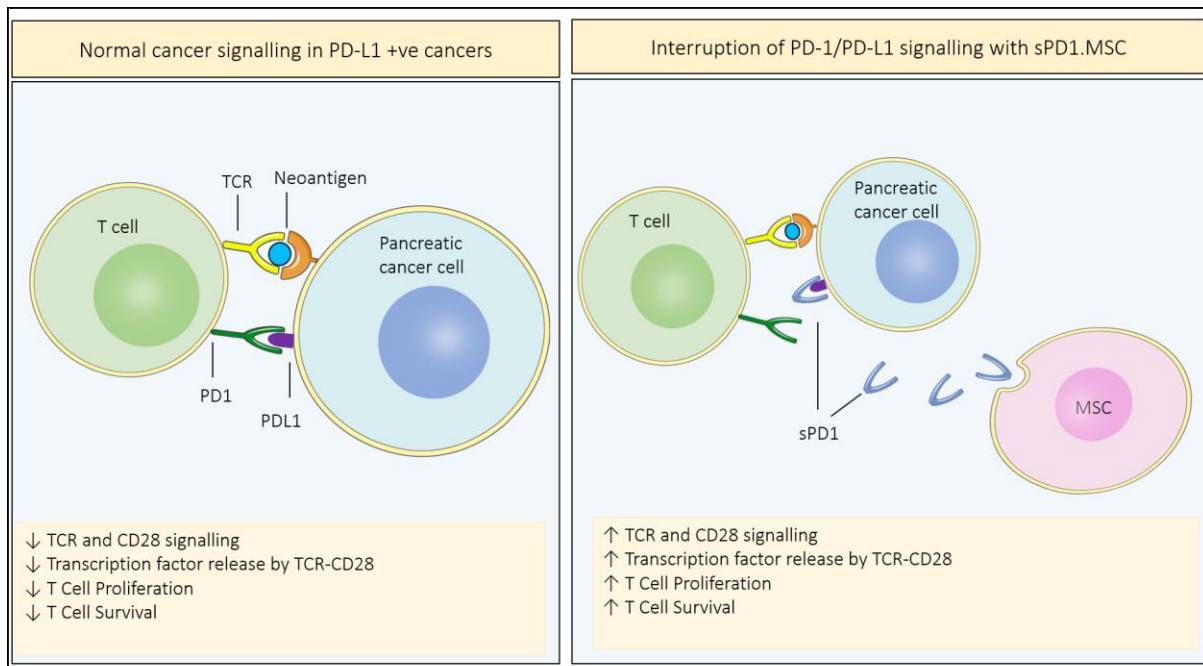


Figure 1.10.1. Interruption of PD1/PD-L1 signalling with mesenchymal stem cells which secrete soluble PD1 (sPD1.MSC). When pancreatic cancer cells begin expressing PD-L1 on their surface it interacts with PD1 on T cells and inhibits T cell and CD28 co-receptor signalling and prevents the activation of transcription factors which would go on to activate genes regulating proliferation and T cell effector functions. This is a method of cancer immune evasion and allows pancreatic cancer to escape immune-mediated death. Introduction of sPD1.MSC would bind to PD-L1 on the cancer and prevent it from interacting with the PD1 on T cells. This would reactivate TCR and CD28 signalling allow the T cell to carry out its effector functions and destroy cancer cells.

Methods

2.1. Generation of the pcDNA.sPD1^{WT}

The sPD1^{WT} fragment was synthesised by an external manufacturer (DC Bioscience, Dundee). It was then amplified with a PCR reaction. The sPD1^{WT} fragment was cloned into the pGEM T-Easy vector, which was obtained from Promega Systems (Catalog no #A1360) with T4 ligase to generate a pGEM.sPD1^{WT} construct. The ligation reaction was transfected into competent Top10 *E. Coli* cells and grown in LB agar supplemented with Ampicillin, X-Gal and IPTG to allow selection of positive bacterial clones. A positive colony was picked and further cultured in LB media. The pGEM.sPD1^{WT} plasmid construct was then isolated with the miniprep technique. pGEM.sPD1^{WT} was digested with EcoRI and NotI restriction enzymes and cloned into the pcDNA3 plasmid vector which was obtained from ThermoFisher Scientific (Catalog no #V790200). This resulted in a final pcDNA.sPD1^{WT} construct.

2.2. – Generation of variants with higher binding affinities

To generate the MM/PBSA variants, site directed mutagenesis on pcDNA.sPD1^{WT} was conducted. A PCR reaction was performed using primers which contained the desired mutations to generate sPD1¹, sPD1²⁷ and fragments with introduced point mutations. The cloning procedure described in section 2.1 was then performed to produce the pcDNA.sPD1¹ and pcDNA.sPD1²⁷ and constructs.

2.3. Generation of the sPD1.pFUSE constructs

The pFUSE-hlgG1-Fc vector was obtained from InvivoGen (Catalog no #pfuse-hg1fc1).

The sPD1 fragment was amplified from the pcDNA.sPD1 expression constructs by using primers with EcoRI and BglII restriction sites. The sPD1 DNA fragment was separated from the pcDNA3 vector via gel electrophoresis, purified and isolated using the miniprep procedure. The sPD1 fragment was then cloned into pFUSE-hlgG1-Fc at the EcoRI and BglII restriction sites with T4 ligase. The ligation reaction was transformed into competent *E. Coli* cells and expanded in liquid culture for isolation by midi prep (Section 2.7).

2.4. Agarose Gel Electrophoresis parameters

The QuickLoad® Purple 1Kb Plus DNA Ladder was purchased from New England BioLabs (Catalog no #N0550S).

DNA was mixed with Sybrgreen and Loading Buffer. Components of different sample types are shown below (Table 2.4.1). Samples were tested on 1% agarose gel in 1X TAE buffer [100 V, 40 mins]. All samples were loaded on gel with a DNA Ladder.

Table 2.4.1. Components of samples used during gel electrophoresis with the volumes shown.

Sample type	DNA	Sybrgreen	Loading Buffer
PCR sample	Whole PCR sample	5 µl	5 µl
DNA for Analytical Digest	10 µl	5 µl	5 µl
DNA for Extraction Digest	20 µl	5 µl	5 µl
DNA Ladder	1 µl	5 µl	5 µl

2.5. DNA gel extraction

DNA was purified from the gel using Sigma-Aldrich GenElute Gel Extraction Kit (Catalog no #NA111) following the manufacturer's instructions. The DNA concentration was tested with a Nanodrop reader.

2.6. Plasmid Miniprep

Minipreps were done using the GenElute Sigma-Aldrich Plasmid Miniprep Kit (Catalog no #PLN10), following the manufacturers guidelines. 1.5 mL of overnight cell cultures was used. The concentration of eluted DNA was measured using a nanodrop.

2.7. DNA Plasmid Midiprep

The Midiprep procedure was done using the NucleoBond® Xtra Midi Kit. For details on *E. Coli* cell culture guidelines, refer to section 2.8.

A 100 mL of overnight *E. Coli* cell culture was centrifuged [4,500 g, 10 mins]. The pellet was resuspended in 8 mL Resuspension Buffer and treated with Lysis Buffer [5 mins] and neutralized with Neutralization Buffer [8 mL]. The NucleoBond® Xtra Column was treated with Equilibration Buffer [12 mL] and loaded with the cell lysate. Equilibration Buffer [5 mL] was used to wash the column and the filter was discarded. The column was then washed with Wash Buffer [8 mL]. Room temperature isopropanol [3.5 mL] was added into a fresh collection tube into which the plasmid DNA was eluted into using Elution Buffer [5 mL]. The DNA plasmid elute was concentrated with a NucleoBond Finalizer. The plunger was

removed from a 30 mL syringe and a NucleoBond finalizer was attached to the outlet. The previously collected elute was then added to the syringe and the plunger was reinserted, and the mixture was slowly pressed through the NucleoBond Finalizer and the flow-through discarded. 70% ethanol [2 mL] was slowly pressed through the NucleoBond Finalizer and the flow-through was discarded. The NucleoBond Finalizer was dried until no ethanol was present. The NucleoBond Finalizer was then attached to a 1 mL syringe outlet and Redissolving Buffer TRIS [400 µl of] was added to the syringe and the plasmid DNA was slowly eluted into a collection tube.

2.8. *E. Coli* culture conditions

The transformation reaction is mixed with 300 µl of LB medium and cultured for 1 hour at 37°C. The cells were then grown on LB agar plates overnight [37°C]. For sPD1.pGEM selection and expansion, the agar was supplemented with 100 µg/mL Ampicillin, 40 µg/mL of X-Gal and 1 mM IPTG. For sPD1.pcDNA construct expansion the agar was supplemented with 100 µg/mL Ampicillin only. To expand sPD1.pFUSE constructs, LB agar was supplanted with 250 µg / mL Zeocin.

For miniprep isolation (Section 2.6) of recombinant plastic vectors, a positive colony was grown in 5 mL of LB supplemented with 100 µg /mL Ampicillin or 250 µg / mL Zeocin for pcDNA3 and pFUSE T-Easy vectors respectively and cultured overnight [37°C, 300 rpm].

For midiprep isolation (section 2.7) of recombinant plasmid vectors, a single transformed colony was picked from a freshly streaked agar plate and placed in 3 mL of LB medium supplemented with 100 µg/mL Ampicillin or 250 µg / mL Zeocin for the pcDNA3 and pFUSE respectively, and grown while shaken [8 hours, 37°C, 300 rpm]. 100 µl of this culture was placed in 100 mL of LB medium supplemented with the antibiotic of choice and grown overnight [37°C, 300 rpm].

2.9. CHO cell Culture

All cell culture was undertaken in a microbiological safety cabinet using aseptic techniques to ensure sterility. Chinese Hamster Ovary (CHO) cells were maintained in DMEM media, supplemented with 10% Foetal Bovine Serum (FBS).

2.10. CHO cell transfection

CHO cells cultured at 70% density were transfected. A mixture of 3 µg pcDNA.sPD1 DNA, FuGene at a 3:1 ratio of FuGene to DNA and 100 µl serum-free media was added to each well of a 6-well plate. The mixture was added in a drop-wise manner at various spots in each well. The cells were incubated for 2 days at 37°C and the supernatant was collected, aliquoted and stored at -20°C.

2.11. ELISA

ELISA tests were carried out using a standard R&D system® Elisa Kit according to the manufacturer's instructions. The antibodies used were also obtained from R&D Systems – Human PD-1 Antibody (Catalog no #AF1086) for the capture antibody, Human PD-1 biotinylated antibody (Catalog no #BAF1086) for the detection antibody and Recombinant Human PD-1 Fc Chimera Protein (Catalog no #1086-PD) for the standard PD-1 sample. The PD-1 capture and detection antibodies were both used at the concentration of 5.6 µl/mL, diluted in blocking buffer (1% BSA in PBS). The wash buffer used was 0.05% Tween in PBS. Sample absorbance was read at 450 nm in a BMG Labtech Clariostar fluorophotometer.

2.12. Solid-phase protein competition assay

The biotin-labelled PD1 Fc-fusion protein was obtained from BPS bioscience (Catalog no #1109). Recombinant human PD-L1 Fc-chimera protein was obtained from R&D systems (Catalog no #156-B7-100). Streptavidin-HRP and the Colour Development solution was obtained from R&D system® Elisa Kit. The Wash Buffer used is 0.05% Tween in PBS. The Blocking Buffer is 1% BSA in PBS.

Wells in a 96-micro well plate were coated with 50 µl of PD-L1 at a concentration of 2 µg/µl. The microplate was incubated at overnight [4°C]. PD-L1 was aspirated and Wash Buffer [100 µl] was added to the wells and removed; this step was repeated three times. The plate was patted against a paper towel until dry. Wells were then treated with blocking buffer [100 µl] and incubated at room temperature [1 hour]. The test samples consisted of CHO supernatant with 50 or 20 ng of the sPD1 variant of interest and an equivalent amount biotin-labelled PD1 (unless stated otherwise) and adjusted with PBS to make a final sample volume of 50 µl. Samples were incubated at room temperature [2 hours]. The wash procedure was repeated, and the wells were blocked with Blocking Buffer [100 µl] and incubated [10 mins] and washed again. 100 µl of streptavidin-HRP was added at the working concentration and incubated at room temperature [20 min], while shielded from direct light. The wash procedure was repeated, and wells were treated with Blocking Buffer [100 µl]. Next, tetramethylbenzidine was added - the colorogenic substrate, and incubated at room temperature for 3 minutes. The reaction was stopped with 50 µl 1M Phosphoric acid. The absorbance was recorded at 450 nm using BMG Labtech Clariostar microplate reader.

2.13. Unspecific Binding Testing

Recombinant human PD-L1 (Catalog no #9049-B7-100) and PDL-2 (Catalog no #9075-PL-100) His-tag proteins were obtained from R&D Systems. Human PD-1 biotinylated antibody (Catalog no #BAF1086) was also obtained from R&D Systems. The Wash Buffer used is 0.05% Tween in PBS. The Blocking Buffer is 1% BSA in PBS.

Wells in a 96-well microplate were coated with 100 μ l of His-PD-L1, His-PD-L2 and His-GST suspended in PBS at a concentration of 2 μ g/ μ l. The microplate was incubated overnight [4°C]. The wells were then aspirated and washed three times with Wash Buffer [400 μ l], dried by blotting against a paper towel. Wells were then blocked with Blocking buffer [400 μ l] at room temperature [1 hour]. Test samples consisted of CHO supernatant containing 20 and 50 ng of sPD1 diluted in PBS with a total sample volume of 100 μ l. The samples were added to appropriate wells alongside a negative control sample without sPD1-containing supernatant present. Samples were incubated at room temperature [2 hours]. The washing procedure was repeated. Wells were then incubated with the anti-PD1, biotinylated antibody which was diluted with PBS to the working at the concentration of 5.6 μ L/mL. The wells were aspirated and washed and coated with streptavidin-HRP [100 μ l] at a 1:40 dilution ratio., and incubated at room temperature [20 mins], while shielded from light. The wash procedure was repeated, and wells were treated with the Colour Development solution [100 μ l] and incubated at room temperature [20 mins]. The reaction was stopped with 100 μ l of the stop solution (1M HCL) and the sample absorbance was read at 450 nm in a Clariostar microplate reader.

2.14. Surface staining and FACS analysis

The human PD-L1 PE-conjugated antibody (Catalog no #FAB1561P) and the mouse IgG1 PE-conjugate antibody (Catalog no #IC002P) were both purchased from RnD Systems. Biotin -labelled PD1, obtained from BPS Bioscience (Catalog no #711090). The streptavidin-PE conjugate was obtained from ThermoFisher Scientific (Catalog no #12-4317-87).

PancTul cells were treated with IFN- γ to induce surface PD-L1 expression. The growth medium was transferred into a universal tube and the cells were washed with 2.5 mL of PBS. 2 mL of Trypsin was added, and the cells were incubated until they detached from the membrane and transferred into the universal tube containing the growth medium. The cell suspension was adjusted to a concentration of 2×10^6 cells/mL in ice cold PBS. A haemocytometer was used to count the cells and 2×10^6 cells were used for the assay. Each cell sample was centrifuged [5000 xg, 1 minute] and the supernatant was discarded.

PancTul cells were treated with the PD-L1 PE-conjugated antibody. To test for background staining a mouse IgG1 PE-conjugate antibody was used. PancTul were treated with 1 μ l of the appropriate

antibody and incubated for 20 mins [4°C]. The cells were then washed with 1 mL PBS, centrifuged [5000 xg, 1 min] and the supernatant was discarded. Next, 50 µl of PBS was added to the cells and gently mixed and the signal was measured using BD Acuri C6 flow cytometer.

To test sPD1 variant competition, CHO supernatant containing 50 ng of sPD1 protein was added to the sample with 50 ng of Biotin -labelled PD1 and incubated [4°C, 20 min]. The sample volume was adjusted to 50 µl with PBS. Each sample was then washed with 1 mL of PBS, centrifuged [5000 xg, 1 min] and the supernatant was discarded. 1 µl of Streptavidin-PE conjugate was added to the samples, adjusted with PBS to make a 50 µl total reaction volume and incubated [4°C, 20 min]. The washing, centrifugation and supernatant removal steps were repeated and then 50 µl of PBS was added to the cells and gently mixed and the signal was measured using BD Acuri C6 flow cytometer.

2.15. Adenoviral vector generation for sPD1 expression

To generate an adenoviral expression vector for sPD1, the pAd/CMV/V5-DEST vector was used, obtained from Invitrogen (Catalog no #V493-20).

First, an LR recombinant reaction between pFUSE.sPD1^{HAC} and the pAd/CMV/V5-DEST vector was set up. The components of each reaction (Table 2.15.1) were added to a 0.5 ml microcentrifuge at room temperature and mixed. To include a negative control, a separate reaction was set up which will not contain LR Clonase II enzyme mix.

Table 2.15.1. Sample components of the LR recombinant reaction between pFUSE.sPD1^{HAC} and pAd/CMV/V5-DEST vector

Component	Sample	Positive Control
pFUSE.sPD1 ^{HAC} (50-150 ng / reaction)	1-7 µl	-
PETR-gus (50 ng/ µl)	-	2 µl
pAd/CMV/V5-DEST vector	2 µl	2 µl
TE Buffer, pH 8.0	To 8 µl	4 µl

Next, 2 µl of the LR Clonase®II enzyme mix was added to each sample excluding the negative control, mixed well and incubated at 25°C overnight. 1 µl of Proteinase K solution was added to each reaction and incubated for 10 mins at 37°C. Next, competent Top10 *E. Coli* cells were transformed with 3 µl of the LR recombination reaction. Positive clones were cultured with ampicillin. The recombinant vector was isolated and purified using the miniprep procedure (section 2.6).

The adenovirus-containing cells and media were harvested into a sterile tube and the adenoviral stock was amplified following Life Technologies' ViralPower Adenoviral Expression System guidelines.

2.16. Mesenchymal stem cell transduction

The MSCs used in this study were bone-marrow derived. They were cultured in complete StemMACS™ culture media from Miltenyi Biotec (Catalog no #130-104-182). On the day of the transduction the cell culture medium was removed from the cells and a MOI of 500 of freshly thawed adenoviral stock was added to each well. The plate was incubated overnight [at 37°C]. The following day the virus-containing medium was removed and replaced with fresh, complete culture medium. The cells were then grown for 2 days and the supernatant was harvested and tested using ELISA for successful protein expression.

Results

3.1. Designing a soluble PD1 DNA construct

In order to generate a soluble version of the PD1 protein, the wild-type PD1 protein sequence was retrieved first. The PD1 sequence was modified to exclude the cytoplasmic and transmembrane domains. The location of the extracellular domain of PD1 is 109 nt – 558 nt; a visual representation of the linear structure of PD1 and the extracellular domain position is shown in Figure 3.1.1. To enable sPD1 protein secretion an exogenous signal peptide was added to the N-terminus of the protein – this sequence directs the protein to the endoplasmic reticulum and tags it for eventual extracellular secretion. The signal peptide was derived from the human fibrillin gene. A Furin protease cleavage site was also introduced to facilitate the removal of the localisation peptide thus producing a mature wild-type sPD1 protein – termed sPD1^{WT}. This method of generating soluble protein variants has achieved success in other studies (Yu et al., 2013).

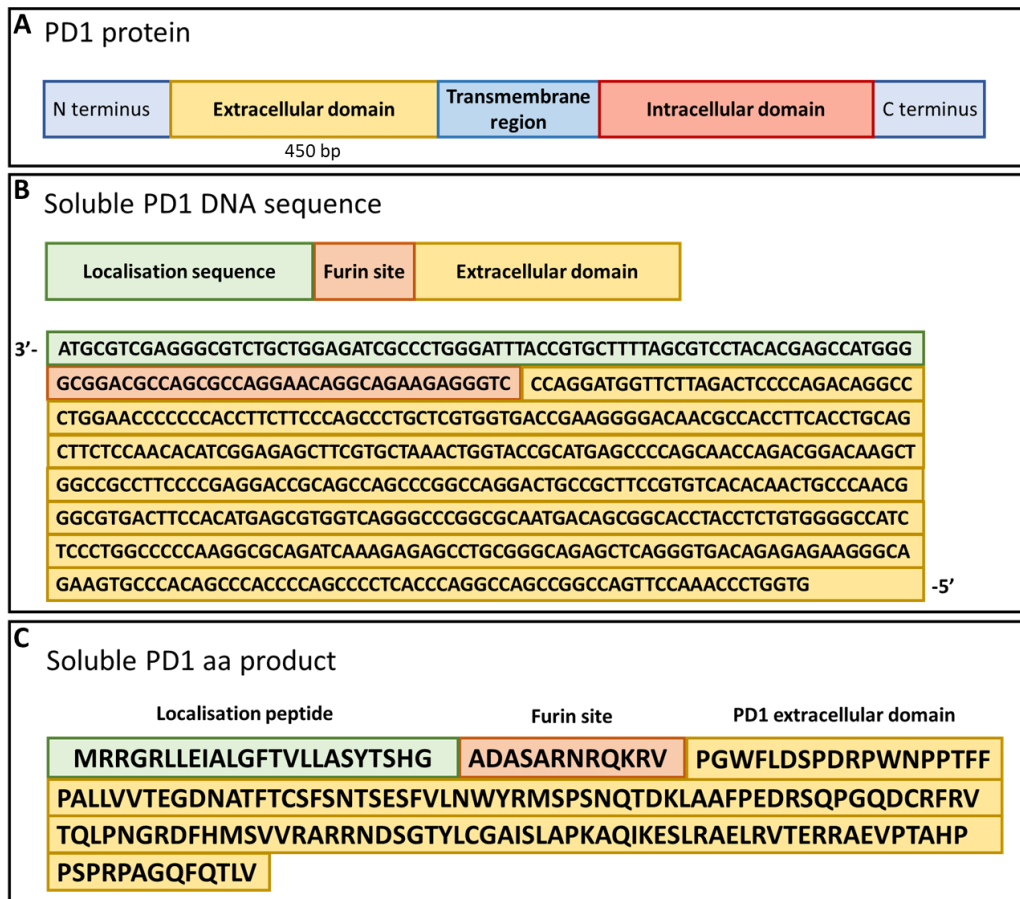


Figure 3.1.1. Design of a soluble wild-type PD1 (sPD1^{WT}) protein variant where the extracellular domain is isolated and fused with a localization sequence and a Furin cleavage site. **A.** A linear diagram indicating the key domains of PD1. It consists of a 450 bp extracellular domain (yellow), a transmembrane region (blue) and an intracellular domain (red). The C terminus and N terminus are indicated. **B.** A diagram showing the design and sequence of soluble PD1^{WT}. The extracellular domain is isolated from the full PD1 sequence and fused with a localisation sequence (green) and a Furin cleavage site (orange). **C.** The final sPD1^{WT} peptide product with the localisation peptide and Furin cleavage site shown.

To produce the sPD1^{WT} expression construct the sPD1^{WT} DNA fragment was amplified using primers with introduced NotI and EcoRI restriction sites (Figure 3.1.2). The forward and reverse primers contain Kozak and Stop Codon sequences respectively which will facilitate the beginning and end of replication of sPD1 within cells. During PCR, DNA Polymerase adds a single deoxyadenosine base to the 3'- ends of the amplified fragments. The pGEM-T Easy vector contains complimentary 3' terminal thymidine overhangs and therefore provides a compatible insertion site for the sPD1 PCR products.

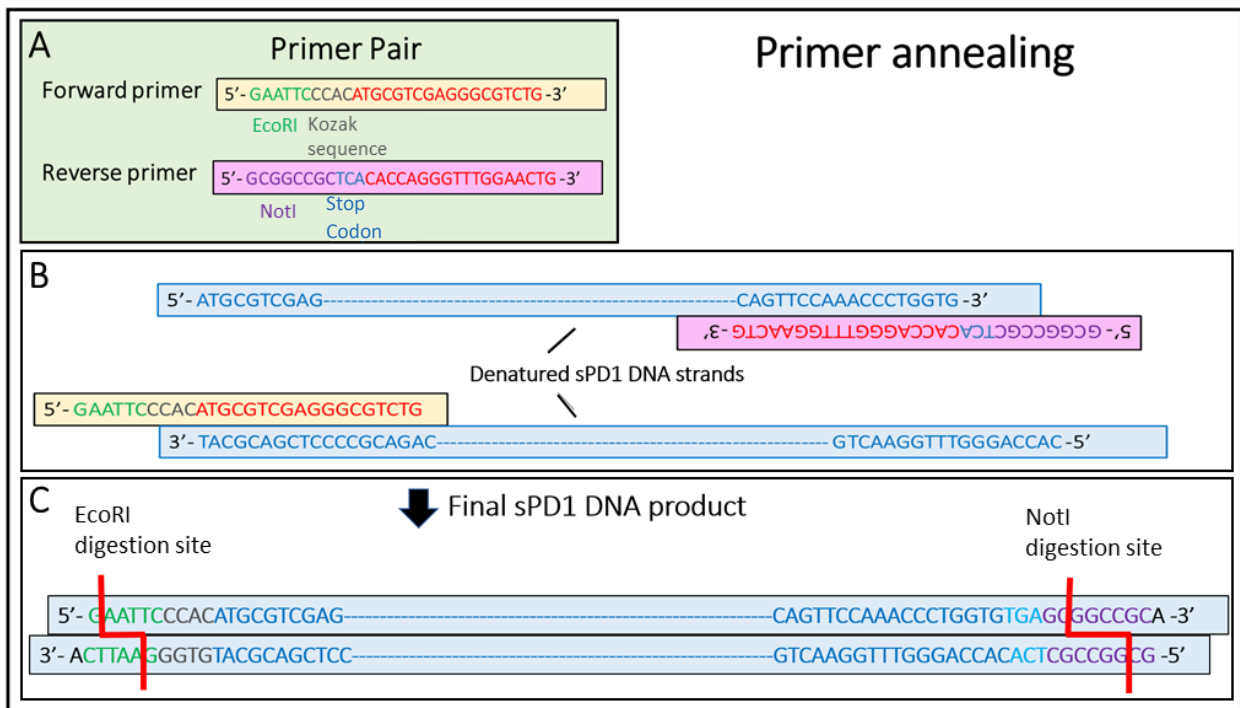


Figure 3.1.2. PCR amplification of sPD1^{WT} with the primer binding location and final PCR product shown. A. The primer pair sequence is shown here with EcoRI (green), NotI (purple) restriction enzyme sites highlighted. The forward primer contains a Kozak consensus sequence (grey) to initiate DNA translation and the reverse primer contains a Stop sequence (blue) to terminate DNA translation. The red sequence in both primers represents the sequence complementary to sPD1. **B.** The primer annealing location is shown here. The sPD1 DNA strands are visualised in blue. **C.** The final sPD1 DNA fragment generated from the PCR process. The 3' adenosine overhangs (black) are a feature of DNA polymerase which adds these during DNA replication. The EcoRI and NotI digestion sites are indicated with a red line.

The pGEM-T-Easy vector contains an ampicillin resistance gene and a LacZ operon to allow for selection of positive bacterial clones (Figure 3.1.3). The PCR sPD1^{WT} fragment and pGEM-T-Easy vector were ligated to generate the pGEM.sPD1^{WT} construct. Insertion of the sPD1^{WT} fragment into the pGEM-T-Easy plasmid disrupts the LacZ α gene within the Lac operon which normally leads to X-gal hydrolysis and a subsequent colour change of the resulting bacterial clones after transformation with the plasmid, from blue for the simply ligated pGEM-T-Easy plasmid to white for insert-containing/positive plasmids. White colonies were amplified in small liquid cultures and the resulting plasmid DNAs after Miniprep purification analysed by restriction digests for the presence of the pGEM.sPD1^{WT} construct. One positive bacterial clone and its purified pGEM.sPD1^{WT} plasmid DNA were used for the next steps.

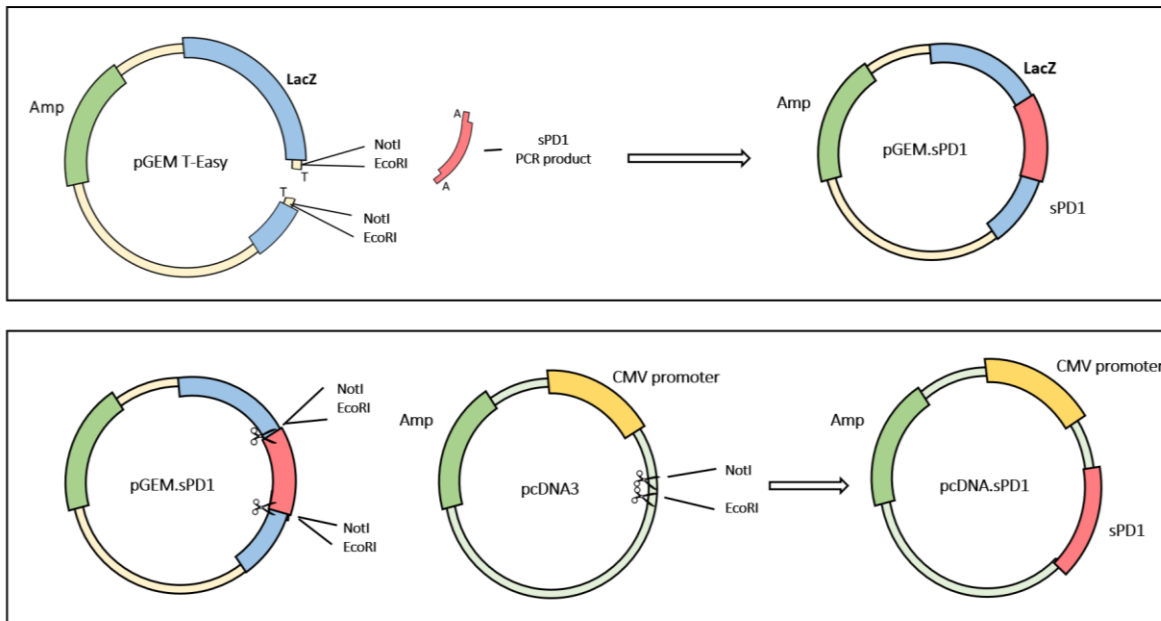


Figure 3.1.3. A visualisation of the genetic engineering procedure to generate an sPD1^{WT} expression construct using pGEM T-Easy as the intermediate cloning vector and pcDNA3 as the final expression vector. The pGEM T-easy vector contains thymidine overhangs and is a compatible vector for PCR sPD1^{WT} variant products which have adenosine base overhangs due to the nature of DNA Polymerase replication. The DNA undergoes a ligation reaction to generate a pGEM.sPD1^{WT} construct. pGEM.sPD1^{WT} is cleaved with NotI and EcoRI enzymes to release the sPD1^{WT} fragment from the pGEM vector. A pcDNA3 vector is cleaved with NotI and EcoRI enzymes to produce complimentary overhangs to the sPD1 fragment and the two are ligated to generate the final pcDNA.sPD1^{WT} vector.

The sPD1^{WT} fragment was then released from the pGEM vector backbone via restriction with EcoRI and NotI at the introduced enzyme cleavage sites (Figure 3.1.2). Next, it was inserted into a pcDNA3 plasmid vector – a mammalian expression vector containing the human cytomegalovirus immediate-early (CMV) promoter and, among others, NotI and EcoRI cleavage sites in the multi-cloning site where DNA fragments are usually inserted. Ligation between sPD1^{WT} and pcDNA3 resulted in a final expression construct termed pcDNA.sPD1^{WT}. A full plasmid map of pcDNA.sPD1^{WT} is shown below (Figure 3.1.4). The vector will be used to transfect mammalian cells and generate and secrete sPD1^{WT} protein.

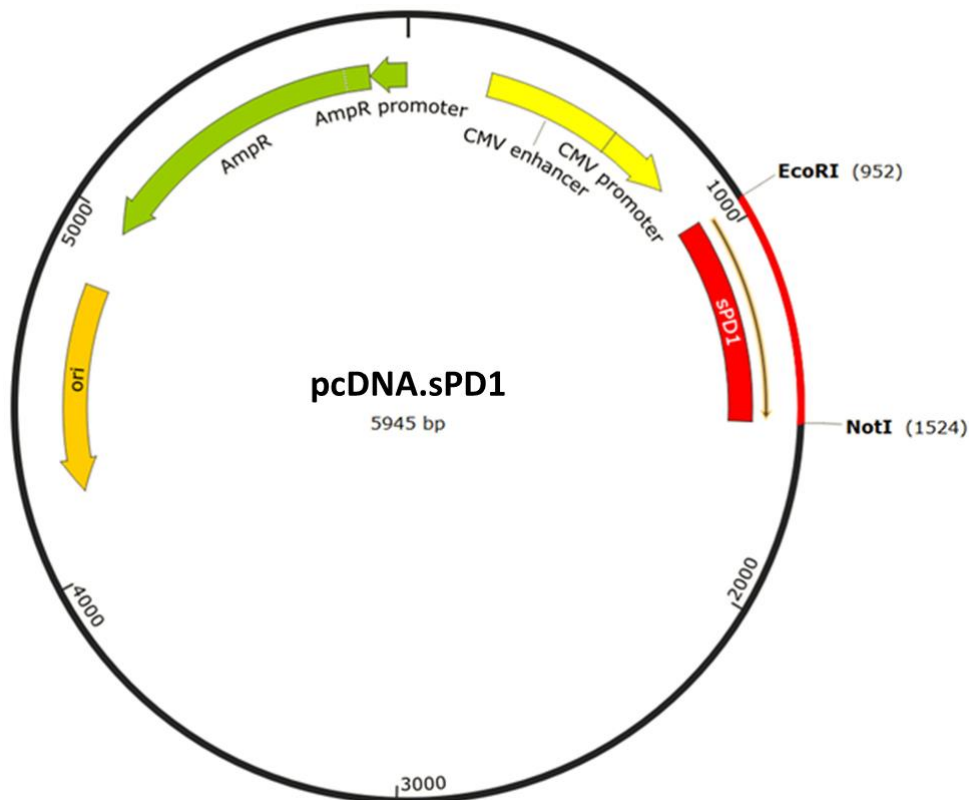


Figure 3.1.4. A map of the recombinant pcDNA.sPD1^{WT} expression construct with the key features shown. The pcDNA.sPD1^{WT} construct is 5945 bp in size. It contains an ampicillin resistance gene (green) for selection of positive bacterial clones, a CMV promoter and enhancer (yellow) which are required for transient expression of transgenes, and other essential plasmid elements including origin of replication (Ori). The sPD1^{WT} fragment was cloned into the multidrug insertion site with EcoRI and NotI enzymes at the location 952-1524 bp (red).

3.2. sPD1^{WT} protein production

To generate the sPD1^{WT} protein Chinese Hamster Ovary (CHO) cells were transfected with pcDNA.sPD1^{WT}. The cell supernatants were analysed for sPD1^{WT} protein presence by ELISA. The results confirm successful extracellular sPD1^{WT} protein secretion (Figure 3.2.1). The average sPD1^{WT} concentration was 1380 ng / mL. A control sample consisting of supernatants from CHO cells transfected with a non-recombinant pcDNA3 vector tested negative for sPD1 protein presence. These results confirm successful sPD1^{WT} production from the pcDNA.sPD1^{WT} expression construct. The produced sPD1^{WT} will be tested further for its functionality.

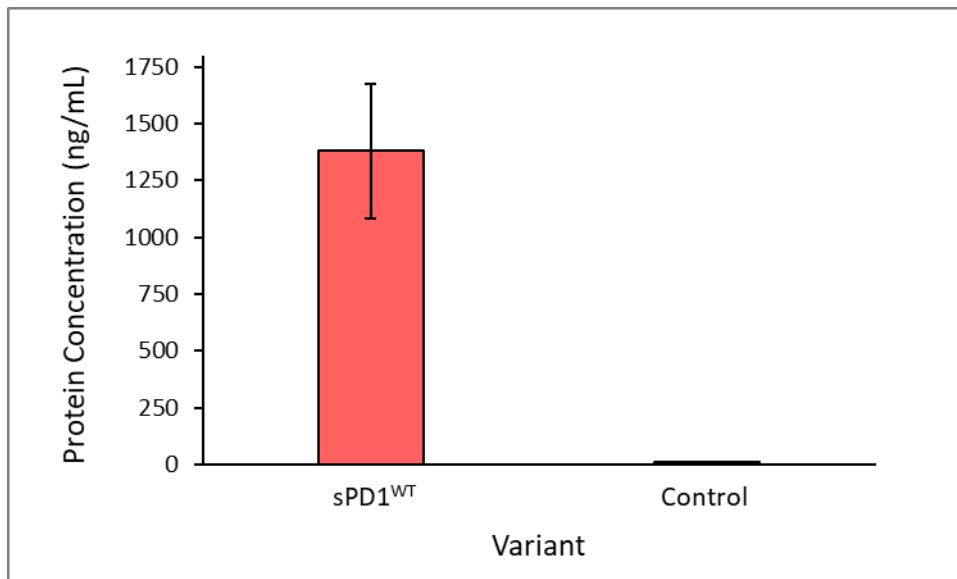


Figure 3.2.1. sPD1^{WT} protein concentration in the supernatant of CHO cells transfected with the pcDNA.sPD1^{WT} construct. Protein concentration in the supernatant was determined via ELISA. The control sample is a supernatant sample from CHO cells transfected with a non-recombinant pcDNA3 parental plasmid. Data is expressed as mean \pm SE and are representative of four independent experiments.

3.3. Testing sPD1^{WT} binding to PD-L1 in a cellular competition assay

To ensure sPD1^{WT} can bind to its ligand - PD-L1, a competition binding experiment was conducted. Pancreatic cancer tumour cells (PancTul) were stimulated with IFN- γ to induce expression of PD-L1 on their surface, to better reflect the nature of cancer cells *in vivo* where PD-L1 is upregulated. PD-L1 was detected with an anti-PD-L1 antibody (Figure 3.3.1). A sample of IFN- γ -stimulated PancTul cells was compared to a sample of non-IFN- γ -stimulated PancTul cells. Background staining was detected using an isotype control. The results show that PancTul cells stimulated with IFN- γ express more PD-L1 than the non-stimulated PancTul cells, visualised by a peak shift to the right. This confirms successful PD-L1 induction on the surface of PancTul cells. The PD-L1 -positive PancTul cells will be used in the protein competition assay to test sPD1^{WT} binding.

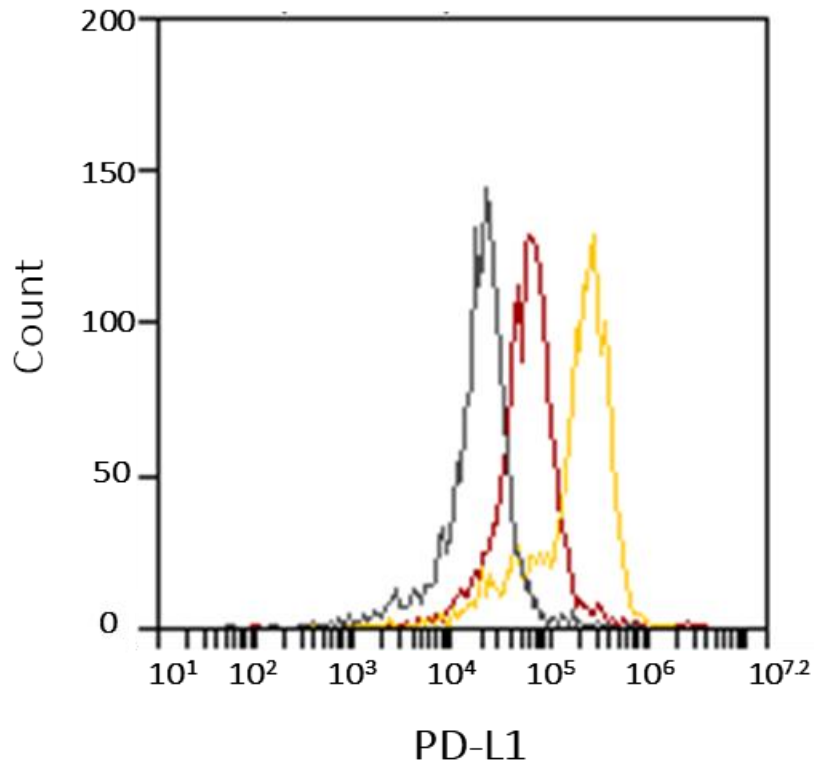


Figure 3.3.1. Induction of PD-L1 on the PancTul cell surface via IFN- γ stimulation. 2×10^6 PancTul cells either stimulated (yellow) or non-stimulated (red) with IFN- γ were incubated with a PE conjugated anti-PD-L1 antibody. Background staining of the IFN- γ -stimulated PancTul cells was detected with an isotype control – PE mouse IgG1 (grey).

IFN-stimulated PancTul cells which tested positive for PD-L1 expression were then incubated with CHO supernatants containing 50 ng of sPD1^{WT} and 50 ng of a commercial recombinant PD1 protein (rPD1), engineered with a biotin tag. The assay was performed with a negative control to detect the background radiation and a control sample (IFN- γ stimulated PancTul cells incubated with supernatant from CHO cells that were transfected with a non-recombinant pcDNA3 plasmid vector). The results (Figure 3.3.2) show a decrease in rPD1 binding when sPD1^{WT} is present in the sample (visualised by a peak shift to the left). This signifies sPD1^{WT} successfully binds to PD-L1 on the PancTul surface and is competing with rPD1 for the binding site of PD-L1. These results suggest that sPD1^{WT} could be effective at inhibiting the PD1/PD-L1 interaction.

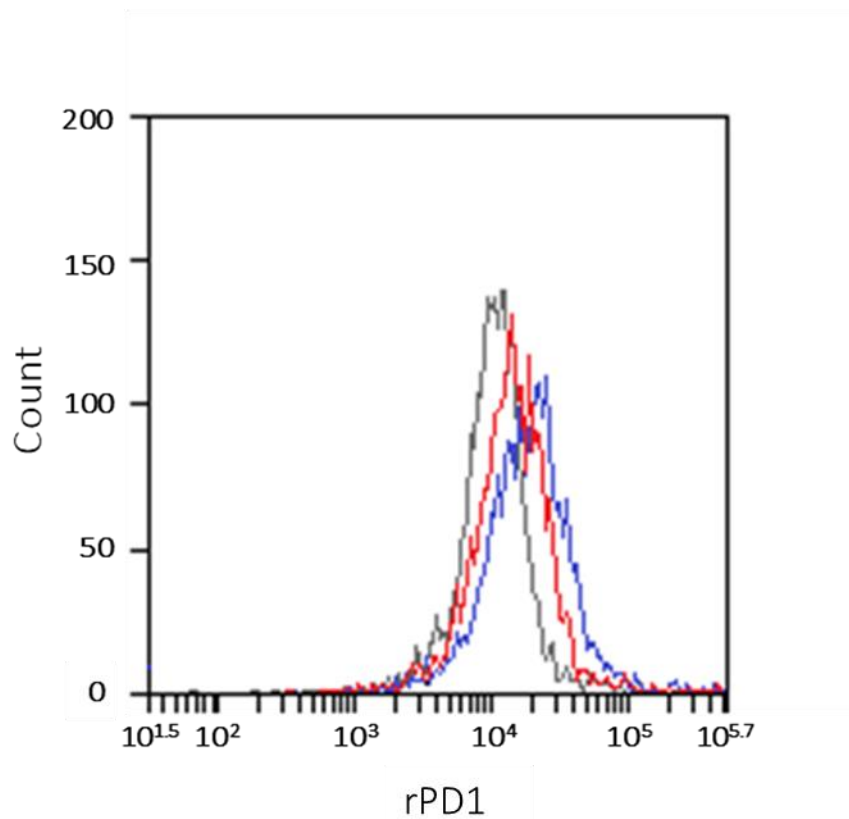


Figure 3.3.2 Flow cytometry results showing competitive binding of recombinant PD1 (rPD1) and sPD1^{WT} to PD-L1 on the surface of PancTul cells. PancTul cells were stimulated with IFN- γ to induce PD-L1 expression on their surface. The binding affinity of sPD1^{WT} to PD-L1 was then analysed in a competition assay where sPD1^{WT} competes for the binding site of PD-L1 on the surface of PancTul cells with rPD1– a commercial recombinant PD1 protein engineered with a biotin tag. First the full binding capacity of rPD1 was tested (blue) – 2×10^6 PancTul cells were coated with 50 ng of rPD1 and the bound rPD1 was detected with streptavidin-PE conjugate and the signal intensity was measured via flow cytometry. To detect protein competition (red), 2×10^6 PancTul cells were incubated with 50 ng of sPD1^{WT} and 50 ng of rPD1. Unbound protein was washed away and PancTul cells were incubated with a streptavidin-PE conjugate and the signal intensity was measured. A negative control to detect background radiation (grey) was tested by incubating 2×10^6 PancTul cells with the streptavidin-PE conjugate.

3.4. Establishing parameters of the microplate-based sPD1 Competition Assay

The cellular protein competition assay can be time-consuming and expensive due to the cell culture and maintenance. To make sPD1 variant testing more efficient a solid-phase competition assay was developed. The assay is derived from the enzyme-linked immunosorbent assay (ELISA) methodology (Figure 3.4.1). It consists of three main stages; immobilisation of commercial, recombinant PD-L1 protein- to the wells of the assay plate, the incubation stage with sPD1 proteins for protein-protein interaction to establish, and the detection of bound sPD1. In the protein interaction stage, the plate is

coated with the sPD1 variant of interest and a commercial, recombinant PD1 protein (rPD1) with an added biotin tag. In the protein-protein interaction stage sPD1 and rPD1 compete for the PD-L1 binding site. The bound rPD1 is quantified via an enzyme-linked reaction which results in a measurable colour change in the assay. The intensity of the colour change is quantitatively dependent on the amount of rPD1 bound to PD-L1. Comparison of signal intensities between the test sample with the sPD1 protein variant and rPD1 and the control sample with just rPD1, allows for analysis of the binding of sPD1 to PD-L1.

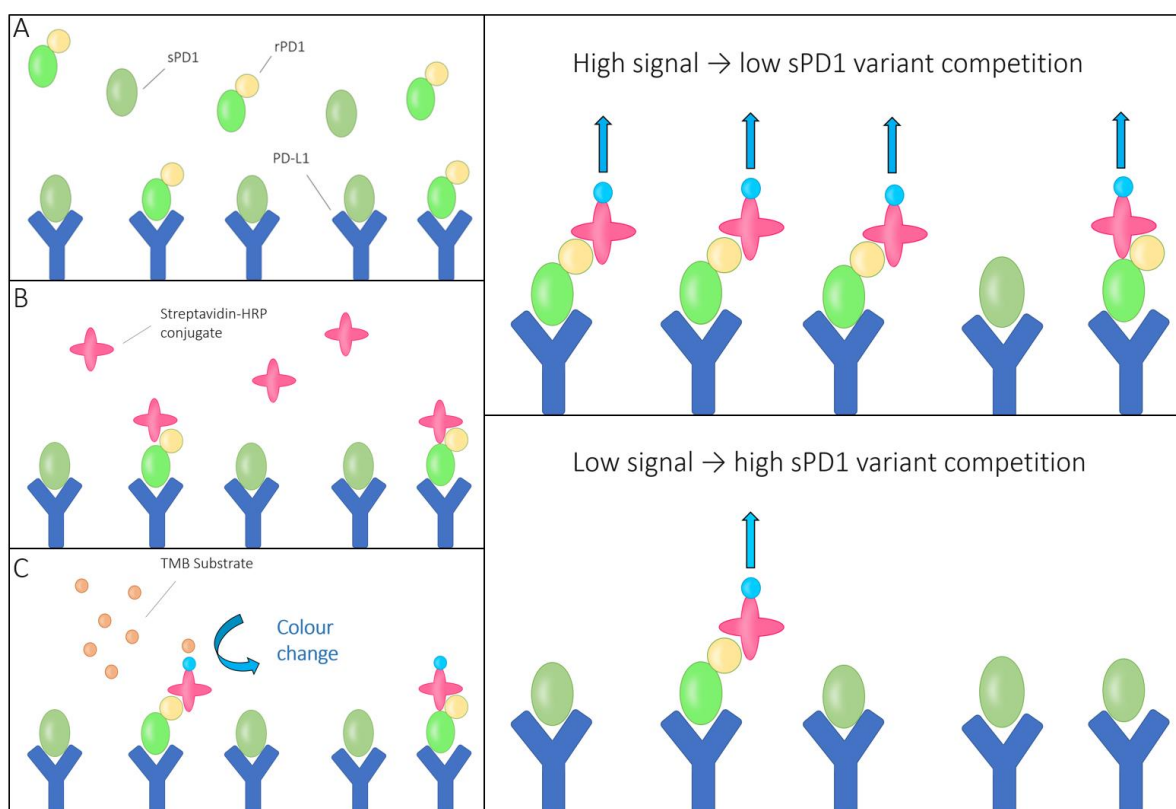


Figure 3.4.1. Principle behind the solid-phase protein competition assay to analyse the binding of sPD1 to PD-L1.

A) Recombinant PD1 (rPD1) engineered with a biotin tag and unlabelled sPD1 protein variant are incubated together on a microplate with PD-L1 attached to the surface. After an incubation period the unbound protein is removed by washing. **B)** The plate is coated with a streptavidin-HRP conjugate protein which strongly binds to biotin in a non-covalent manner. The unbound conjugate protein is washed away. **C)** The addition of TMB substrate results in a colour change catalysed by the HRP enzyme in the wells, which can be measured. sPD1 protein variants can be tested for their ability to outcompete the binding of rPD1 using this assay. A weak signal suggests that sPD1 is successfully outcompeting rPD1 binding and therefore has a higher affinity for PD-L1.

To provide a sensitive assay for effective testing of sPD1 variants, the assay parameters were tested and optimised. To determine the working concentration of rPD1 for the assay a PD-L1 saturation curve was generated. rPD1 dilutions in the concentration range of 10 - 900 ng were added to wells with 100

ng of PD-L1 immobilised to the surface and allowed to reach binding equilibrium. The signal intensity of each well was recorded via spectroscopy and the optical density value was converted into a percentage of PD-L1 saturation and plotted (Figure 3.4.2). For a sensitive assay, the protein association must be higher than the dissociation rate, which occurs in the linear range of the curve. In this assay, this is between 10 and 100 ng with the curve starting to flatten at 200 ng - and binding beginning to reach equilibrium at 500 ng of rPD1. Thus, it was decided to use rPD1 concentrations between 10 and 50 ng in further solid-phase experiments to test sPD1 variant ligand binding.

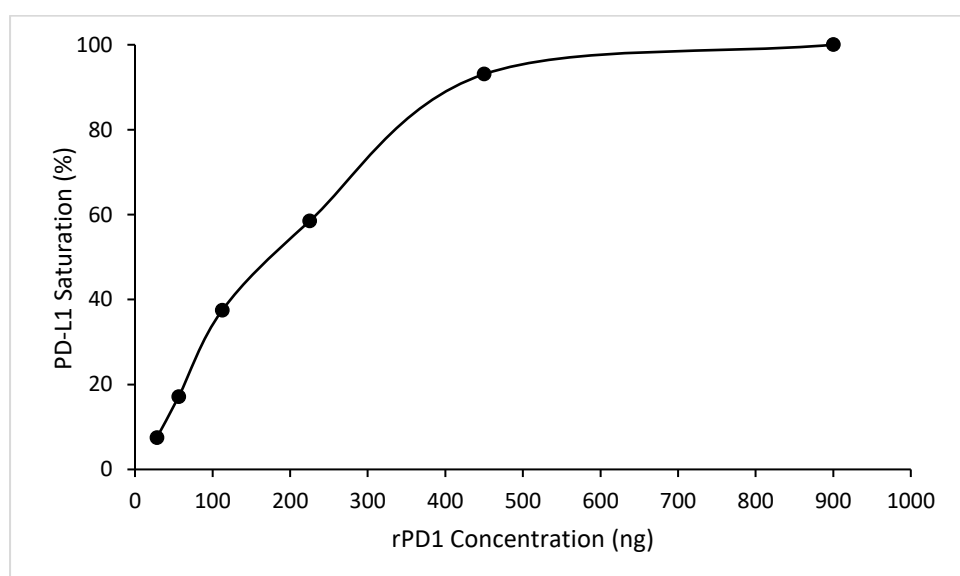


Figure 3.4.2 Saturation of PD-L1 with recombinant PD1 (rPD1). A microplate with PD-L1 attached to the surface was incubated with a rPD1 (PD1 engineered with a biotin tag) in concentration ranges of 10 – 900 ng to generate a PD-L1 saturation curve. Data shows percentage of PD-L1 saturation at different rPD1 concentrations.

To determine the appropriate concentration of PD-L1 for the assay to be sensitive, an experiment was conducted where PD-L1 was the variable parameter. The microplate surface was coated with PD-L1 concentrations of 0, 12.5, 25, 50 and 100 ng. The wells were incubated with either 20 or 50 ng of rPD1. The optical density data was converted into a percentage value where the standard 100% rPD1 binding sample is the 100 ng of PD-L1 incubated with 50 ng of rPD1 sample. The assay results are shown in Figure 3.4.3. Coating the plate with 0 ng of PD-L1 did not result in a signal from rPD1 indicating that it does not bind to the plate surface or the BSA protein. Increasing the coating surface of PD-L1 leads to a proportional signal increase in each sample. Coating the plate with 12.5 ng of PD-L1 resulted in a weak

signal with no significant variation between the 20 ng and 50 ng rPD1 concentration groups, suggesting an excess of rPD1 protein in both samples. Increasing the PD-L1 coating concentration to 25 ng results in a higher overall signal, however no distinct difference between the different rPD1 concentration conditions was observed. An increase to 50 ng of PD-L1 resulted in 54% more rPD1 binding in the 50 ng rPD1 group compared to the 20 ng group. Coating with 100 ng PD-L1 resulted in the highest signal intensity and the highest sensitivity to distinguish between the different rPD1 concentration groups. An 88% signal increase has been recorded between the 20 ng and 50 ng rPD1 concentration samples in this group. In future experiments, each well will be coated with 100 ng of PD-L1 as this condition provides for the highest assay sensitivity.

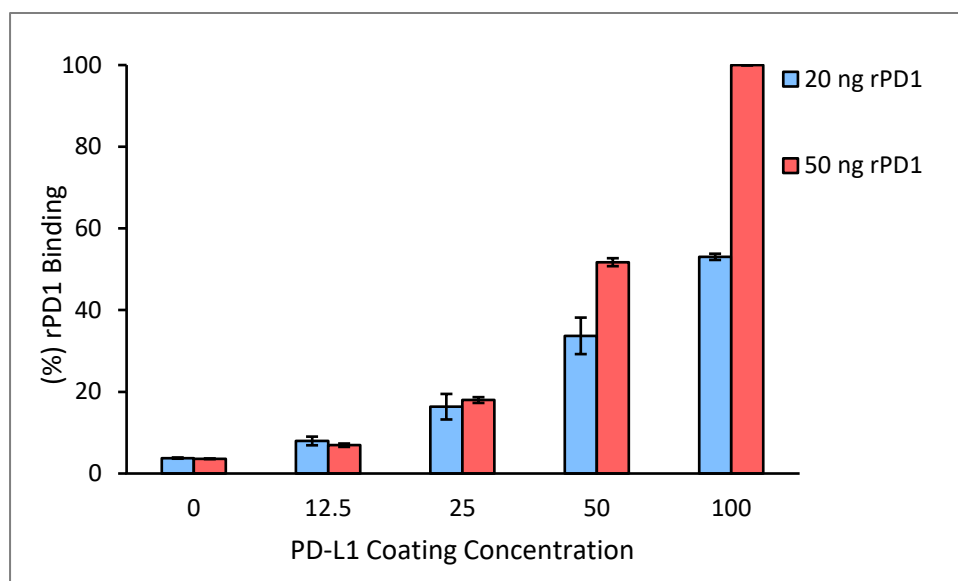


Figure 3.4.3. Percentage of recombinant PD1 (rPD1) Binding PD-L1 coating concentration in a solid-phase microplate-based assay. Microplate wells were coated with PD-L1 (0, 12.5, 25, 50, 100 ng). The wells were incubated with either 20 or 50 ng of rPD1 and the signal intensity was measured and converted into % of rPD1 binding. Data is expressed as mean \pm SE of duplicate wells.

3.5 Generation of sPD1 variants with mutations to increase binding affinity to PD-L1

The sPD1 variants were designed using the MM/PBSA method; single point mutations were introduced into the protein coding sequence to increase the sPD1 binding affinity to PD-L1. These mutations were introduced via site-directed mutagenesis of the sPD1^{WT} fragment using primers containing desired mutations. Variants termed sPD1¹ and sPD1²⁷ were generated in this way and were transfected into CHO cells alongside sPD1^{WT}. The supernatants were analysed to determine protein concentrations via ELISA (Figure 3.5.1). The highest protein expression levels are seen in sPD1^{WT} with values of 1379 ng /

mL. The expression level of sPD1²⁷ was on average 1017 ng / mL. Variant sPD1¹ exhibited an average expression level of 1027 ng / mL. Overall, there is no evidence that any of the introduced mutations is having an adverse effect on sPD1 protein production and expression.

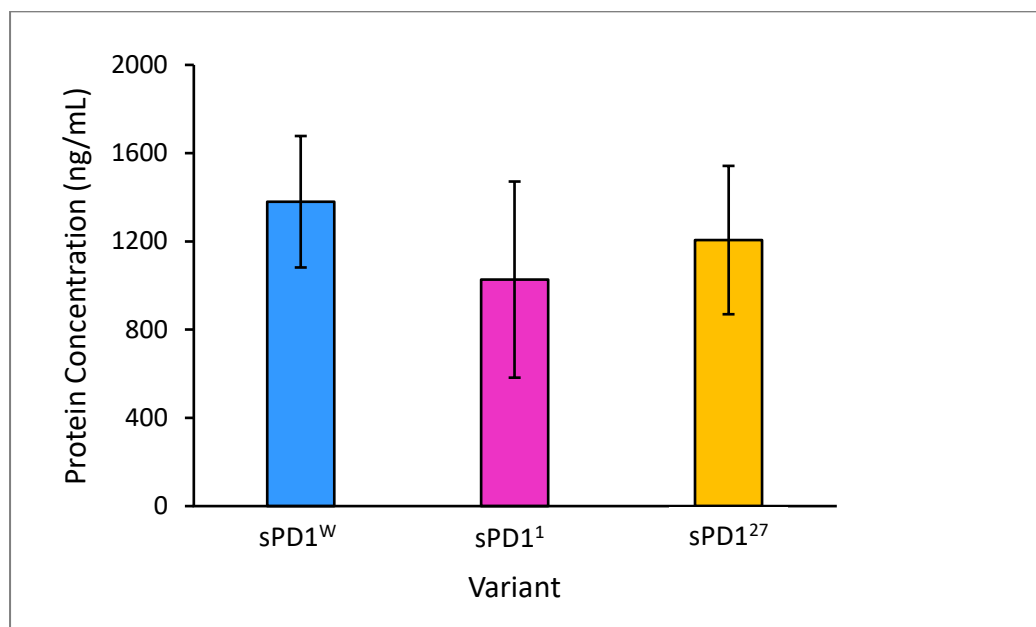


Figure 3.5.1. sPD1 variant protein concentration in the supernatant of transfected CHO cells. CHO cells were transfected with pcDNA.sPD1 variants and sPD1 protein concentration in cell supernatants were determined by ELISA. Data is expressed as mean \pm SE of duplicate wells and are representative of three independent experiments.

The sPD1 variants were then tested for the strength of their binding to PD-L1 using the solid-phase protein competition assay. CHO supernatant containing 50 ng of sPD1 variant and 50 ng of rPD1 was added to wells coated with 100 ng of PD-L1. Variant binding to PD-L1 was compared to that of sPD1^{WT} with this setting the 100% rPD1 binding. The results (Figure 3.5.2) show that the variants are moderately more effective than sPD1^{WT} at binding to PD-L1 and can outcompete rPD1. On average, sPD1²⁷ outcompetes 22% more rPD1 than sPD1^{WT}. sPD1¹ outcompetes 26% more rPD1 than sPD1^{WT} and is the most effective protein inhibitor out of the tested variants. These are promising results showing that binding affinity of sPD1 to PD-L1 has been successfully increased by using synthetic variants.

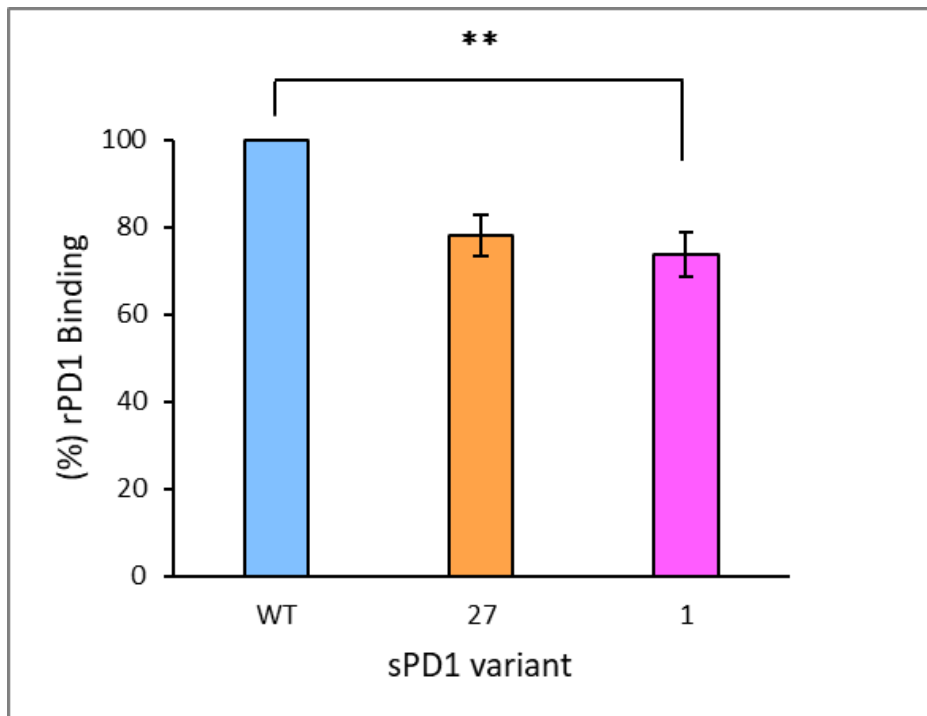


Figure 3.5.2. Solid-phase protein competition assay testing sPD1 variant binding (sPD1^{WT}, sPD1²⁷ and sPD1¹) to PD-L1 at different recombinant PD1 (rPD1) concentrations. A microplate with 100 ng of PD-L1 attached to the surface of each well was incubated with 50 ng of sPD1^{WT}, sPD1²⁷ or sPD1¹ with 50 ng of rPD1. All data is expressed as mean \pm SE of duplicate wells and are representative of three independent experiments.

Based on the hypothesis that PD1 and PD-L1 interact as dimers rather than monomers, we generated a tetramerisation variant of sPD1 (sPD1^{TETR}) through the addition of a p53-derived tetramerisation site into the DNA sequence. The theory is that by enforcing a tetramer structure of sPD1, the dimeric interaction between sPD1 and PD-L1 will be able to occur more readily and therefore this variant will have an increased binding affinity to PD-L1 than the monomeric sPD1. sPD1^{TETR} was expressed in a pcDNA.sPD1^{TETR} expression construct and used to transfect CHO cells alongside sPD1^{WT} to observe if the introduced tetramerisation site interferes with protein production or secretion. The ELISA results (Figure 3.5.3) show that the mean concentration of sPD1^{TETR} in cell supernatant was 1194 ng / mL and the mean concentration of sPD1^{WT} was 1177 ng / mL. While the amount of protein expression varied between transfection experiments, the sPD1^{WT} and sPD1^{TETR} were expressed in comparable concentrations in each of the individual experiments. From these results, it can be concluded that a tetramerization site does not interfere with sPD1 protein production and secretion.

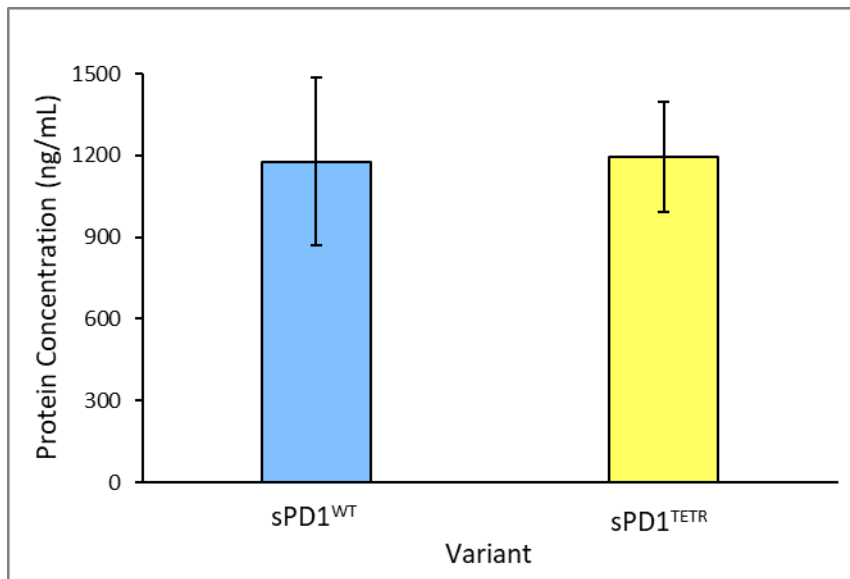


Figure 3.5.3. Average protein concentration of sPD1^{WT} and sPD1^{TETR} in CHO cell supernatant. The supernatants of CHO cells transfected with pcDNA.sPD1^{WT} and pcDNA.sPD1^{TETR} expression constructs were analysed by ELISA to determine the sPD1 (variant) concentration in cell. Data is expressed as mean \pm SE of duplicate wells and are representative of three independent experiments.

To determine if the tetramerisation site does, in fact increase the binding of sPD1 to PD-L1, sPD1^{TETR} was assessed in a solid-phase binding assay and compared to a control sample with sPD1^{WT} present as the rPD1 competitor. The results (Figure 3.5.4) show that the addition of a tetramerisation site leads to less rPD1 binding to PD-L1 and the tetramerization site therefore appears to increase the affinity to PD-L1. The results show that sPD1^{TETR} decreases rPD1 binding by 24% compared to sPD1^{WT}. This finding opens up the possibility of a future design of a tetramerisation domain containing high-affinity sPD1 variant to inhibit the PD1/PD-L1 pathway interaction even further.

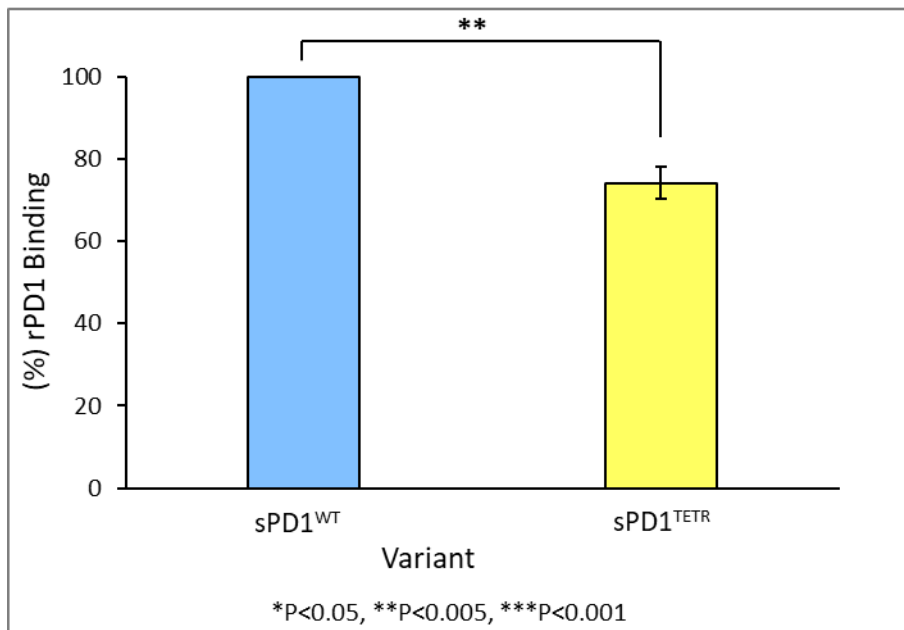


Figure 3.5.4. Comparison of recombinant PD1 (rPD1) binding to PD-L1 in samples with sPD1^{WT} and sPD1^{TETR} as competitors. PD-L1 was immobilised to the microplate surface (100 ng per well) and wells treated with supernatant from transfected CHO cells that contained either sPD1^{WT} or sPD1^{TETR} protein, together with 50 ng of rPD1. Values were converted into percentage wherein the binding of rPD1 in the presence of sPD1^{WT} is set as 100%. Data is expressed as mean \pm SE of duplicate wells and are representative of three independent experiments.

3.6 Generation of a soluble High Affinity Consensus (HAC) sequence PD1 variant

A published high-affinity consensus sequence mutant (HAC) of PD1 was found in the literature (Maute et al., 2015). This sequence contains 10 point mutations, as opposed to our variants which only contain a single point mutation. It was also generated in a soluble form using our general design with signal peptide and Furin cleavage site and termed sPD1^{HAC} (Figure 3.1.3). A pcDNA.sPD1^{HAC} expression construct was generated (Section 3.1) and transfected into CHO cells to express the protein. An ELISA was used to measure protein expression of this variant. The results revealed that sPD1^{HAC} is expressed in much lower concentrations than other variants - the average sPD1^{HAC} concentration was 15 ng / mL while the concentration of our variants was on average of 1000 ng / mL. To ensure the low protein concentration was not a consequence of sPD1^{HAC} DNA degradation, pcDNA.sPD1^{HAC} was tested using gel electrophoresis alongside pcDNA.sPD1^{WT}. No signs of DNA degradation were visible on the gel - typically characterised by a smeared appearance, instead DNA presented itself as a solid band on the gel (Figure 3.6.1). To further confirm DNA integrity the sPD1^{HAC} DNA was sequenced and analysed to confirm the presence of all introduced mutations and to verify that no random undesired mutations have emerged. The amino acid sequence is shown (Figure 3.6.1) aligned with sPD1^{WT} sequence with the

mutations highlighted. The 10 mutations present are all the introduced mutations to increase binding affinity to PD-L1 and no additional random mutations emerged confirming DNA integrity. Therefore, the low protein expression must be a result of ineffective protein production and/or secretion.

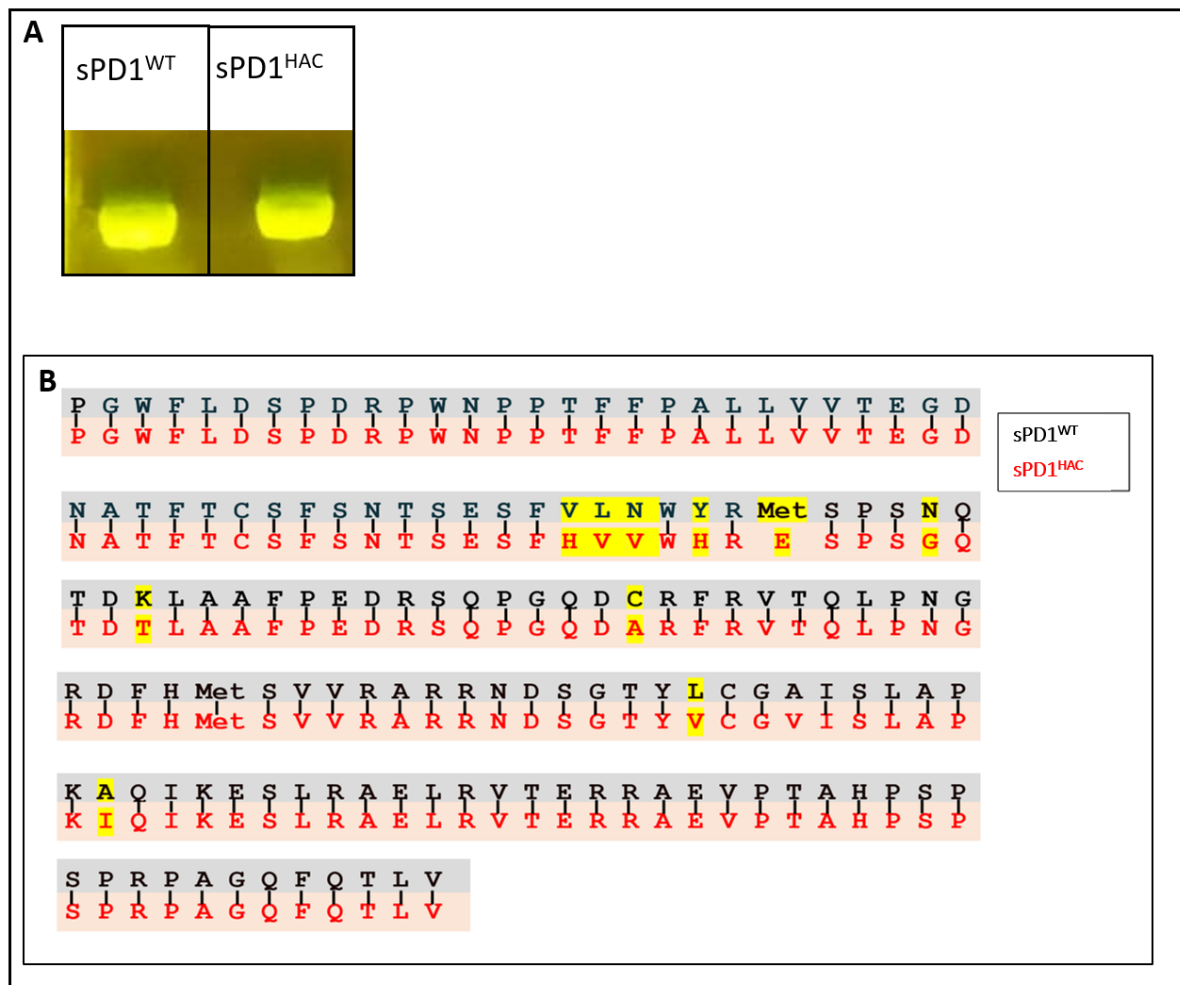


Figure 3.6.1. Analysis of sPD1^{HAC} DNA integrity with the amino acid sequencing results of sPD1^{HAC} shown aligned with sPD1^{WT} sequence. A) Gel image of pcDNA.sPD1^{HAC} alongside pcDNA.sPD1^{WT} to detect DNA degradation. **B)** Amino acid sequence of sPD1^{HAC} (black) aligned with the sPD1^{WT} (red) amino acid sequence. The amino acid sequences were derived from the sequencing results of the respective plasmids. The mutations within the sPD1^{HAC} sequence are indicated (yellow).

To examine whether the levels of the sPD1^{HAC} could be increased, we expressed sPD1^{HAC} as a fusion protein with IgG-Fc. For this the sPD1^{HAC} fragment was engineered onto an IgG1-based expression plasmid (pFUSE-hIgG1-fc1). This plasmid generates Fc-fusion proteins that express the Fc region (CH2 and CH3 domains) of the human IgG1 heavy chain and the hinge region. The sPD1^{HAC} fragment was amplified from the pcDNA.sPD1^{HAC} expression plasmid by PCR introducing EcoRI and BglII restriction sites and inserted into the pFUSE-hIgG1-Fc vector, which contains the same restriction in its multi-cloning site. In this way, a final pFUSE.sPD1 expression construct was generated with the DNA map shown in Figure 3.6.2.

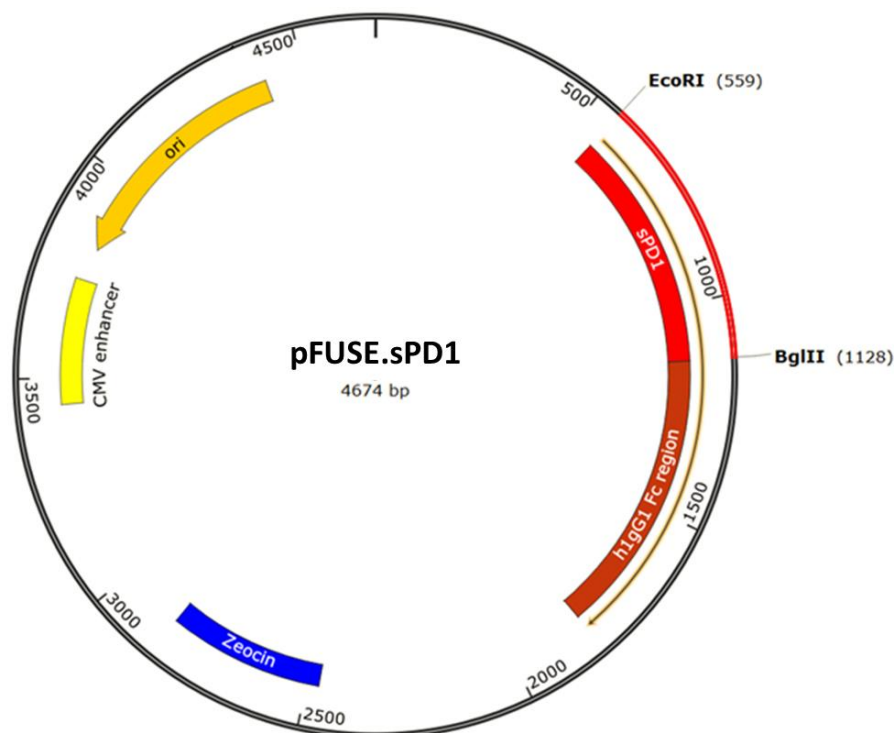


Figure 3.6.2. A map of the recombinant pFUSE.sPD1 expression construct with the key features shown. The pFUSE.sPD1 construct is 4674 bp in size. It contains an EF-1 α core promoter (dark green) which drives strong gene expression, a gene for Zeocin resistance (blue) to allow selection of positive bacterial clones and a region coding for the human IgG1 region (dark red). The sPD1 gene is inserted at the EcoRI and bglII cleavage sites and is located at 559 – 1128 bp.

A pFUSE.sPD1^{HAC} expression construct was generated as well as pFUSE.sPD1^{WT} and pFUSE.sPD1^{TETR}. These constructs were used to transfect Human Embryonic Kidney Cells 293 cells (HEK293) cells to test protein secretion in human cells and the protein concentration was measured via ELISA (Figure 3.6.3). The control sample used here is a supernatant from non-transfected HEK293 cells, which tested negative for sPD1 expression. The results show significantly higher sPD1 protein concentrations in all sPD1 variants when the protein is expressed as an IgG-Fc fusion protein, with pcDNA.sPD1^{HAC} having a significantly lower expression rate than both pcDNA.sPD1^{WT} and pcDNA.sPD1^{TETR}. The concentration of pcDNA.sPD1^{WT} and pcDNA.sPD1^{TETR} proteins is 120 ng / mL and 142 ng / mL respectively while the concentration of pcDNA.sPD1^{HAC} is 24 ng / mL. The concentration of pFUSE.sPD1^{HAC} is significantly higher at 2127 ng / mL. pFUSE.sPD1^{WT} and pFUSE.sPD1^{TETR} protein concentrations are 1904 ng / mL and 552 ng / mL respectively. The results suggest that the tetramerization site interferes with protein production when sPD1^{TETR} is engineered into the pFUSE-hIgG1-Fc expression vector, but not when in the pcDNA3 vector.

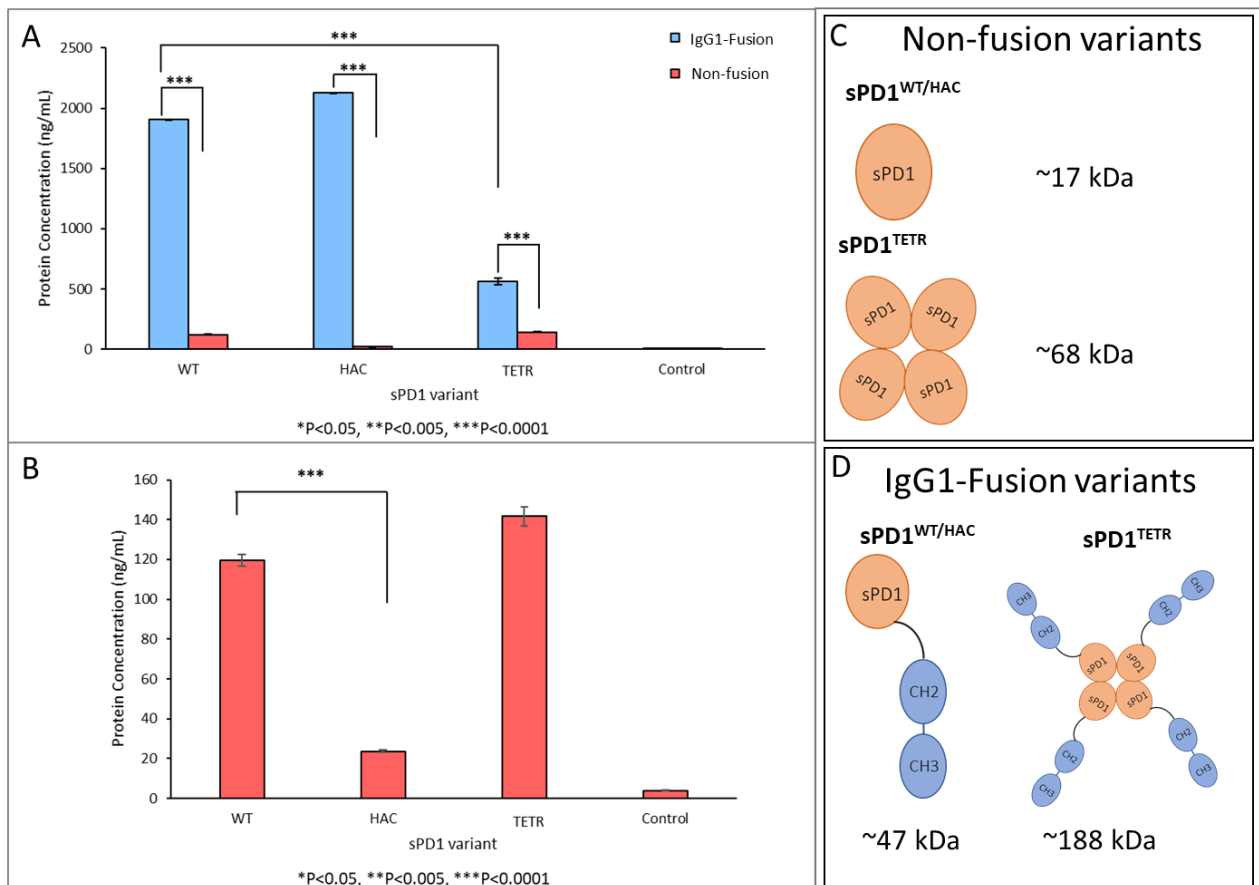


Figure 3.6.3 Comparison of protein expression of IgG1-Fc Fusion and non-Fusion sPD1 variants in HEK293 supernatants. HEK293 cells were transfected with sPD1^{WT}, sPD1^{HAC} and sPD1^{TETR} variants cloned into pFUSE-hIgG1-Fc or pcDNA3 plasmids to produce IgG1-Fc Fusion and non-fusion proteins, respectively. The concentration of the sPD1 variants in the supernatant was analysed using the ELISA method. **A)** Comparison of protein expression of the IgG1 fusion and non-fusion sPD1 variants. **B)** Comparison of protein expression of non-fusion sPD1^{WT}, sPD1^{HAC} and sPD1^{TETR} variants. **C)** Schematics visualising the structure of the non-fusion sPD1 variants and their molecular weights. **D)** Schematics visualising the structure of IgG1-Fusion sPD1 variants and their molecular weights. The CH2 and CH3 groups of the FC region are shown. All data is expressed as mean \pm SE of duplicate wells and are representative of three independent experiments.

To detect any variances in pcDNA.sPD1^{WT} and pFUSE.sPD1^{WT} binding to PD-L1 the proteins were tested in a solid-phase protein competition assay. The signal from the pcDNA.sPD1^{WT} sample was set as 100% rPD1 binding. The results (Figure 3.6.4) show no significant difference in the binding of sPD1^{WT} to PD-L1 when expressed on different vectors. This suggests that while IgG1-Fc gives sPD1 variants better stability, it does not interfere with binding and competition. sPD1^{WT} and sPD1^{HAC} IgG1-Fc fusion proteins - termed sPD1^{WT}.IgG and sPD1^{HAC}.IgG respectively - will be used in further functionality experiments.

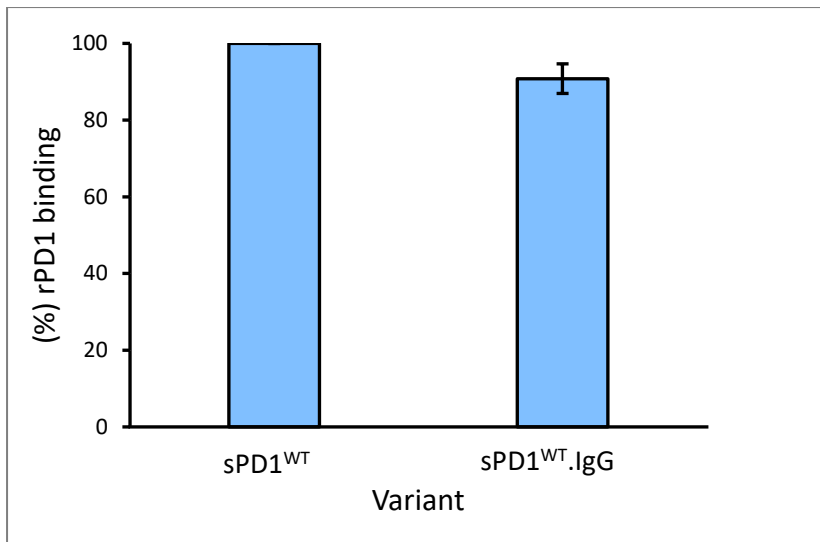


Figure 3.6.4. Comparison of recombinant PD1 (rPD1) binding to PD-L1 in samples with sPD1^{WT} and sPD1^{WT}.IgG as competitors. A microplate was coated with 100 ng of PD-L1 per well. 50 ng of each sPD1 variant was incubated with 50 ng of rPD1 in a solid-phase protein competition assay. Competition of pFUSE.sPD1^{WT} is shown as percentage of competition of pcDNA.sPD1^{WT}. Data is expressed as mean \pm SE of duplicate wells and are representative of three independent experiments.

3.7. Protein affinity testing to PD-L1 of the sPD1^{HAC} protein

sPD1^{HAC}.IgG was tested in a solid-phase protein competition assay to analyse the binding to PD-L1. 50 ng of rPD1 was incubated with CHO supernatant containing sPD1^{HAC} in the amounts of 20, 10 and 1 ng to observe protein competition rates. The results (Figure 3.7.1) revealed sPD1^{HAC}.IgG to be a strong inhibitor of the PD1/PD-L1 signalling interaction. 20 and 10 ng of sPD1^{HAC}.IgG were sufficient to completely outcompete 50 ng of rPD1. Even at quantities of 1 ng sPD1^{HAC}.IgG can still outcompete 97% of rPD1 binding. These results reveal that the binding of sPD1^{HAC}.IgG to PD-L1 is approximately 50 times stronger than that of rPD1.

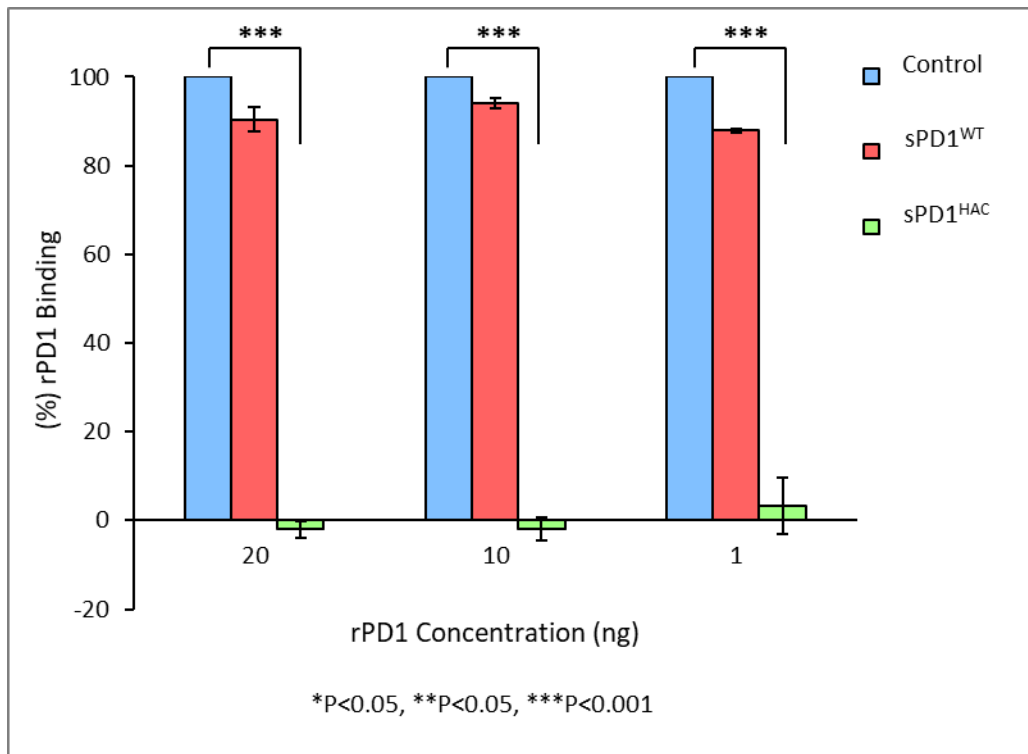


Figure 3.7.1 Competition assay testing the binding of sPD1^{HAC}.IgG and sPD1^{WT}.IgG at decreasing concentrations to PD-L1 against 50 ng of recombinant PD1 (rPD1). A microplate with 100 ng of PD-L1 attached to the surface of each well was treated with 20, 10 or 1 ng of sPD1^{WT}.IgG and sPD1^{HAC}.IgG protein variants with 50 ng of rPD1. Data is expressed as mean \pm SE of duplicate wells and are representative of three independent experiments.

The binding of sPD1^{HAC} is a magnitude stronger than other sPD1 variants tested which led to the question if the stronger binding is specific for PD-L1 or if the protein is 'adhesive' in nature. To test this, a microplate was coated with PD-L1, PD-L2 and an unrelated protein – Glutathione S-transferase (GST) and incubated with 20 ng of either sPD1^{WT} or sPD1^{HAC}. Bound protein was detected with a PD1 detection antibody and quantified via an enzyme-linked reaction. The results revealed that sPD1^{HAC} only binds to PD-L1 and does not bind to PD-L2 or GST (Figure 3.7.2). These results demonstrate that sPD1^{HAC} binds strongly and specifically to PD-L1.

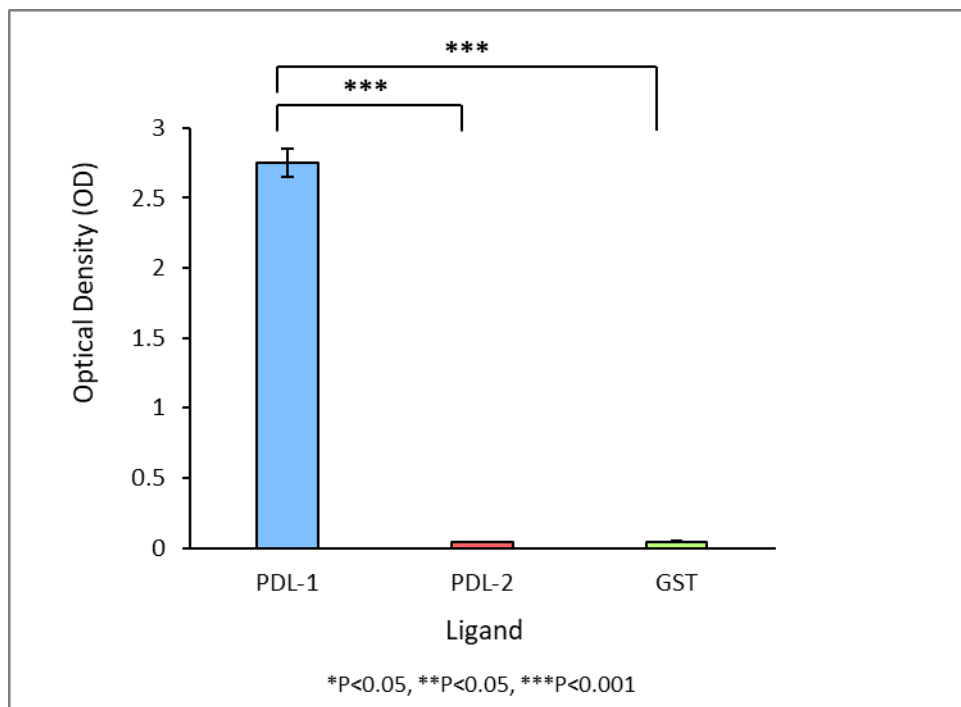


Figure 3.7.2. Analysis of sPD1^{HAC}.IgG binding to PD-L1, PD-L2 and Glutathione S-transferase (GST). 20 ng of sPD1^{HAC}.IgG was added to wells with PD-L1 (blue), PD-L2 (red) and GST (green) immobilised to the surface. Bound sPD1^{HAC} was detected using an anti-PD1 antibody and quantified via an enzyme-linked reaction. Coated wells incubated without sPD1^{HAC}.IgG were used as controls. All data are expressed as mean \pm SE of duplicate wells and are representative of three independent experiments.

To determine the minimum quantity of sPD1^{HAC}.IgG needed to maintain the competitive effect on rPD1, CHO supernatant containing sPD1^{HAC}.IgG in the amounts of 20 – 0.001 ng was incubated with 50 ng of rPD1. The results (Figure 3.7.3) show that even at a quantity of 0.1 ng sPD1^{HAC}.IgG can exert competitive binding effects. In this condition 16% less rPD1 binds to PD-L1 compared to the control sample. Binding of sPD1^{HAC}.IgG is no longer detected with 0.01 ng protein in the sample. These results display that even when rPD1 is in excess of 500:1 to sPD1^{HAC}.IgG, there is still a blocking effect of rPD1/PD-L1.

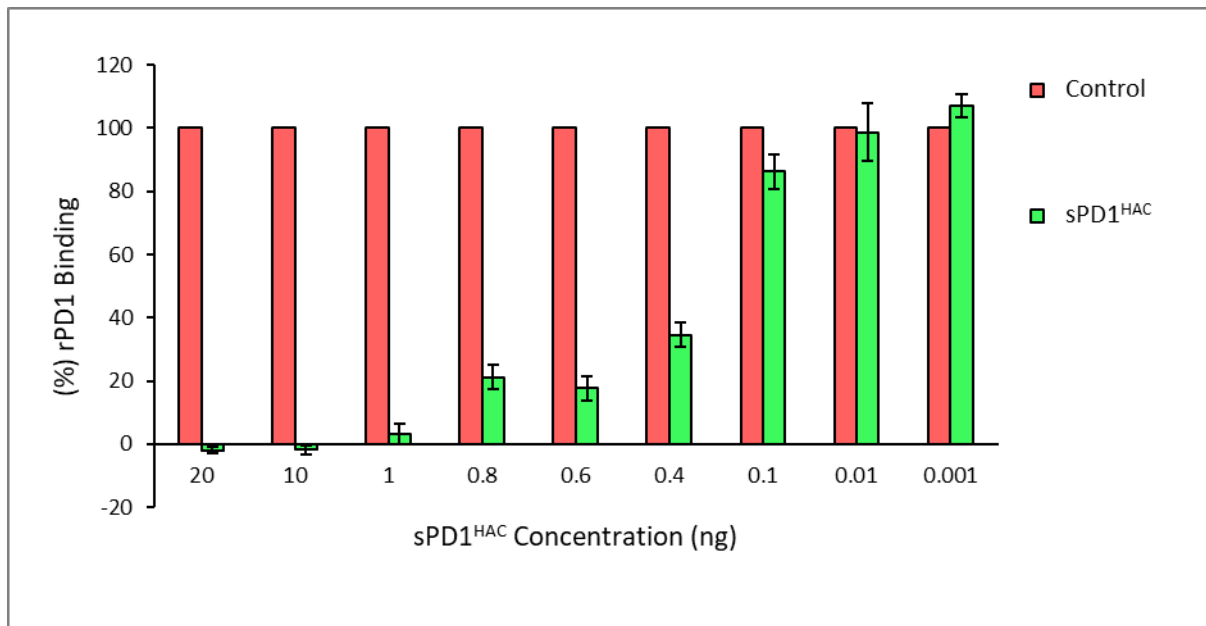


Figure 3.7.3. Determination of the minimum quantity of sPD1^{HAC}.IgG required to outcompete 50 ng of recombinant PD1 (rPD1). A microplate with 100 ng of PD-L1 attached to the surface of each well was treated with sPD1^{HAC}.IgG quantities ranging from 20 ng to 0.001 ng together with 50 ng of rPD1. All data are expressed as mean \pm SE of duplicate wells and are representative of three independent experiments.

To ensure that sPD1^{HAC}.IgG does not denature or lose function in an acidic environment which might exist inside of tumours, a solid-phase competition assay was conducted in buffers with pH values of 6.5 and 7.5. Cell supernatant containing 0.1 ng of sPD1^{HAC}.IgG was incubated with 20 ng of rPD1. For comparison, a control sample was used which consisted of supernatant from non-transfected cells. The results (Figure 3.7.4) reveal that sPD1^{HAC}.IgG binding to PD-L1 is not affected by a lowering of pH - 0.1 ng of sPD1^{HAC}.IgG outcompetes approximately 19% of rPD1 at pH 6.5 and 28% at pH 7.5. These results suggest that sPD1^{HAC}.IgG could still be effective within a tumour microenvironment.

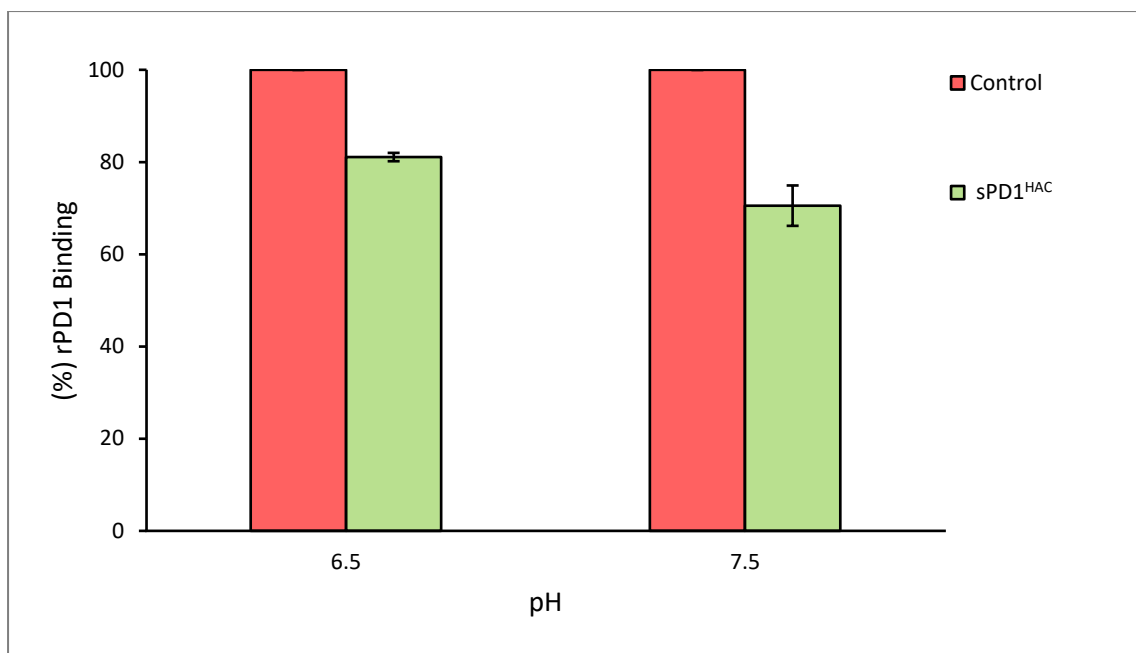


Figure 3.7.4 sPD1^{HAC}.IgG binding to PD-L1 in a solid-phase protein competition assay at pH values of 6.5 and 7.5.

A microplate with 100 ng of PD-L1 attached to the surface of each well was treated with 0.1ng sPD1^{HAC}.IgG and 20ng rPD1. The control sample contains supernatant from non-transfected cells. All data is expressed as mean \pm SE of duplicate wells and are representative of two independent experiments.

3.8. Analysis of sPD1^{HAC}.IgG binding to PD-L1 in a cellular competition assay

To ensure sPD1^{HAC}.IgG exhibits the same binding affinity to a membrane-bound PD-L1 as to plate-bound PD-L1, protein binding was tested in a cellular competition assay. The sPD1^{HAC}.IgG test sample consisted of PD-L1-positive PancTul cells, which were incubated with 50 ng of sPD1^{HAC}.IgG and 50 ng of rPD1. The results (Figure 3.8.1) show a drastic reduction in rPD1 binding to PD-L1 in the sPD1^{HAC}.IgG test sample compared to the control sample where no sPD1^{HAC}.IgG is present. The test sample and isotype sample both exhibit the same signal indicating that sPD1^{HAC}.IgG is completely outcompeting the rPD1 binding in the test sample. These results suggest that sPD1^{HAC}.IgG will be effective in blocking the PD-L1 signal from cancer cells in an *in vivo* setting.

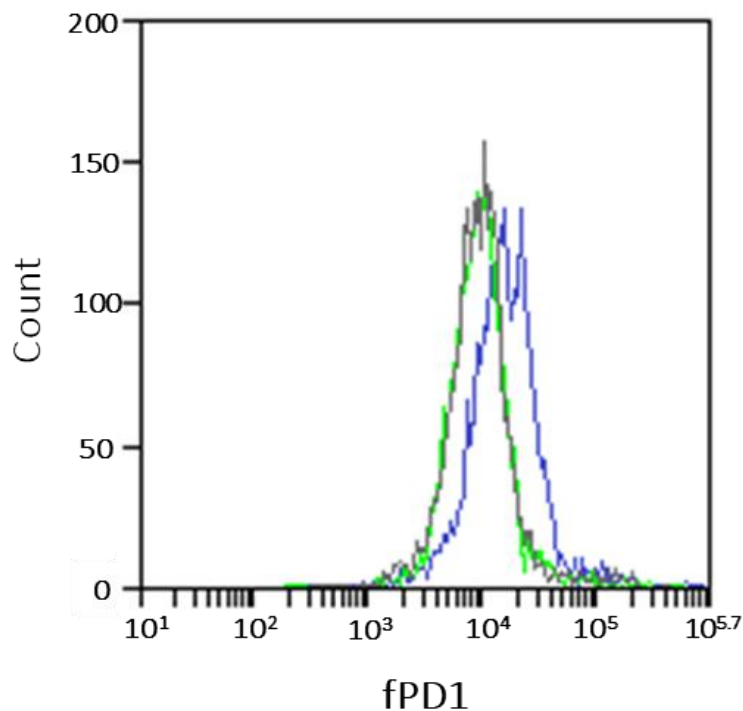


Figure 3.8.1. Flow cytometry results showing competitive binding of recombinant PD1 (rPD1) and sPD1^{HAC} to PD-L1 on the surface of PancTul cells. PancTul cells were stimulated with IFN- γ to induce PD-L1 expression on their surface. The binding affinity of sPD1^{HAC} to PD-L1 was then analysed in a competition assay where sPD1^{HAC} competes for the binding site of PD-L1 on the surface of PancTul cells with rPD1—a commercial recombinant PD1 protein engineered with a biotin tag. First the full binding capacity of rPD1 was tested (blue) – 2×10^6 PancTul cells were coated with 50 ng of rPD1 and the bound rPD1 was detected with streptavidin-PE conjugate and the signal intensity was measured via flow cytometry. To observe protein competition (green), 2×10^6 PancTul cells were incubated with 50 ng of sPD1^{HAC} and 50 ng of rPD1. Unbound protein was washed away and PancTul cells were incubated with a streptavidin-PE conjugate and the signal intensity was measured. A negative control to detect background radiation (grey) was tested by incubating 2×10^6 PancTul cells with the streptavidin-PE conjugate.

3.9. sPD1^{HAC}.IgG adenoviral vector generation

The affinity of sPD1^{HAC}.IgG to PD-L1 is very strong, even at small concentrations. It is much more effective than any of the other sPD1 variants at inhibiting the binding between rPD1 and PD-L1 and was selected as a suitable candidate for further studies. The sPD1^{HAC}.IgG fragment was cloned into an adenoviral expression vector - pAd/CMV/V5-DEST. With this plasmid an adenoviral vector (Ad.CMV.sPD1^{HAC}) was produced and purified by a company (Vector Biolabs) which was then used to transduce MSCs. A plasmid map for Ad.CMV.sPD1^{HAC} is shown in Figure 3.9.1.

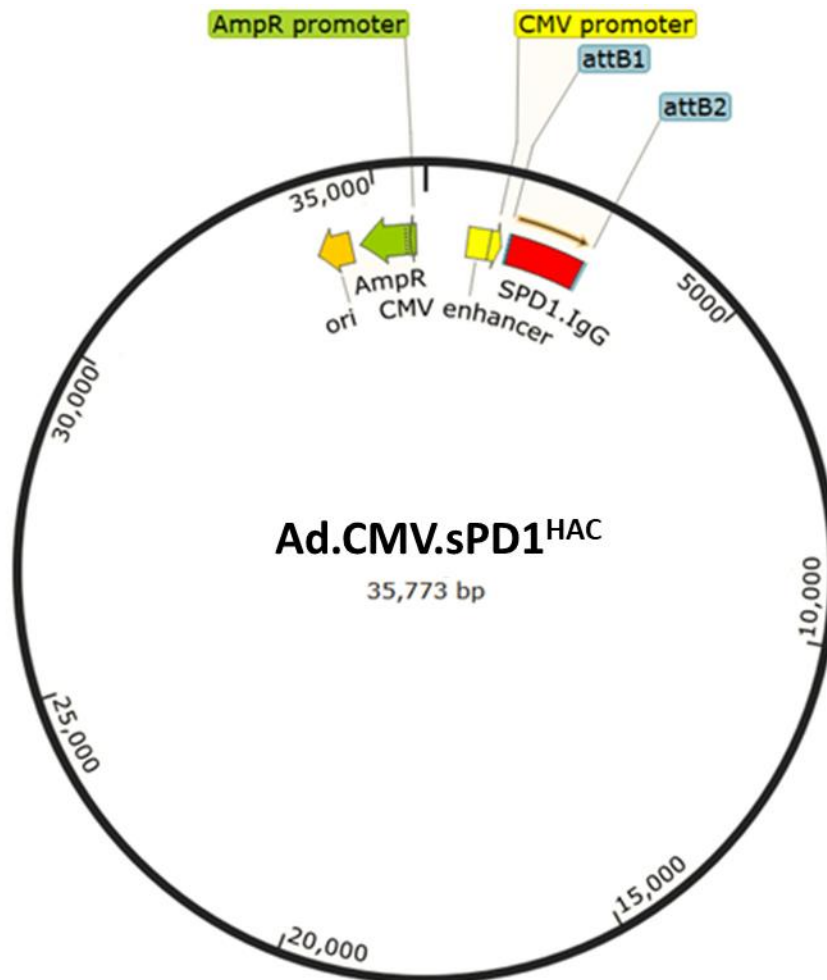


Figure 3.9.1. Plasmid map of the Ad.CMV.sPD1^{HAC} construct. A plasmid map showing a recombinant 35,773 bp construct containing the sPD1^{HAC}.IgG fragment (red) within a pAd/CMV/V5-DEST adenoviral expression vector. The vector contains an Ampicillin resistance gene (green) to allow selection, and a CMV promoter and enhancer (yellow) required for transient expression of the transgene.

The supernatant of the MSCs was harvested and analysed via ELISA (Figure 3.9.2). The results revealed that the sPD1^{HAC}.IgG protein was successfully produced and secreted by MSCs at the concentration of 6.55 ng / mL. The control used alongside the sample is supernatant from MSCs transduced with a control adenoviral vector.

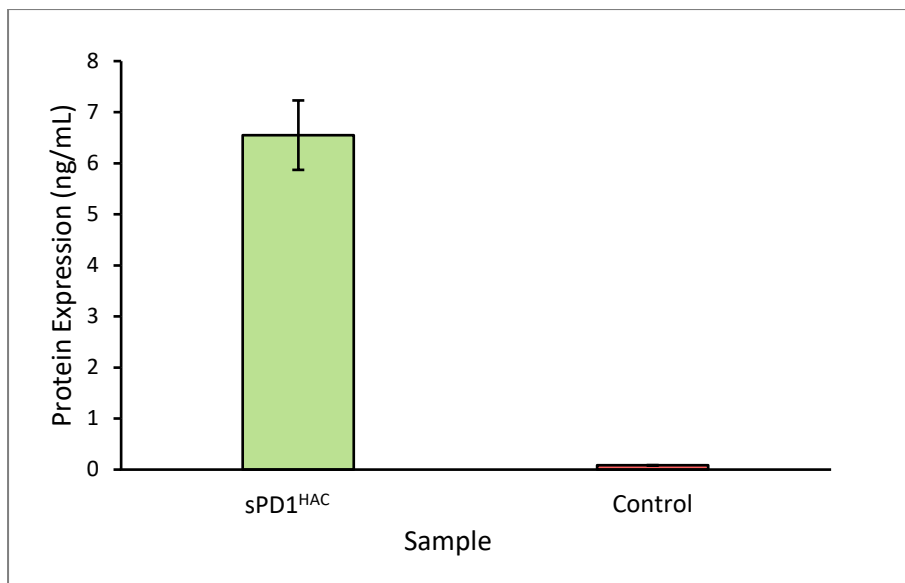


Figure 3.9.2. ELISA results showing protein concentration of sPD1^{HAC}.IgG secreted by mesenchymal stem cells (MSCs). A recombinant Ad.CMV.sPD1^{HAC} vector was used to transduce MSCs. The supernatant was harvested, and protein expression was analysed via ELISA. The negative control is a sample of MSC supernatant from cells transfected with a control vector. Data is expressed as mean \pm SE of triplicate wells and are representative of two independent experiments.

The generation of sPD1^{HAC}.IgG -expressing MSCs was successful, and these cells can be used in future *in vivo* experiments to deliver sPD1^{HAC} to tumours to block the PD1/PD-L1 pathway and act as an immune checkpoint inhibitor.

DISCUSSION

In this study, sPD1 variants with stronger binding characteristics to PD-L1 than the wild-type sPD1 were engineered. They were produced in CHO cells and successfully secreted into the medium. After having confirmed protein expression and measured protein concentration, they were analysed in vitro with the use of solid-phase and live pancreatic cell assays to determine the effectiveness of the variants at outcompeting the sPD1^{WT} binding to PD-L1. Protein variants were generated via MMBSA computational modelling studies and one variant was found through a literature search. The sPD1 variants designed via the MMPBSA computational molecular method showed modestly increased binding affinities. While the single point mutations led to a change in binding properties of sPD1 variant proteins, their affinity was not improved enough for them to be deemed effective as an anti-PD-L1 therapeutic. The sPD1^{HAC}.IgG variant which contains mutations identified via directed evolution with yeast-surface display by Maute et al (2015) revealed itself to be far more effective. Perhaps the reason for such a drastic difference in binding affinities between sPD1^{HAC}.IgG and our variants, is that sPD1^{HAC}.IgG contains ten point mutations, while sPD1¹ and sPD1²⁷ only contain one. The stacking of multiple mutations considerably increases protein binding.

The sPD1^{HAC}.IgG variant was found to outcompete sPD1^{WT} 500-fold even at very low concentrations. Protein functionality testing revealed that sPD1^{HAC}.IgG binds to PD-L1 specifically and does not bind to PD-L2 and unrelated proteins thus posing as a promising candidate for anti- PD-L1 therapy. The sPD1^{HAC}.IgG variant was engineered into MSCs and the protein was successfully expressed and secreted from these cells too. The engineered MSCs can provide a novel anti- PD-L1 therapeutic for difficult to treat cancer types such as pancreatic cancer.

PD1^{HAC} was generated through a directed evolution with yeast-surface display (Maute et al., 2015). The point amino acid substitutions present in the DNA sequence compose of 8 contact residues and 2 core residues. This study used plasmon resonance to reveal sPD1^{HAC} has a 15,000-40,000-fold increase in affinity for PD-L1 compared to the wild-type. Molecular dynamics of the structure of the PD1^{HAC} /PD-L1 complex show the mechanisms by which the point mutations enhance binding affinity (Pascolutti, 2016). The complex has close resemblance to the structure of wild-type human PD1/PD-L1 complex, with a few key changes. PD1^{HAC} engages in a more extensive polar network with PD-L1, which is likely contributing to the higher affinity of the protein. The polar interactions in the PD1^{HAC} mutant also show greater conformational stability than in the wild-type variant. The mutations cause formations of new hydrogen bonds and salt bridges between the PD1^{HAC} and PD-L1. Maute and colleagues tested PD1^{HAC} functionality by fusing it to a dimeric CH3 domain of a human IgG1 to create a HAC 'microbody'. It was

tested in *in vivo* studies in murine models of colon cancer alongside an anti-PD1 antibody to analyse PD-L1 binding and tumour penetrance. In PD-L1 positive tumours there was clear binding of both PD1^{HAC} and an anti-PD1 antibody, however in very different distributions. The antibody signal was mainly constrained to the peripheral regions of the tumour while the staining for PD1^{HAC} was widespread, confirming improved tissue penetrance. Tumour-size was significantly reduced with the use of PD1^{HAC} in comparison to antibody injection. More so, there is supporting evidence that a sPD1^{HAC}.IgG protein variant would be more effective than an antibody in antagonizing the PD1/PD-L1 pathway *in vivo*. Mice injected with anti-mouse PD-L1 antibody exhibited a 15% decrease in circulating peripheral blood CD8+ T cells (Maute et al., 2015) – an effect that was not visible after administration with PD1^{HAC}.

In our study, instead of a microbody, the PD1^{HAC} protein was engineered as a soluble IgG1-Fc fusion protein. We found that the IgG1-Fc significantly increases the stability of the protein and leads to increased protein secretion while conferring no negative effects to protein functionality. The IgG1-Fc group is known to allow easier protein expression and can improve the solubility and stability of the fused partner molecule both *in vitro* and *in vivo* as well as conferring several other beneficial biological and pharmacological properties to proteins (Czajkowsky et al., 2012). Notably, the presence of the Fc domain extends the plasma half-life of protein thus prolonging therapeutic activity. This is due to the reduced renal filtration and elimination rate of larger molecules (Kontermann, 2011) and the Fc domain interacting with neonatal Fc-receptor (FcRn) in a pH-dependant manner. This prevents the protein from being degraded in endosomes and instead allows it to be released back into circulation (Roopenian and Akilesh, 2007). Through the binding of Fc to its receptor Fc-gamma receptor (FcγR), immune system cells expressing FcγRs are recruited and activated, triggering antibody-dependant cell-mediated cytotoxicity (ADCC). ADCC destroys and clears target cells (including tumour cells) via the secretion of various substances (perforin, granzyme, TNF) that mediate target cell destruction (Wang et al., 2015). In addition to this, Fc binding to the serum complement molecule (C1q) initiates complement-dependant cytotoxicity (CDC) by initiating the assembly of a membrane attack complex (Meyer et al., 2014). Out of the four IgG subtypes, IgG1 has the highest affinity to FcγRs and is one of the most cytotoxic IgG groups (Bruhns et al., 2009). These features make IgG1-Fc desirable in oncological therapies which selectively target tumour cells for destruction and therefore may increase the effectiveness of sPD1^{HAC} as a therapeutic.

Based on the recent evidence that PD-L1 exists in a dimeric state (Lin et al., 2008; Chen et al., 2010), an sPD1 tetramerisation variant (sPD1^{TETR}) was produced and analysed to determine improved binding abilities. Solid-phase analyses revealed that sPD1^{TETR} possesses slightly stronger binding characteristics to PD-L1 in comparison to sPD1^{WT}. These results may support the hypothesis that PD-L1 interacts in a dimeric manner and sPD1^{TETR} may be decreasing the off-rate of the reaction by promoting dimerization

by decreasing the entropic penalty compared to when monomeric sPD1 proteins are distributed randomly. Our results show that in non-IgG-Fc fusion sPD1 variants introduction of a tetramerisation site does not interfere with protein production or secretion and therefore tetramerisation does not seem to destabilise the protein. However, the combination of the IgG-Fc domain with a tetramerisation domain results in significantly decreased protein concentration in the supernatant. This is likely due to the fact that the CH3 domains within the Fc interact with each other to form homodimers resulting in dimerization of Fc (Yu et al., 2017). The Fc dimerization site and introduced p53 tetramerisation site likely combine to produce a protein aggregate with decreased stability. Due to this it is unlikely that an sPD1^{HAC/TETR}.IgG mutant would have improved therapeutic functionality as its potentially higher binding activity is compromised by the lower expression levels.

Protein binding analyses show that at pH values of 6.5 and 7.5 sPD1^{HAC}.IgG maintains a comparable binding affinity to PD-L1. Tumour microenvironment pH values can range from 5.5 – 7 (Justus et al., 2013), so it is vital that sPD1^{HAC}.IgG can maintain its function in such conditions. Our results did not show any evidence of pH-dependent affinity in sPD1^{HAC} – a contrasting result to Pascolutti et al (2016) who reported pseudo-irreversible binding to PD-L1 in low pH conditions. They found that at a pH of 6.5 the affinity to PD1 increased 100-fold compared to a basic environment and the interaction became so strong at pH 5.5, it no longer showed any detectable dissociation in a 600 second timeframe. Perhaps the reason these effects were not observed in our study is due to the editing of PD1^{HAC} into a soluble, secreted protein which alters its structure in such a way that limits the pH effects. Another explanation for the discrepancy in the results may be the difference in the nature of the IgG molecule fused to the protein. The sPD1^{HAC}.IgG protein contains both CH2 and CH3 domains of the human heavy chain and hinge region. Instead, in the Pascolutti study PD1^{HAC} is fused only to a dimeric CH3 domain. The study states that lower pH conditions stabilise the PD1^{HAC} structure and in turn increase binding affinity of PD1^{HAC} to PD-L1. It has been observed that CH2 domain exerts a certain level of stability to proteins and the presence of this domain in our sPD1^{HAC}.IgG variant may already exert a degree of protein stabilization to the protein; perhaps in such a way that limits pH-dependant stabilisation. PD1^{HAC} was produced in insect cells while we produced the sPD1^{HAC}.IgG variant in mammalian cells. One of the main differences in the two systems, is that insect cells are unable to produce complex, terminally sialylated *N*-glycans such as those produced by mammalian cells. These side-chains are instead replaced by paucimannosidic *N*-glycans, which are not found in mammalian cells (Shi and Jarvis., 2007). These slight changes in the modifications of the protein may be generating a protein surface that is affected differently by pH variations.

The inhibitory signals transduced by PD1 in T cells have been well characterised, however the activities of PD-L1 have been less so. Recent hypothesis suggests that PD-L1 can propagate signals in the cell on

which it is expressed (Lecis et al., 2019). This reverse signalling is not very well defined; however, research suggests that it can deliver pro-proliferative and protective signals to the tumour (Jalali et al., 2019). This poses a challenge in anti-PD-L1 therapies as the prolonged binding to PD-L1 by high-affinity therapeutics may inadvertently trigger pro-tumour signalling in cancer cells, thus affecting the clinical outcome of the therapy. There is evidence to show that in the case of neoplastic cells, the short intracytoplasmic tail of PD-L1 contains signal transduction motifs that mediate cell protection through a STAT3/caspase-7-mediated pathway (Gato-Cañas et al., 2017). This protective function ultimately contributes to tumour growth and progression. One study found that PD-L1 signalling promotes the EMT phenotype in human oesophageal cancer as well as playing roles in viability and migration (Chen et al., 2017). Another study demonstrated an association of PD-L1 with a stem-like phenotype and using PD-L1 knockout experiments found that PD-L1 is involved in maintaining stemness markers (Oct-4, Nanog, BMI1). Down-regulation of PD-L1 caused a reduction in the self-renewal capacity of breast cancer stem cells in both *in vitro* and *in vivo* (Almozyan et al., 2017). Antagonising PD-L1 engagement with an antibody in classical Hodgkin lymphoma cells resulted in increased proliferation and survival of cells and reduced apoptosis, likely through the activation of the MAPK pathway (Jalali et al., 2019). This finding highlights the importance of the need to characterise the mechanisms of PD-L1 signalling and its potential implications in therapy. It is crucial we monitor sPD1^{HAC}.IgG binding in pancreatic cancer cells to detect the extent, if any of the pro-proliferative signalling from PD-L1 as not to accelerate tumour growth.

In this study we successfully generated MSCs that secrete the sPD1^{HAC}.IgG protein, revealing a promising new method of targeting the PD1/PD-L1 pathway in pancreatic cancer. It must be noted however, that the expression of sPD1^{HAC}.IgG is significantly lower in MSCs than in the HEK293A cells and CHO cells. Future studies should attempt to increase the expression of sPD1^{HAC}.IgG in MSCs to maximise clinical potency. Although clinical trials demonstrate that MSC injection in high doses is safe (Lalu et al., 2016); systemic infusion of MSCs for therapeutic applications requires efficient migration and homing to the target tumour and this process is inefficient. There is abundant evidence of MSC homing, however only a small percentage of systematically administered MSCs actually reach the target tissue – typically less than 1% (Zhang et al., 2007). After injection, MSCs appear to be cleared and trapped in the lungs, compromising homing to target tissues. It also appears that MSCs downregulate the expression of homing molecules during *in vitro* expansion (Rombouts and Ploemacher, 2003). There is a lot of interest in current research to increase the homing efficacy of MSCs; the strategies involve specific cell preconditioning and modification of culture conditions. For example, an important homing molecule on the cell surface – CXCR4 can be increased by the addition of cytokines or cytokine cocktails to the culture medium during MSC expansion. Exposure to flt3 ligand, stem cell factor (SCF), IL-3, IL-6 and HGF

was found to increase both the intracellular and membrane expression of CXCR4 on cultured MSCs (Shi et al., 2007). However, the degree of improvement in homing efficiency that these methods provide is still unclear and MSCs should be engineered to be as efficient as possible in providing the drug load.

These cells can be used in future *in vivo* assays to determine the effectiveness MSC therapy at delivering an anti-PD-L1 therapeutic agent to pancreatic cancer. The ability of MSCs to accumulate at tumour sites is indeed an attractive feature for directed cancer therapy, however MSCs are not inert vectors and have their own properties that can affect tumour growth. Current literature is divided on the effects of MSCs on cancer growth, with research indicating MSCs can exert both pro-tumour and anti-tumour effects. One important feature of MSCs that needs to be considered in the context of cancer immunotherapy, is the profound immunosuppressive effects they possess. Numerous studies converged on the findings that MSCs contribute to cancer pathogenesis via the release of inflammatory factors which promote immunosuppressive effects. One study found that human MSCs exert immunosuppressive effects through the production of indoleamine 2,3-dioxygenase (IDO) (Ling et al., 2015). These IDO-expressing MSCs were capable of suppressing T cell proliferation *in vitro* and dramatically reduced both tumour-infiltrating CD8⁺ T cells and B cells. Another study revealed that MSCs isolated from gastric tumours mediate cancer progression through the secretion of IL-8 – a pro-inflammatory chemokine involved in the recruitment of leukocytes (Li et al., 2015). Leukocytes such as macrophages and neutrophils are known to be involved in cancer initiation and progression (Guo et al., 2017, Powell et al., 2018). MSCs can also secrete TGF β which can promote macrophage infiltration at the tumour site and facilitates tumour escape from immune surveillance. The ability of MSCs to create an immunosuppressive environment is unfavourable in cancer checkpoint inhibition therapy as it can negate or reduce the effects of delivered sPD1 and limit overall therapeutic outcome.

Compelling evidence also points to the role of MSCs in tumour angiogenesis. For instance, bone-marrow derived MSCs were found to increase the expression of angiogenic factors (TGF β , VEGF and IL-6) which contribute to tumour vascularization and growth (Zhang et al., 2013). A correlation between expression of TGF β 1 and higher microvessel density was observed in hepatocellular carcinomas in mice that received intravenous injections of human MSCs (Li et al., 2016). Another issue with the use of MSCs is their potential to promote metastasis. MSCs can induce cancer cell distribution in tumours that would not normally form metastatic lesions, however MSCs do not further increase metastasis in tumours with a high metastatic potential (Albarenque, 2011). PDAC has an unusually high tendency for metastasis, and it is therefore likely that MSCs introduction would not further increase the metastatic potential. On top of this, MSCs can differentiate into cancer-associated fibroblasts (CAFs) due to soluble factors secreted from cancer cells. CAFs contribute to tumour progression due to their active secretome which includes immune-modulating agents (CXCL12, GM-CSF), pro-angiogenic factors (VEGF, TGF β ,

PDGF), pro-survival factors (Hepatocyte GF, Insulin-like GF, IL6), and extracellular matrix modulators (MMP, Tissue Inhibitor of Metalloproteinases) among others (Kalluri, 2016). The aforementioned factors have the potential to exacerbate tumour growth and could lead to an adverse clinical response. The goal is to one day re-engineer MSCs and develop safer cells which lack the expression of pro-tumour factors for a safer treatment of cancer.

Interestingly recent research indicates that MSCs may promote apoptosis and suppress growth of glioma cells through downregulation of the PI3K/AKT signalling pathway (Lu et al., 2019). They found that treatment with human bone-marrow derived MSCs could suppress phosphorylation of PI3K and AKT in U251 cells. This pathway is related to advancement of cell proliferation, suppression of apoptosis, change in cell cycle distribution, promotion of invasion, and induction of EMT in most tumour cells. In pancreatic cancer cells, downregulation of the PI3K/Akt pathway induced cell cycle apoptosis and G1 phase cell cycle arrest and suppressed EMT (Xu et al., 2014). The PI3K/Akt pathway is one of the signalling cascades inhibited by PD1 and is one of the targets for sPD1^{HAC}.IgG. MSC-induced downregulation of this pathway could enhance the therapeutic effects of sPD1^{HAC}.IgG and provide a better overall clinical outcome.

Overall, while MSC-based drug delivery is extremely promising, a number of issues have to be addressed. Notwithstanding MSCs have the advantage that they would act as a drug depot within the tumour site and through a continuous release of sPD1^{HAC}.IgG would extend the time frame of sufficiently high drug concentration to exert pharmacological activity. In this way renal clearance is further overcome by the constant release of the protein into circulation. However, due to the conflicting actions of MSCs they should only be used in a clinical setting after a detailed risk-benefit analysis.

CONCLUSIONS

In this study we generated engineered MSCs which successfully produce and secrete a soluble, high-affinity PD1 protein variant (sPD1^{HAC}.IgG). The sPD1^{HAC}.IgG exhibits success in antagonising the PD1/PD-L1 pathway *in vitro* in solid-phase and live pancreatic cell assays. The MSCs offer a novel delivery vector to transport this immune-therapeutic into pancreatic cancer and has the potential to overcome current challenges with drug delivery into the pancreatic microenvironment. Despite the great promise of using MSCs to target cancers, they are associated with several unfavourable biological side effects and should be used with caution until they can be overcome.

BIBLIOGRAPHY

- . "Pancreatic cancer statistics." Retrieved 14 September, 2019, from <https://www.pancreaticcancer.org.uk/statistics/>.
- Agata, Y., A. Kawasaki, H. Nishimura, Y. Ishida, T. Tsubata, H. Yagita and T. Honjo (1996). "Expression of the PD-1 antigen on the surface of stimulated mouse T and B lymphocytes." *Int Immunol* **8**(5): 765-772.
- Albarenque, S. M., R. M. Zwacka and A. Mohr (2011). "Both human and mouse mesenchymal stem cells promote breast cancer metastasis." *Stem Cell Res* **7**(2): 163-171.
- Almozyan, S., D. Colak, F. Mansour, A. Alaiya, O. Al-Harazi, A. Qattan, F. Al-Mohanna, M. Al-Alwan and H. Ghebeh (2017). "PD-L1 promotes OCT4 and Nanog expression in breast cancer stem cells by sustaining PI3K/AKT pathway activation." *Int J Cancer* **141**(7): 1402-1412.
- Ansell, S. M., A. M. Lesokhin, I. Borrello, A. Halwani, E. C. Scott, M. Gutierrez, S. J. Schuster, M. M. Millenson, D. Cattray, G. J. Freeman, S. J. Rodig, B. Chapuy, A. H. Ligon, L. Zhu, J. F. Grosso, S. Y. Kim, J. M. Timmerman, M. A. Shipp and P. Armand (2015). "PD-1 blockade with nivolumab in relapsed or refractory Hodgkin's lymphoma." *N Engl J Med* **372**(4): 311-319.
- Apte, M. V., S. Park, P. A. Phillips, N. Santucci, D. Goldstein, R. K. Kumar, G. A. Ramm, M. Buchler, H. Friess, J. A. McCarroll, G. Keogh, N. Merrett, R. Pirola and J. S. Wilson (2004). "Desmoplastic reaction in pancreatic cancer: role of pancreatic stellate cells." *Pancreas* **29**(3): 179-187.
- Apte, M. V. and J. S. Wilson (2012). "Dangerous liaisons: pancreatic stellate cells and pancreatic cancer cells." *J Gastroenterol Hepatol* **27 Suppl 2**: 69-74.
- Arasanz, H., M. Gato-Cañas, M. Zuazo, M. Ibañez-Vea, K. Breckpot, G. Kochan and D. Escors (2017). "PD1 signal transduction pathways in T cells." *Oncotarget* **8**(31): 51936-51945.
- Arvelo, F., F. Sojo and C. Cotte (2016). "Tumour progression and metastasis." *Ecanccermedicalscience* **10**: 617.
- Bachem, M. G., E. Schneider, H. Gross, H. Weidenbach, R. M. Schmid, A. Menke, M. Siech, H. Beger, A. Grünert and G. Adler (1998). "Identification, culture, and characterization of pancreatic stellate cells in rats and humans." *Gastroenterology* **115**(2): 421-432.
- Bachem, M. G., M. Schünemann, M. Ramadani, M. Siech, H. Beger, A. Buck, S. Zhou, A. Schmid-Kotsas and G. Adler (2005). "Pancreatic carcinoma cells induce fibrosis by stimulating proliferation and matrix synthesis of stellate cells." *Gastroenterology* **128**(4): 907-921.
- Balar, A. V. and J. S. Weber (2017). "PD-1 and PD-L1 antibodies in cancer: current status and future directions." *Cancer Immunol Immunother* **66**(5): 551-564.
- Bardhan, K., T. Anagnostou and V. A. Boussiotis (2016). "The PD1:PD-L1/2 Pathway from Discovery to Clinical Implementation." *Front Immunol* **7**: 550.
- Beatty, G. L., E. G. Chiorean, M. P. Fishman, B. Saboury, U. R. Teitelbaum, W. Sun, R. D. Huhn, W. Song, D. Li, L. L. Sharp, D. A. Torigian, P. J. O'Dwyer and R. H. Vonderheide (2011). "CD40 agonists alter tumor stroma and show efficacy against pancreatic carcinoma in mice and humans." *Science* **331**(6024): 1612-1616.
- Beckman, R. A., L. M. Weiner and H. M. Davis (2007). "Antibody constructs in cancer therapy: protein engineering strategies to improve exposure in solid tumors." *Cancer* **109**(2): 170-179.
- Birnbaum, D. J., P. Finetti, A. Lopresti, M. Gilabert, F. Poizat, O. Turrini, J. L. Raoul, J. R. Delpero, V. Moutardier,

D. Birnbaum, E. Mamessier and F. Bertucci (2016). "Prognostic value of PDL1 expression in pancreatic cancer." *Oncotarget* **7**(44): 71198-71210.

Borghaei, H., L. Paz-Ares, L. Horn, D. R. Spigel, M. Steins, N. E. Ready, L. Q. Chow, E. E. Vokes, E. Felip, E. Holgado, F. Barlesi, M. Kohlhäufel, O. Arrieta, M. A. Burgio, J. Fayette, H. Lena, E. Poddubskaya, D. E. Gerber, S. N. Gettinger, C. M. Rudin, N. Rizvi, L. Crinò, G. R. Blumenschein, S. J. Antonia, C. Dorange, C. T. Harbison, F. Graf Finckenstein and J. R. Brahmer (2015). "Nivolumab versus Docetaxel in Advanced Nonsquamous Non-Small-Cell Lung Cancer." *N Engl J Med* **373**(17): 1627-1639.

Boussiotis, V. A. (2016). "Molecular and Biochemical Aspects of the PD-1 Checkpoint Pathway." *N Engl J Med* **375**(18): 1767-1778.

Bray, F., J. Ferlay, I. Soerjomataram, R. L. Siegel, L. A. Torre and A. Jemal (2018). "Global cancer statistics 2018: GLOBOCAN estimates of incidence and mortality worldwide for 36 cancers in 185 countries." *CA Cancer J Clin* **68**(6): 394-424

Bruhns, P., B. Iannascoli, P. England, D. A. Mancardi, N. Fernandez, S. Jorieux and M. Daëron (2009). "Specificity and affinity of human Fcγ receptors and their polymorphic variants for human IgG subclasses." *Blood* **113**(16): 3716-3725.

Chames, P., M. Van Regenmortel, E. Weiss and D. Baty (2009). "Therapeutic antibodies: successes, limitations and hopes for the future." *Br J Pharmacol* **157**(2): 220-233.

Chan, D. A. and A. J. Giaccia (2007). "Hypoxia, gene expression, and metastasis." *Cancer Metastasis Rev* **26**(2): 333-339.

Chemnitz, J. M., R. V. Parry, K. E. Nichols, C. H. June and J. L. Riley (2004). "SHP-1 and SHP-2 associate with immunoreceptor tyrosine-based switch motif of programmed death 1 upon primary human T cell stimulation, but only receptor ligation prevents T cell activation." *J Immunol* **173**(2): 945-954.

Chen, J., C. C. Jiang, L. Jin and X. D. Zhang (2016). "Regulation of PD-L1: a novel role of pro-survival signalling in cancer." *Ann Oncol* **27**(3): 409-416.

Chen, L. and D. B. Flies (2013). "Molecular mechanisms of T cell co-stimulation and co-inhibition." *Nat Rev Immunol* **13**(4): 227-242.

Chen, L., Y. Xiong, J. Li, X. Zheng, Q. Zhou, A. Turner, C. Wu, B. Lu and J. Jiang (2017). "PD-L1 Expression Promotes Epithelial to Mesenchymal Transition in Human Esophageal Cancer." *Cell Physiol Biochem* **42**(6): 2267-2280.

Chen, T., Q. Li, Z. Liu, Y. Chen, F. Feng and H. Sun (2019). "Peptide-based and small synthetic molecule inhibitors on PD-1/PD-L1 pathway: A new choice for immunotherapy?" *Eur J Med Chem* **161**: 378-398.

Chen, X., M. Song, B. Zhang and Y. Zhang (2016). "Reactive Oxygen Species Regulate T Cell Immune Response in the Tumor Microenvironment." *Oxid Med Cell Longev* **2016**: 1580967.

Chen, Y., P. Liu, F. Gao, H. Cheng, J. Qi and G. F. Gao (2010). "A dimeric structure of PD-L1: functional units or evolutionary relics?" *Protein Cell* **1**(2): 153-160.

Cheng, S., S. K. Nethi, S. Rath, B. Layek and S. Prabha (2019). "Engineered Mesenchymal Stem Cells for Targeting Solid Tumors: Therapeutic Potential beyond Regenerative Therapy." *J Pharmacol Exp Ther* **370**(2): 231-241.

Comerford, K. M., T. J. Wallace, J. Karhausen, N. A. Louis, M. C. Montalto and S. P. Colgan (2002). "Hypoxia-inducible factor-1-dependent regulation of the multidrug resistance (MDR1) gene." *Cancer Res* **62**(12): 3387-3394.

Czajkowsky, D. M., J. Hu, Z. Shao and R. J. Pleass (2012). "Fc-fusion proteins: new developments and future

perspectives." EMBO Mol Med **4**(10): 1015-1028.

Deng, L., H. Liang, B. Burnette, M. Beckett, T. Darga, R. R. Weichselbaum and Y. X. Fu (2014). "Irradiation and anti-PD-L1 treatment synergistically promote antitumor immunity in mice." J Clin Invest **124**(2): 687-695.

Dunn, G. P., A. T. Bruce, H. Ikeda, L. J. Old and R. D. Schreiber (2002). "Cancer immunoediting: from immunosurveillance to tumor escape." Nat Immunol **3**(11): 991-998.

Eliopoulos, N., M. Francois, M. N. Boivin, D. Martineau and J. Galipeau (2008). "Neo-organoid of marrow mesenchymal stromal cells secreting interleukin-12 for breast cancer therapy." Cancer Res **68**(12): 4810-4818.

Erkan, M., S. Hausmann, C. W. Michalski, A. A. Fingerle, M. Dobritz, J. Kleeff and H. Friess (2012). "The role of stroma in pancreatic cancer: diagnostic and therapeutic implications." Nat Rev Gastroenterol Hepatol **9**(8): 454-467.

Escors, D., M. Gato-Cañas, M. Zuazo, H. Arasanz, M. J. García-Granda, R. Vera and G. Kochan (2018). "The intracellular signalosome of PD-L1 in cancer cells." Signal Transduct Target Ther **3**: 26.

Fang, D. and Y. C. Liu (2001). "Proteolysis-independent regulation of PI3K by Cbl-b-mediated ubiquitination in T cells." Nat Immunol **2**(9): 870-875.

Francisco, L. M., V. H. Salinas, K. E. Brown, V. K. Vanguri, G. J. Freeman, V. K. Kuchroo and A. H. Sharpe (2009). "PD-L1 regulates the development, maintenance, and function of induced regulatory T cells." J Exp Med **206**(13): 3015-3029.

Gao, X., K. S. Kim and D. Liu (2007). "Nonviral gene delivery: what we know and what is next." AAPS J **9**(1): E92-104.

Gato-Cañas, M., M. Zuazo, H. Arasanz, M. Ibañez-Vea, L. Lorenzo, G. Fernandez-Hinojal, R. Vera, C. Smerdou, E. Martisova, I. Arozarena, C. Wellbrock, D. Llopiz, M. Ruiz, P. Sarobe, K. Breckpot, G. Kochan and D. Escors (2017). "PDL1 Signals through Conserved Sequence Motifs to Overcome Interferon-Mediated Cytotoxicity." Cell Rep **20**(8): 1818-1829.

Genheden, S. and U. Ryde (2015). "The MM/PBSA and MM/GBSA methods to estimate ligand-binding affinities." Expert Opin Drug Discov **10**(5): 449-461.

Gong, W., Q. Song, X. Lu, J. Zhao, P. Min and X. Yi (2011). "Paclitaxel induced B7-H1 expression in cancer cells via the MAPK pathway." J Chemother **23**(5): 295-299.

Green, M. R., S. Monti, S. J. Rodig, P. Juszczynski, T. Currie, E. O'Donnell, B. Chapuy, K. Takeyama, D. Neuberg, T. R. Golub, J. L. Kutok and M. A. Shipp (2010). "Integrative analysis reveals selective 9p24.1 amplification, increased PD-1 ligand expression, and further induction via JAK2 in nodular sclerosing Hodgkin lymphoma and primary mediastinal large B-cell lymphoma." Blood **116**(17): 3268-3277.

Greenwald, R. J., G. J. Freeman and A. H. Sharpe (2005). "The B7 family revisited." Annu Rev Immunol **23**: 515-548.

Guo, J., K. Xie and S. Zheng (2016). "Molecular Biomarkers of Pancreatic Intraepithelial Neoplasia and Their Implications in Early Diagnosis and Therapeutic Intervention of Pancreatic Cancer." Int J Biol Sci **12**(3): 292-301.

Guo, X., Y. Zhao, H. Yan, Y. Yang, S. Shen, X. Dai, X. Ji, F. Ji, X. G. Gong, L. Li, X. Bai, X. H. Feng, T. Liang, J. Ji, L. Chen, H. Wang and B. Zhao (2017). "Single tumor-initiating cells evade immune clearance by recruiting type II macrophages." Genes Dev **31**(3): 247-259.

Hanahan, D. and R. A. Weinberg (2011). "Hallmarks of cancer: the next generation." Cell **144**(5): 646-674.

Hirano, F., K. Kaneko, H. Tamura, H. Dong, S. Wang, M. Ichikawa, C. Rietz, D. B. Flies, J. S. Lau, G. Zhu, K. Tamada

- and L. Chen (2005). "Blockade of B7-H1 and PD-1 by monoclonal antibodies potentiates cancer therapeutic immunity." Cancer Res **65**(3): 1089-1096.
- Hiraoka, N., K. Onozato, T. Kosuge and S. Hirohashi (2006). "Prevalence of FOXP3+ regulatory T cells increases during the progression of pancreatic ductal adenocarcinoma and its premalignant lesions." Clin Cancer Res **12**(18): 5423-5434.
- Huse, M. (2009). "The T-cell-receptor signaling network." J Cell Sci **122**(Pt 9): 1269-1273.
- Hwang, R. F., T. Moore, T. Arumugam, V. Ramachandran, K. D. Amos, A. Rivera, B. Ji, D. B. Evans and C. D. Logsdon (2008). "Cancer-associated stromal fibroblasts promote pancreatic tumor progression." Cancer Res **68**(3): 918-926.
- Ikemizu, S., R. J. Gilbert, J. A. Fennelly, A. V. Collins, K. Harlos, E. Y. Jones, D. I. Stuart and S. J. Davis (2000). "Structure and dimerization of a soluble form of B7-1." Immunity **12**(1): 51-60.
- Ishida, Y., Y. Agata, K. Shibahara and T. Honjo (1992). "Induced expression of PD-1, a novel member of the immunoglobulin gene superfamily, upon programmed cell death." EMBO J **11**(11): 3887-3895.
- Jalali, S., T. Price-Troska, C. Bothun, J. Villasboas, H. J. Kim, Z. Z. Yang, A. J. Novak, H. Dong and S. M. Ansell (2019). "Reverse signaling via PD-L1 supports malignant cell growth and survival in classical Hodgkin lymphoma." Blood Cancer J **9**(3): 22.
- Justus, C. R., L. Dong and L. V. Yang (2013). "Acidic tumor microenvironment and pH-sensing G protein-coupled receptors." Front Physiol **4**: 354.
- Kalluri, R. (2016). "The biology and function of fibroblasts in cancer." Nat Rev Cancer **16**(9): 582-598.
- Kambayashi, T., J. Michaëlsson, L. Fahlén, B. J. Chambers, C. L. Sentman, K. Kärre and H. G. Ljunggren (2001). "Purified MHC class I molecules inhibit activated NK cells in a cell-free system in vitro." Eur J Immunol **31**(3): 869-875.
- Karwacz, K., C. Bricogne, D. MacDonald, F. Arce, C. L. Bennett, M. Collins and D. Escors (2011). "PD-L1 co-stimulation contributes to ligand-induced T cell receptor down-modulation on CD8+ T cells." EMBO Mol Med **3**(10): 581-592.
- Kikuta, K., A. Masamune, T. Watanabe, H. Ariga, H. Itoh, S. Hamada, K. Satoh, S. Egawa, M. Unno and T. Shimosegawa (2010). "Pancreatic stellate cells promote epithelial-mesenchymal transition in pancreatic cancer cells." Biochem Biophys Res Commun **403**(3-4): 380-384.
- Kinter, A. L., E. J. Godbout, J. P. McNally, I. Sereti, G. A. Roby, M. A. O'Shea and A. S. Fauci (2008). "The common gamma-chain cytokines IL-2, IL-7, IL-15, and IL-21 induce the expression of programmed death-1 and its ligands." J Immunol **181**(10): 6738-6746.
- Kontermann, R. E. (2011). "Strategies for extended serum half-life of protein therapeutics." Curr Opin Biotechnol **22**(6): 868-876.
- Koorstra, J. B., G. Feldmann, N. Habbe and A. Maitra (2008). "Morphogenesis of pancreatic cancer: role of pancreatic intraepithelial neoplasia (PanINs)." Langenbecks Arch Surg **393**(4): 561-570.
- Korc, M., B. Chandrasekar and G. N. Shah (1991). "Differential binding and biological activities of epidermal growth factor and transforming growth factor alpha in a human pancreatic cancer cell line." Cancer Res **51**(23 Pt 1): 6243-6249.
- Kunk, P. R., T. W. Bauer, C. L. Slingluff and O. E. Rahma (2016). "From bench to bedside a comprehensive review of pancreatic cancer immunotherapy." J Immunother Cancer **4**: 14.

Lalu, M. M., L. McIntyre, C. Pugliese, D. Fergusson, B. W. Winston, J. C. Marshall, J. Granton, D. J. Stewart and C. C. T. Group (2012). "Safety of cell therapy with mesenchymal stromal cells (SafeCell): a systematic review and meta-analysis of clinical trials." PLoS One **7**(10): e47559.

Lecis, D., S. Sangaletti, M. P. Colombo and C. Chiodoni (2019). "Immune Checkpoint Ligand Reverse Signaling: Looking Back to Go Forward in Cancer Therapy." Cancers (Basel) **11**(5).

Li, G. C., H. W. Zhang, Q. C. Zhao, L. I. Sun, J. J. Yang, L. Hong, F. Feng and L. Cai (2016). "Mesenchymal stem cells promote tumor angiogenesis via the action of transforming growth factor β 1." Oncol Lett **11**(2): 1089-1094.

Li, W., Y. Zhou, J. Yang, X. Zhang, H. Zhang, T. Zhang, S. Zhao, P. Zheng, J. Huo and H. Wu (2015). "Gastric cancer-derived mesenchymal stem cells prompt gastric cancer progression through secretion of interleukin-8." J Exp Clin Cancer Res **34**: 52.

Lin, D. Y., Y. Tanaka, M. Iwasaki, A. G. Gittis, H. P. Su, B. Mikami, T. Okazaki, T. Honjo, N. Minato and D. N. Garboczi (2008). "The PD-1/PD-L1 complex resembles the antigen-binding Fv domains of antibodies and T cell receptors." Proc Natl Acad Sci U S A **105**(8): 3011-3016.

Ling, Q., X. Xu, X. Wei, W. Wang, B. Zhou, B. Wang and S. Zheng (2011). "Oxymatrine induces human pancreatic cancer PANC-1 cells apoptosis via regulating expression of Bcl-2 and IAP families, and releasing of cytochrome c." J Exp Clin Cancer Res **30**: 66.

Ling, W., J. Zhang, Z. Yuan, G. Ren, L. Zhang, X. Chen, A. B. Rabson, A. I. Roberts, Y. Wang and Y. Shi (2014). "Mesenchymal stem cells use IDO to regulate immunity in tumor microenvironment." Cancer Res **74**(5): 1576-1587.

Lu, L., G. Chen, J. Yang, Z. Ma, Y. Yang, Y. Hu, Y. Lu, Z. Cao, Y. Wang and X. Wang (2019). "Bone marrow mesenchymal stem cells suppress growth and promote the apoptosis of glioma U251 cells through downregulation of the PI3K/AKT signaling pathway." Biomed Pharmacother **112**: 108625.

Luke, J. J., K. T. Flaherty, A. Ribas and G. V. Long (2017). "Targeted agents and immunotherapies: optimizing outcomes in melanoma." Nat Rev Clin Oncol **14**(8): 463-482.

Löhr, M., G. Klöppel, P. Maisonneuve, A. B. Lowenfels and J. Lüttges (2005). "Frequency of K-ras mutations in pancreatic intraductal neoplasias associated with pancreatic ductal adenocarcinoma and chronic pancreatitis: a meta-analysis." Neoplasia **7**(1): 17-23.

Ma, F., D. Chen, F. Chen, Y. Chi, Z. Han, X. Feng and X. Li (2015). "Human Umbilical Cord Mesenchymal Stem Cells Promote Breast Cancer Metastasis by Interleukin-8- and Interleukin-6-Dependent Induction of CD44(+)/CD24(-) Cells." Cell Transplant **24**(12): 2585-2599.

Masamune, A., T. Watanabe, K. Kikuta and T. Shimosegawa (2009). "Roles of pancreatic stellate cells in pancreatic inflammation and fibrosis." Clin Gastroenterol Hepatol **7**(11 Suppl): S48-54.

Matthaei, H., R. D. Schulick, R. H. Hruban and A. Maitra (2011). "Cystic precursors to invasive pancreatic cancer." Nat Rev Gastroenterol Hepatol **8**(3): 141-150.

Maute, R. L., S. R. Gordon, A. T. Mayer, M. N. McCracken, A. Natarajan, N. G. Ring, R. Kimura, J. M. Tsai, A. Manglik, A. C. Kruse, S. S. Gambhir, I. L. Weissman and A. M. Ring (2015). "Engineering high-affinity PD-1 variants for optimized immunotherapy and immuno-PET imaging." Proc Natl Acad Sci U S A **112**(47): E6506-6514.

McCarroll, J. A., S. Naim, G. Sharbeen, N. Russia, J. Lee, M. Kavallaris, D. Goldstein and P. A. Phillips (2014). "Role of pancreatic stellate cells in chemoresistance in pancreatic cancer." Front Physiol **5**: 141.

Mews, P., P. Phillips, R. Fahmy, M. Korsten, R. Pirola, J. Wilson and M. Apte (2002). "Pancreatic stellate cells respond to inflammatory cytokines: potential role in chronic pancreatitis." Gut **50**(4): 535-541.

- Meyer, S., J. H. Leusen and P. Boross (2014). "Regulation of complement and modulation of its activity in monoclonal antibody therapy of cancer." MABs **6**(5): 1133-1144.
- Mitchem, J. B., D. J. Brennan, B. L. Knolhoff, B. A. Belt, Y. Zhu, D. E. Sanford, L. Belaygorod, D. Carpenter, L. Collins, D. Piwnica-Worms, S. Hewitt, G. M. Udipi, W. M. Gallagher, C. Wegner, B. L. West, A. Wang-Gillam, P. Goedegebuure, D. C. Linehan and D. G. DeNardo (2013). "Targeting tumor-infiltrating macrophages decreases tumor-initiating cells, relieves immunosuppression, and improves chemotherapeutic responses." Cancer Res **73**(3): 1128-1141.
- Neel, B. G., H. Gu and L. Pao (2003). "The 'Shp'ing news: SH2 domain-containing tyrosine phosphatases in cell signaling." Trends Biochem Sci **28**(6): 284-293.
- Noman, M. Z., G. Desantis, B. Janji, M. Hasmim, S. Karray, P. Dessen, V. Bronte and S. Chouaib (2014). "PD-L1 is a novel direct target of HIF-1 α , and its blockade under hypoxia enhanced MDSC-mediated T cell activation." J Exp Med **211**(5): 781-790.
- Oestreich, K. J., H. Yoon, R. Ahmed and J. M. Boss (2008). "NFATc1 regulates PD-1 expression upon T cell activation." J Immunol **181**(7): 4832-4839.
- Okazaki, T. and T. Honjo (2007). "PD-1 and PD-1 ligands: from discovery to clinical application." Int Immunol **19**(7): 813-824.
- Okita, R., A. Maeda, K. Shimizu, Y. Nojima, S. Saisho and M. Nakata (2017). "PD-L1 overexpression is partially regulated by EGFR/HER2 signaling and associated with poor prognosis in patients with non-small-cell lung cancer." Cancer Immunol Immunother **66**(7): 865-876.
- Okkenhaug, K. and B. Vanhaesebroeck (2003). "PI3K in lymphocyte development, differentiation and activation." Nat Rev Immunol **3**(4): 317-330.
- Olive, K. P., M. A. Jacobetz, C. J. Davidson, A. Gopinathan, D. McIntyre, D. Honess, B. Madhu, M. A. Goldgraben, M. E. Caldwell, D. Allard, K. K. Frese, G. Denicola, C. Feig, C. Combs, S. P. Winter, H. Ireland-Zecchini, S. Reichelt, W. J. Howat, A. Chang, M. Dhara, L. Wang, F. Rückert, R. Grützmann, C. Pilarsky, K. Izeradjene, S. R. Hingorani, P. Huang, S. E. Davies, W. Plunkett, M. Egorin, R. H. Hruban, N. Whitebread, K. McGovern, J. Adams, C. Iacobuzio-Donahue, J. Griffiths and D. A. Tuveson (2009). "Inhibition of Hedgehog signaling enhances delivery of chemotherapy in a mouse model of pancreatic cancer." Science **324**(5933): 1457-1461.
- Parsa, A. T., J. S. Waldron, A. Panner, C. A. Crane, I. F. Parney, J. J. Barry, K. E. Cachola, J. C. Murray, T. Tihan, M. C. Jensen, P. S. Mischel, D. Stokoe and R. O. Pieper (2007). "Loss of tumor suppressor PTEN function increases B7-H1 expression and immunoresistance in glioma." Nat Med **13**(1): 84-88.
- Pascolutti, R., X. Sun, J. Kao, R. L. Maute, A. M. Ring, G. R. Bowman and A. C. Kruse (2016). "Structure and Dynamics of PD-L1 and an Ultra-High-Affinity PD-1 Receptor Mutant." Structure **24**(10): 1719-1728.
- Patsoukis, N., K. Bardhan, P. Chatterjee, D. Sari, B. Liu, L. N. Bell, E. D. Karoly, G. J. Freeman, V. Petkova, P. Seth, L. Li and V. A. Boussiotis (2015). "PD-1 alters T-cell metabolic reprogramming by inhibiting glycolysis and promoting lipolysis and fatty acid oxidation." Nat Commun **6**: 6692.
- Pollard, T. D. (2010). "A guide to simple and informative binding assays." Mol Biol Cell **21**(23): 4061-4067.
- Powell, D., M. Lou, F. Barros Becker and A. Huttenlocher (2018). "Cxcr1 mediates recruitment of neutrophils and supports proliferation of tumor-initiating astrocytes in vivo." Sci Rep **8**(1): 13285.
- Quigley, M., F. Pereyra, B. Nilsson, F. Porichis, C. Fonseca, Q. Eichbaum, B. Julg, J. L. Jesneck, K. Brosnahan, S. Imam, K. Russell, I. Toth, A. Piechocka-Trocha, D. Dolfi, J. Angelosanto, A. Crawford, H. Shin, D. S. Kwon, J. Zupkosky, L. Francisco, G. J. Freeman, E. J. Wherry, D. E. Kaufmann, B. D. Walker, B. Ebert and W. N. Haining (2010). "Transcriptional analysis of HIV-specific CD8+ T cells shows that PD-1 inhibits T cell function by upregulating BATF." Nat Med **16**(10): 1147-1151.

- Rahib, L., B. D. Smith, R. Aizenberg, A. B. Rosenzweig, J. M. Fleshman and L. M. Matrisian (2014). "Projecting cancer incidence and deaths to 2030: the unexpected burden of thyroid, liver, and pancreas cancers in the United States." Cancer Res **74**(11): 2913-2921.
- Reeves, E. and E. James (2017). "Antigen processing and immune regulation in the response to tumours." Immunology **150**(1): 16-24.
- Rojewski, M. T., B. M. Weber and H. Schrezenmeier (2008). "Phenotypic Characterization of Mesenchymal Stem Cells from Various Tissues." Transfus Med Hemother **35**(3): 168-184.
- Rombouts, W. J. and R. E. Ploemacher (2003). "Primary murine MSC show highly efficient homing to the bone marrow but lose homing ability following culture." Leukemia **17**(1): 160-170.
- Roopenian, D. C. and S. Akilesh (2007). "FcRn: the neonatal Fc receptor comes of age." Nat Rev Immunol **7**(9): 715-725.
- Ruddon, R. W. (2007). Cancer biology. Oxford ; New York, Oxford University Press.
- Röder, P. V., B. Wu, Y. Liu and W. Han (2016). "Pancreatic regulation of glucose homeostasis." Exp Mol Med **48**: e219.
- Saad, A. M., T. Turk, M. J. Al-Husseini and O. Abdel-Rahman (2018). "Trends in pancreatic adenocarcinoma incidence and mortality in the United States in the last four decades; a SEER-based study." BMC Cancer **18**(1): 688.
- Sato, N., N. Fukushima, R. H. Hruban and M. Goggins (2008). "CpG island methylation profile of pancreatic intraepithelial neoplasia." Mod Pathol **21**(3): 238-244.
- Shi, M., J. Li, L. Liao, B. Chen, B. Li, L. Chen, H. Jia and R. C. Zhao (2007). "Regulation of CXCR4 expression in human mesenchymal stem cells by cytokine treatment: role in homing efficiency in NOD/SCID mice." Haematologica **92**(7): 897-904.
- Shi, X. and D. L. Jarvis (2007). "Protein N-glycosylation in the baculovirus-insect cell system." Curr Drug Targets **8**(10): 1116-1125.
- Son, B. R., L. A. Marquez-Curtis, M. Kucia, M. Wysoczynski, A. R. Turner, J. Ratajczak, M. Z. Ratajczak and A. Janowska-Wieczorek (2006). "Migration of bone marrow and cord blood mesenchymal stem cells in vitro is regulated by stromal-derived factor-1-CXCR4 and hepatocyte growth factor-c-met axes and involves matrix metalloproteinases." Stem Cells **24**(5): 1254-1264.
- Song, C., J. Xiang, J. Tang, D. G. Hirst, J. Zhou, K. M. Chan and G. Li (2011). "Thymidine kinase gene modified bone marrow mesenchymal stem cells as vehicles for antitumor therapy." Hum Gene Ther **22**(4): 439-449.
- Spranger, S., R. M. Spaapen, Y. Zha, J. Williams, Y. Meng, T. T. Ha and T. F. Gajewski (2013). "Up-regulation of PD-L1, IDO, and T(regs) in the melanoma tumor microenvironment is driven by CD8(+) T cells." Sci Transl Med **5**(200): 200ra116.
- Studeny, M., F. C. Marini, R. E. Champlin, C. Zompetta, I. J. Fidler and M. Andreeff (2002). "Bone marrow-derived mesenchymal stem cells as vehicles for interferon-beta delivery into tumors." Cancer Res **62**(13): 3603-3608.
- Swann, J. B. and M. J. Smyth (2007). "Immune surveillance of tumors." J Clin Invest **117**(5): 1137-1146.
- Tan, M. C., P. S. Goedegebuure, B. A. Belt, B. Flaherty, N. Sankpal, W. E. Gillanders, T. J. Eberlein, C. S. Hsieh and D. C. Linehan (2009). "Disruption of CCR5-dependent homing of regulatory T cells inhibits tumor growth in a murine model of pancreatic cancer." J Immunol **182**(3): 1746-1755.

Tang, H., Y. Wang, L. K. Chlewicki, Y. Zhang, J. Guo, W. Liang, J. Wang, X. Wang and Y. X. Fu (2016). "Facilitating T Cell Infiltration in Tumor Microenvironment Overcomes Resistance to PD-L1 Blockade." Cancer Cell **29**(3): 285-296.

Tkachev, V., S. Goodell, A. W. Opipari, L. Y. Hao, L. Franchi, G. D. Glick, J. L. Ferrara and C. A. Byersdorfer (2015). "Programmed death-1 controls T cell survival by regulating oxidative metabolism." J Immunol **194**(12): 5789-5800.

Topalian, S. L., F. S. Hodi, J. R. Brahmer, S. N. Gettinger, D. C. Smith, D. F. McDermott, J. D. Powderly, R. D. Carvajal, J. A. Sosman, M. B. Atkins, P. D. Leming, D. R. Spigel, S. J. Antonia, L. Horn, C. G. Drake, D. M. Pardoll, L. Chen, W. H. Sharfman, R. A. Anders, J. M. Taube, T. L. McMiller, H. Xu, A. J. Korman, M. Jure-Kunkel, S. Agrawal, D. McDonald, G. D. Kollia, A. Gupta, J. M. Wigginton and M. Sznol (2012). "Safety, activity, and immune correlates of anti-PD-1 antibody in cancer." N Engl J Med **366**(26): 2443-2454.

Tsushima, F., S. Yao, T. Shin, A. Flies, S. Flies, H. Xu, K. Tamada, D. M. Pardoll and L. Chen (2007). "Interaction between B7-H1 and PD-1 determines initiation and reversal of T-cell anergy." Blood **110**(1): 180-185.

van Heek, N. T., A. K. Meeker, S. E. Kern, C. J. Yeo, K. D. Lillemo, J. L. Cameron, G. J. Offerhaus, J. L. Hicks, R. E. Wilentz, M. G. Goggins, A. M. De Marzo, R. H. Hruban and A. Maitra (2002). "Telomere shortening is nearly universal in pancreatic intraepithelial neoplasia." Am J Pathol **161**(5): 1541-1547.

Vonlaufen, A., S. Joshi, C. Qu, P. A. Phillips, Z. Xu, N. R. Parker, C. S. Toi, R. C. Pirola, J. S. Wilson, D. Goldstein and M. V. Apte (2008). "Pancreatic stellate cells: partners in crime with pancreatic cancer cells." Cancer Res **68**(7): 2085-2093.

Wachsmann, M. B., L. M. Pop and E. S. Vitetta (2012). "Pancreatic ductal adenocarcinoma: a review of immunologic aspects." J Investig Med **60**(4): 643-663.

Wang, W., A. K. Erbe, J. A. Hank, Z. S. Morris and P. M. Sondel (2015). "NK Cell-Mediated Antibody-Dependent Cellular Cytotoxicity in Cancer Immunotherapy." Front Immunol **6**: 368.

Woods, D. M., R. Ramakrishnan, A. S. Laino, A. Berglund, K. Walton, B. C. Betts and J. S. Weber (2018). "Decreased Suppression and Increased Phosphorylated STAT3 in Regulatory T Cells are Associated with Benefit from Adjuvant PD-1 Blockade in Resected Metastatic Melanoma." Clin Cancer Res **24**(24): 6236-6247.

Xie, C., Z. Yang, Y. Suo, Q. Chen, D. Wei, X. Weng, Z. Gu and X. Wei (2017). "Systemically Infused Mesenchymal Stem Cells Show Different Homing Profiles in Healthy and Tumor Mouse Models." Stem Cells Transl Med **6**(4): 1120-1131.

Xu, Q., J. Ma, J. Lei, W. Duan, L. Sheng, X. Chen, A. Hu, Z. Wang, Z. Wu, E. Wu, Q. Ma and X. Li (2014). "α-Mangostin suppresses the viability and epithelial-mesenchymal transition of pancreatic cancer cells by downregulating the PI3K/Akt pathway." Biomed Res Int **2014**: 546353.

Xu, Z., A. Vonlaufen, P. A. Phillips, E. Fiala-Beer, X. Zhang, L. Yang, A. V. Biankin, D. Goldstein, R. C. Pirola, J. S. Wilson and M. V. Apte (2010). "Role of pancreatic stellate cells in pancreatic cancer metastasis." Am J Pathol **177**(5): 2585-2596.

Yamazaki, T., H. Akiba, H. Iwai, H. Matsuda, M. Aoki, Y. Tanno, T. Shin, H. Tsuchiya, D. M. Pardoll, K. Okumura, M. Azuma and H. Yagita (2002). "Expression of programmed death 1 ligands by murine T cells and APC." J Immunol **169**(10): 5538-5545.

Yin, J., J. K. Kim, J. H. Moon, S. Beck, D. Piao, X. Jin, S. H. Kim, Y. C. Lim, D. H. Nam, S. You, H. Kim and Y. J. Choi (2011). "hMSC-mediated concurrent delivery of endostatin and carboxylesterase to mouse xenografts suppresses glioma initiation and recurrence." Mol Ther **19**(6): 1161-1169.

Yu, J., X. Wang, T. Xu, Q. Jin, J. Duan, J. Wu, H. Wu and S. Ye (2017). "A rational approach to enhancing antibody Fc homodimer formation for robust production of antibody mixture in a single cell line." J Biol Chem **292**(43):

17885-17896.

Yu, R., L. Deedigan, S. M. Albarenque, A. Mohr and R. M. Zwacka (2013). "Delivery of sTRAIL variants by MSCs in combination with cytotoxic drug treatment leads to p53-independent enhanced antitumor effects." Cell Death Dis **4**: e503.

Yu, Y. and J. Cui (2018). "Present and future of cancer immunotherapy: A tumor microenvironmental perspective." Oncol Lett **16**(4): 4105-4113.

Zak, K. M., R. Kitel, S. Przetocka, P. Golik, K. Guzik, B. Musielak, A. Dömling, G. Dubin and T. A. Holak (2015). "Structure of the Complex of Human Programmed Death 1, PD-1, and Its Ligand PD-L1." Structure **23**(12): 2341-2348.

Zhang, M., N. Mal, M. Kiedrowski, M. Chacko, A. T. Askari, Z. B. Popovic, O. N. Koc and M. S. Penn (2007). "SDF-1 expression by mesenchymal stem cells results in trophic support of cardiac myocytes after myocardial infarction." FASEB J **21**(12): 3197-3207.

Zhang, T., Y. W. Lee, Y. F. Rui, T. Y. Cheng, X. H. Jiang and G. Li (2013). "Bone marrow-derived mesenchymal stem cells promote growth and angiogenesis of breast and prostate tumors." Stem Cell Res Ther **4**(3): 70.

Zhang, X., J. C. Schwartz, S. C. Almo and S. G. Nathenson (2003). "Crystal structure of the receptor-binding domain of human B7-2: insights into organization and signaling." Proc Natl Acad Sci U S A **100**(5): 2586-2591.